A new class of coherent states and its properties

A thesis submitted in fulfilment of the requirements

for the degree of Doctor of Philosophy

The University of Bradford, 2011

Abdlgader Mohamed

Department of Computing

Abstract

The study of coherent states (CS) for a quantum mechanical system has received a lot of attention. The definition, applications, generalizations of such states have been the subject of work by researchers. A common starting point of all these approaches is the observation of properties of the original CS for the harmonic oscillator. It is well-known that they are described equivalently as (a) eigenstates of the usual annihilation operator, (b) from a displacement operator acting on a fundamental state and (c) as minimum uncertainty states. What we observe in the different generalizations proposed is that the preceding definitions are no longer equivalent and only some of the properties of the harmonic oscillator CS are preserved.

In this thesis we propose to study a new class of coherent states and its properties. We note that in one example our CS coincide with the ones proposed by Glauber where a set of three requirements for such states has been imposed. The set of our generalized coherent states remains invariant under the corresponding time evolution and this property is called **temporal stability**. Secondly, there is no state which is orthogonal to all coherent

states (the coherent states form a total set). The third property is that we get all coherent states by acting on one of these states ['fiducial vector'] with operators. They are highly non-classical states, in the sense that in general, their Bargmann functions have zeros which are related to negative regions of their Wigner functions. Examples of these coherent states with Bargmann function that involve the Gamma and also the Riemann ξ functions are represented. The zeros of these Bargmann functions and the paths of the zeros during time evolution are also studied.

Acknowledgements

My deepest thanks firstly go to God, who created me, helps me and has given me the ability to reach this stage.

I would like to thank Professor A. Vourdas, my supervisor, for his great support and guidance during this research. His inspiring suggestions and constant encouragement have had a great effect on my study, and I count myself fortunate to have been given the valuable opportunity to work under his supervision throughout this journey. I need to thank Dr C Lei for our joint work on the Gamma state. I would also like to thank all members of the Quantum Information research group in the school. Many thanks go also to my research colleagues for their invaluable discussions, as well as the School of Computing, Informatics and Media at the University of Bradford for the financial and technical support and all the staff who helped me during my study. I should also mention that my research study in the UK was sponsored totally by Libyan Cultural Affairs. Finally, I am grateful to my parents for their encouragement and support and also my wife Yasmina for patience and sacrifice.

Declaration

Some parts of the work presented in this thesis have been published in the following article:

A. Mohamed, C. Lei, A. Vourdas "Weak coherent states related to the multiplicative group $\mathbb{C}^*$", Journal of Physics A: Mathematical and Theoretical, vol 44, pp 215-304, 2011.

List of Figures

List of Tables

Contents

Chapter 1

Introduction

The thesis is devoted to the study of a new class of coherent states and its properties. The coherent states of a harmonic oscillator were first constructed by **Schrodinger** as "the most classical" states of the oscillator [1]. The properties of these states have been studied in a systemetic way by Glauber, who showed their importance for the quantum mechanical treatment of optical coherence and who introduced the name "**coherent state**". They are the states of harmonic oscillator system which have the minimum uncertainty in position and momentum allowed by the Heisenberg uncertainty principle. Coherent states have been studied extensively in the literature [2, 3].

When two such classical states are superposed the resultant states exhibit many non-classical features. An important case is the superposition of two coherent states of some amplitude with their phases differing by π. The symmetric combination $|z\rangle + |-z\rangle$ is $|z\rangle_e$, $z \in \mathbb{C}$. The state $|z\rangle_e$ is called an even coherent state. The antisymmetric superposition $|z\rangle - |-z\rangle$ is $|z\rangle_o$ involves only the odd number states. The even and odd coherent states for

harmonic oscillator, introduced in the 1970s by Dodonov, Malkin and Man'ko and later called "Schrodinger cat" [1]. The name "Schrodinger cat" is based on the thought experiment which Schrodinger used to discuss philosophy aspects of quantum mechanics (see subsection 2.2.4).

There are many types of generalized coherent states which are related to some groups and have some properties. $SU(1,1)$ and $SU(2)$ coherent states are some of them. In this thesis we consider the set of states with Bargmann function $g(Az)$ where $A \in \mathbb{C}$. They are generalized coherent states, in the sense that they have three the following properties. The first property is that the set of coherent state is a total set in the Hilbert space. Our states may not have the stronger property of the resolution of the identity. The second property is that we get all coherent states by acting on one of these states ['fiducial vector'] with operators which form a representation of the multiplicative group of non-zero complex numbers $\mathbb{C}^* = \mathbb{C} - \{0\}$. The third property is sometimes called temporal stability [2, 3]. For some Hamiltonian H, the set of coherent states remains invariant under the corresponding time evolution (i.e, if $|s\rangle$ is a coherent state then $\exp(itH)|s\rangle$ is also a coherent state).

We consider various examples, for $g(z) = \exp(z)$ we get the Glauber coherent states. When $g(z) = \sin(z)$ or $g(z) = \cos(z)$ we get the odd and even coherent states. We also consider the case where $g(z) = \frac{\exp(Bz)}{[\Gamma(Az)]^k}$ where Γ is a Gamma function and study the corresponding coherent states. We also study the time evolution of these states for various Hamiltonians and in particular the paths of the zeros of their Bargmann functions. We study in detail the properties of these states photon number $\langle N \rangle$, second order correlation $g^{(2)}$,

wave function, Wigner function, etc. The zeros of a Bargmann function do not define the function uniquely. For this reason we study the functions $\frac{1}{\Gamma(Az)}$ and $\frac{\exp(Bz)}{\Gamma(Az)}$ which have the same zeros but are different. We also study the case where $g(Az) = \xi(Az)$, the Riemann xi function.

The motivation for this work is to introduce a methodology which leads to wide classes with properties similar to coherent states. In the general case, we do not have a resolution of the identity in terms of these states. However, we have the weaker property that these states are a total set in some space. An important open question is to find a resolution of the identity in terms of states which are a total set in some space.

This thesis consists of seven chapters. Chapter one is an introduction to the thesis. Chapter 2 gives a review on phase space methods for quantum particles on a real line. A number of fundamental aspects in quantum systems with a continuous Hilbert space are discussed. The Wigner and Weyl functions are introduced in different quantum states (number states, coherent states, squeezed states). Chapter 3 gives a brief introduction to two types of generalized coherent states based on $SU(1,1)$ and $SU(2)$ Lie groups. Our generalized coherent states and their properties are introduced in chapter 4; with the " Schrödinger cat states" as an example. The wave function, Wigner function and also the motion of its Bargmann function at different Hamiltonians are discussed. In chapter 5 a few examples based on Gamma function are discussed. In addition to this two methods are used to compute the overlaps of our states, one by using zeta function and the other by using integration. Chapter 6 gives a brief introduction to Riemann zeta state $\zeta(z)$ and Riemann ξ state $\xi(z)$. The wave function, Wigner function and also the

motion of $\xi(Az)$ function for different Hamiltonian are discussed. " In the final chapter we conclude and discuss the contributions of this thesis, and suggest further work."

Chapter 2

Quantum Harmonic Oscillator

2.1 Introduction

The quantum harmonic oscillator holds a unique importance in quantum mechanics, as it is both one of the few problems that can really be solved in closed form. It introduces the methods of analytically solving the differential equations frequently encountered in quantum mechanics. It also provides a good introduction to the use of raising and lowering operators, and using the abstract vectors that are frequently used in quantum mechanics to solve problems by knowing the action of operators upon state vectors, rather than using integration to evaluate expectation values [4, 5, 6].

The harmonic oscillator is characterized by the Hamilltonian;

$$\hat{H} = \frac{\hat{p}^2}{2m} + \frac{1}{2}m\omega^2\hat{x}^2, \tag{2.1}$$

where $\hat{p}$ is the momentum operator and $\hat{x}$ is the position operator . For simplicity, let us first consider the Hamilltonian for the harmonic oscillator

with unitary mass $m = 1$ and unitary frequency $\omega = 1$

$$\hat{H} = \frac{\hat{p}^2}{2} + \frac{1}{2}\hat{x}^2. \tag{2.2}$$

2.1.1 Position and Momentum operators

The position operator $\hat{x}$ is a Hermitian operator, and we can use its eigenstates as an orthogonal basis. The state $|x\rangle$ is defined to be the eigenstate of $\hat{x}$ with eigenvalue x ;

$$\hat{x}|x\rangle = x|x\rangle. \tag{2.3}$$

The states of the position operator $\hat{x}$ form an orthogonal basis

$$\langle x|x'\rangle = \delta(x - x'). \tag{2.4}$$

The eigenstates $|x\rangle$ of the position operator $\hat{x}$ form a complete basis

$$\int dx|x\rangle\langle x| = \hat{1}. \tag{2.5}$$

We can expand arbitrary state $|\psi\rangle$ in terms of the $|x\rangle$ basis states,

$$|\psi\rangle = \hat{1}|\psi\rangle = \int dx|x\rangle\langle x|\psi\rangle = \int dx\psi(x)|x\rangle. \tag{2.6}$$

Another useful basis is formed by the eigenstates of the momentum operator $\hat{p}$; The momentum operator $\hat{p}$ is a Hermitian operator, and we can

use its eigenstates as an orthogonal basis. The state $|p\rangle$ is defined to be the eigenstate of $\hat{p}$ with eigenvalue p :

$$\hat{p}|p\rangle = p|p\rangle. \tag{2.7}$$

The states of momentum operator $\hat{p}$ form an orthogonal basis

$$\langle p|p'\rangle = \delta(p - p'). \tag{2.8}$$

The eigen states $|p\rangle$ of momentum operator $\hat{p}$ form a complete basis

$$\int dp|p\rangle\langle p| = \hat{1} \qquad . \tag{2.9}$$

We can expand our state $|\psi\rangle$ in terms of the $|p\rangle$ basis states.

$$|\psi\rangle = \hat{1}|\psi\rangle = \int dp|p\rangle\langle p|\psi\rangle = \int dp\psi(p)|p\rangle. \tag{2.10}$$

The state $|x\rangle$ and $|p\rangle$ are related to each other by Fourier transform

$$|x\rangle = (2\pi)^{-1/2} \int_{-\infty}^{\infty} \exp(-ixp)|p\rangle dp, \tag{2.11}$$

$$|p\rangle = (2\pi)^{-1/2} \int_{-\infty}^{\infty} \exp(ixp)|x\rangle dx. \tag{2.12}$$

The inner product between $|x\rangle$ and $|p\rangle$

$$\langle x|p\rangle = (2\pi)^{-1/2} \exp(ixp). \tag{2.13}$$

For any pair of non commuting operators such as $\hat{x}$ and $\hat{p}$, there is an un-

certainty relation that quantifies to what the two observables can be specified simultaneously. In this case, the position-momentum uncertainty relation is

$$\triangle x \triangle p \geq \frac{1}{2}, \tag{2.14}$$

where $\triangle x$ and $\triangle p$ are the standard deviations of $\hat{x}$ and $\hat{p}$ measurements respectively.

2.2 States of the quantum harmonic oscillator

We shall now describe several states of a quantum harmonic oscillator such as number states, coherent states, squeezed states, and also we will discuss their properties.

2.2.1 Number states $|n\rangle$

Number states play an important role in quantum optics. They are an orthogonal basis in the Hilbert space and each state can be expanded in terms of them.

It is convenient to introduce the non-Hermitian combinations of $\hat{x}$ and $\hat{p}$:

$$\begin{aligned} \hat{a} &= (2)^{-1/2} (\hat{x} + i\hat{p}) , \\ \hat{a}^{\dagger} &= (2)^{-1/2} (\hat{x} - i\hat{p}) , \end{aligned} \tag{2.15}$$

where $\hat{a}$ is the annihilation operator and $\hat{a}^\dagger$ the creation operator.

These two operators obey the canonical commutation relation [7].

$$[\hat{a}, \hat{a}^\dagger] = I. \tag{2.16}$$

The eigenstates $|n\rangle$ of the number operator $\hat{n}$ are known as the number states satisfying:

$$\hat{H}|n\rangle = E_n|n\rangle, \qquad E_n = (n + \frac{1}{2}), \quad n = 0, 1, 2, \ldots, \tag{2.17}$$

where the non-negative integers n characterize the energy spectrum of the linear harmonic oscillator. One quantum of energy is called one photon in quantum optics. The eigenstate $|0\rangle$ with the lowest energy $E_n = 1/2$ is generally called the vacuum state. The number states $\hat{n} = \hat{a}^\dagger\hat{a}$ is defined as

$$\hat{n} = \sum_{n=0}^{\infty} n|n\rangle\langle n| \quad and \quad \hat{n} = n|n\rangle. \tag{2.18}$$

Apparently, the Hamitonian operator in Eq (2.17) is $\hat{H} = \hat{n} + \frac{1}{2}$. Since $\hat{n}$ is a Hermitian, we next introduce the fractional Fourier operator $\hat{U}(\theta)$ as follows:

$$\hat{U}(\theta) = \exp(i\theta\hat{n}) \qquad \theta \in \Re, \tag{2.19}$$

which is a unitary operator. We can show that

$$\hat{U}(\theta)\hat{x}\hat{U}(\theta)^{\dagger} = \hat{x}\cos(\theta) + \hat{p}\sin(\theta). \tag{2.20}$$

$$\hat{U}(\theta)\hat{p}\hat{U}(\theta)^{\dagger} = -\hat{x}\sin(\theta) + \hat{p}\cos(\theta). \tag{2.21}$$

By using this expression

$$\exp(X)Y\exp(-X) = Y + [X,Y] + \frac{1}{2!}[X,[X,Y]] + ... \tag{2.22}$$

It is seen that the fractional Fourier operator $\hat{U}(\theta)$ creates rotations in the x-p plane quantum phase space.

For $\theta = \pi$ this operator is called **parity operator**

$$\hat{U}(\pi) = \exp(i\pi\hat{a}^{\dagger}\hat{a}) = \sum_{n=0}^{\infty}(-1)^n|n\rangle\langle n|, \qquad [\hat{U}(\pi)]^2 = \hat{1}. \tag{2.23}$$

It is easy seen that

$$\hat{U}(\pi)|x\rangle = |-x\rangle, \qquad \hat{U}(\pi)|p\rangle = |-p\rangle \tag{2.24}$$

$$\hat{U}(\pi)\hat{x}\hat{U}(\pi)^{\dagger} = -\hat{x}, \qquad \hat{U}(\pi)\hat{p}\hat{U}(\pi)^{\dagger} = -\hat{p}. \tag{2.25}$$

For $\theta = \frac{\pi}{2}$ this operator is called **Fourier transform operator**

$$\hat{U}(\frac{\pi}{2}) = \exp(i\frac{\pi}{2}\hat{a}^\dagger\hat{a}) = \sum_{n=0}^{\infty}(i)^n|n\rangle\langle n|, \qquad [\hat{U}(\frac{\pi}{2})]^4 = \hat{1}. \tag{2.26}$$

It is easy seen that

$$\hat{U}(\frac{\pi}{2})|x\rangle = |p\rangle, \qquad \hat{U}(\frac{\pi}{2})|p\rangle = |x\rangle \tag{2.27}$$

$$\hat{U}(\frac{\pi}{2})\hat{x}\hat{U}(\pi)^\dagger = \hat{p}, \qquad \hat{U}(\frac{\pi}{2})\hat{p}\hat{U}(\pi)^\dagger = -\hat{x}. \tag{2.28}$$

The ladder of excitation can be climbed up and down via the application of creation and annihilation operators

$$\hat{a}^\dagger|n\rangle = \sqrt{n+1}|n+1\rangle. \tag{2.29}$$

$$\hat{a}|n\rangle = \sqrt{n}|n-1\rangle. \tag{2.30}$$

The set of number states $\{|n\rangle, \quad n = 0, 1, 2, \ldots\}$ forms a complete and orthogonal set of states i.e

$$\sum_{n=0}^{\infty}|n\rangle\langle n| = I \quad and \quad \langle n|m\rangle = \delta_{nm}. \tag{2.31}$$

The position $\hat{x}$ and momentum $\hat{p}$ operators can be written in terms of $\hat{a}$

and $\hat{a}^\dagger$ as follows:

$$\hat{x} = \frac{1}{\sqrt{2}}(\hat{a} + \hat{a}^\dagger), \qquad \hat{p} = -i\partial_x = \frac{1}{\sqrt{2}i}(\hat{a} - \hat{a}^\dagger). \tag{2.32}$$

The position representation of the number states $|n\rangle$

$$\langle x|n\rangle = (\sqrt{\pi}2^n n!)^{-1/2} H_n(x) \exp(-x^2/2). \tag{2.33}$$

The momentum representation of the number states $|n\rangle$

$$\langle p|n\rangle = (\sqrt{\pi}2^n n!)^{-1/2} (-1)^n H_n(p) \exp(-p^2/2), \tag{2.34}$$

where $H_n(x)$ are the Hermite polynomials of order n [8, 9].

Figures (2.1) and (2.2) show the link between the Wave function of the number state $|3\rangle$ and its Fourier transformation.

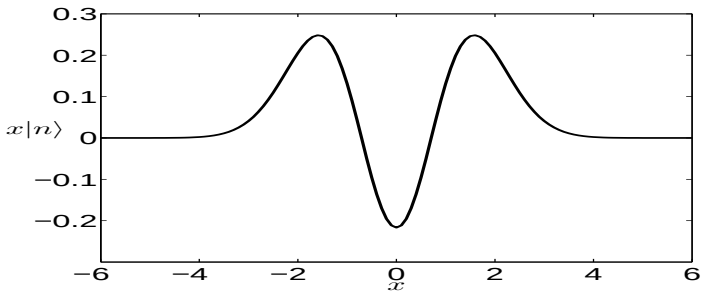

Figure 2.1: The x representation $f(x) = \langle x|3\rangle$ for the number state $|3\rangle$

The states $|x\rangle$ and $|p\rangle$ are eigen states of the position and momentum operators.

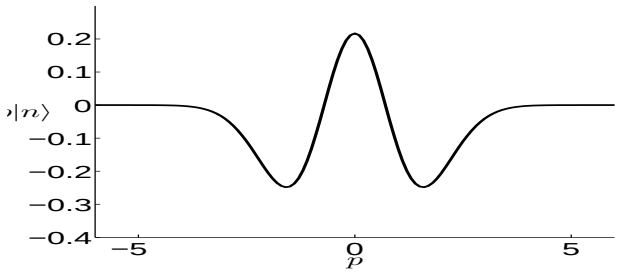

Figure 2.2: The p representation $f(p) = \langle p|3\rangle$ for the number state $|3\rangle$

.

Number states provide a frequently used representation of a pure state

$$|f\rangle = \sum_{n=0}^{\infty} f_n |n\rangle. \tag{2.35}$$

The average of photon number of $|n\rangle$

$$\langle n\rangle = \langle n|\hat{n}|n\rangle = \langle n|\hat{a}^\dagger \hat{a}|n\rangle = n. \tag{2.36}$$

The photon variance of $|n\rangle$

$$(\Delta n)^2 = \langle n^2\rangle - \langle n\rangle^2 = 0. \tag{2.37}$$

The expectation value of $\hat{x}$ for $|n\rangle$

$$\langle x\rangle = \langle n|\hat{x}|n\rangle = \langle n|\frac{1}{\sqrt{2}}(\hat{a} + \hat{a}^\dagger)|n\rangle = 0. \tag{2.38}$$

The expectation value of $\hat{p}$ for $|n\rangle$

$$\langle p\rangle = \langle n|\hat{p}|n\rangle = \langle n|\frac{1}{\sqrt{2}i}(\hat{a}-\hat{a}^{\dagger})|n\rangle = 0. \tag{2.39}$$

The variances of $\hat{x}$ and $\hat{p}$ are equal

$$(\Delta x)^2 = (\Delta p)^2 = n + 1/2. \tag{2.40}$$

The second order coherence $g^{(2)} = 1$ for the ground state $|0\rangle$

The second order coherence $g^{(2)}$ of $|n\rangle$ for $n \geq 1$

$$g^{(2)} = \frac{\langle \hat{a}^{\dagger}\hat{a}^{\dagger}\hat{a}\hat{a}\rangle}{\langle \hat{a}^{\dagger}\hat{a}\rangle^2} = 1 - \frac{1}{n}. \tag{2.41}$$

We present in tables 2.1 and 2.2 the quantum statistical quantities like the average number of photons $\langle n\rangle$, the variances of $\hat{x}$ and $\hat{p}$, and the second-order correlations $g^{(2)}$ for the number states $|n\rangle$ at $n = 0, 1, 2, 3$.

Table 2.1: The values of $\langle n\rangle$, $\langle n^2\rangle$, $(\Delta n)^2$ and $g^{(2)}$ for number states $|n\rangle$ at $n = 0, 1, 2, 3$

$\|n\rangle$	$\langle n\rangle$	$\langle n^2\rangle$	$(\Delta n)^2$	$g^{(2)}$
$\|0\rangle$	0	0	0	1
$\|1\rangle$	1	1	0	0
$\|2\rangle$	2	4	0	1/2
$\|3\rangle$	3	9	0	2/3

Table 2.2: The values of $\langle x\rangle$, $\langle x^2\rangle$,$(\Delta x)^2$ $\langle p\rangle$, $\langle p^2\rangle$ and $(\Delta p)^2$ for number states $|n\rangle$ at $n = 0, 1, 2, 3$

$\|n\rangle$	$\langle x\rangle$	$\langle x^2\rangle$	$(\Delta x)^2$	$\langle p\rangle$	$\langle p^2\rangle$	$(\Delta p)^2$
$\|0\rangle$	0	1/2	1/2	0	1/2	1/2
$\|1\rangle$	0	3/2	3/2	0	3/2	3/2
$\|2\rangle$	0	5/2	5/2	0	5/2	5/2
$\|3\rangle$	0	7/2	7/2	0	7/2	7/2

2.2.2 Coherent states $|z\rangle$

In this subsection we introduce another set of states, the coherent states. They most closely resemble those of a classical field, like a laser pulse. The coherent state can be define as; [3, 10]

$$|z\rangle \;=\; \exp\left(-\frac{|z|^2}{2}\right)\sum_{n=0}^{\infty}\frac{z^n}{\sqrt{n!}}\,|n\rangle. \tag{2.42}$$

We recall that the parameter $z = s\exp(i\theta)$ describing the coherent state is a complex number which has a real and imaginary part $Re(z), Im(z)$ respectively.

The coherent state can also defined by

$$|z\rangle = D(z)|0\rangle, \tag{2.43}$$

where $D(z)$ is a displacement operator and can be written as:

$$D(z) = \exp(z\hat{a}^\dagger - z^*\hat{a}). \tag{2.44}$$

The displacement operator $D(z)$ satisfies the following properties:

$$D^\dagger(z)D(z) = \hat{1}, \tag{2.45}$$

$$D^\dagger(z) = D(-z), \tag{2.46}$$

$$D^\dagger(z)\hat{a}D(z) = \hat{a} + z, \quad D^\dagger(z)\hat{a}^\dagger D(z) = \hat{a}^\dagger + z, \tag{2.47}$$

$$D^\dagger(z)f(\hat{a}, \hat{a}^\dagger)D(z) = f(\hat{a} + z, \hat{a}^\dagger + z^*), \tag{2.48}$$

$$D(z_1)D(z_2) = \exp((z_1 z_2^* - z_1^* z_2)/2)D(z_1 + z_2), \tag{2.49}$$

$$D(z_1)D(z_2) = \exp(z_1 z_2^* - z_1^* z_2)D(z_2)D(z_1), \tag{2.50}$$

where $D^\dagger(z)$ is the conjugate transpose of $D(z)$, and z^* is the conjugate of z.

The Baker-Haussdorf formula states that:

$$\exp(A + B) = \exp(A)\exp(B)\exp(-[A, B]/2), \tag{2.51}$$

when $[A, [A, B]] = 0$ and $[B, [A, B]] = 0$.

The proof of the Baker-Haussdorf formula employs the following identity valid for arbitrary operators (without assuming vanishing of commutators):

$$\exp(A)B\exp(-A) = B + [A, B]/1! + [A, [A, B]]/2!.... \tag{2.52}$$

with the identity we can derive Eqs (2.47) and (2.48)

The number z can be any complex number. We now discuss the basic features of the coherent states and photon operators $\hat{a}$ and $\hat{a}^\dagger$. For example,

one can easily show that the states $|z\rangle$ are normalized.

$$\langle z|z\rangle = \exp(-|z|^2)\sum_{n=0}^{\infty}\frac{|z|^{2n}}{n!}\langle n|n\rangle = \exp(-|z|^2\exp(|z|^2) = 1. \tag{2.53}$$

Coherent states are also useful in calculations, since they are the eigenstates of the annihilation operator $\hat{a}$ with eigen value z. To show this, we calculate:

$$\hat{a}|z\rangle = exp(-\frac{|z|^2}{2})\sum_{n=1}^{\infty}\frac{z^n}{\sqrt{n!}}\sqrt{n}|n-1\rangle = z|z\rangle \tag{2.54}$$

.

The time evolution of any such coherent state remains within the family of coherent states [2, 3, 11].

$$\exp(-iHt)|z\rangle = \exp(-i\hat{a}^{\dagger}\hat{a}t)|z\rangle = |\exp(-it)z\rangle. \tag{2.55}$$

This property is called **temporal stability**

The mean number of photons for a system prepared in take$|z\rangle$ equals

$$\langle n\rangle = \langle z|\hat{a}^{\dagger}\hat{a}|z\rangle = z^*\langle z|\hat{a}|z\rangle = z^*z\langle z|z\rangle = |z|^2 \tag{2.56}$$

.

The expectation value of the position operator $\hat{x}$ in the coherent state $|z\rangle$ is

$$\langle x\rangle = \langle z|\hat{x}|z\rangle = \langle z|\frac{1}{\sqrt{2}}(\hat{a}+\hat{a}^{\dagger})|z\rangle = \sqrt{2}Re(z). \tag{2.57}$$

The expectation value of the momentum operator $\hat{p}$ in the coherent state

$|z\rangle$ is

$$\langle p\rangle = \langle z|\hat{p}|z\rangle = \langle z|\frac{1}{\sqrt{2}i}(\hat{a}-\hat{a}^{\dagger})|z\rangle = \sqrt{2}Im(z). \tag{2.58}$$

The variances of $\hat{x}$ and $\hat{p}$ in the coherent state $|z\rangle$ are

$$(\Delta x)^2 = (\Delta p)^2 = \frac{1}{2}. \tag{2.59}$$

The second order coherence $g^{(2)}$ of $|z\rangle$

$$g^{(2)} = \frac{\langle \hat{a}^{\dagger}\hat{a}^{\dagger}\hat{a}\hat{a}\rangle}{\langle \hat{a}^{\dagger}\hat{a}\rangle^2} = 1. \tag{2.60}$$

We present in tables 2.3 and 2.4 the quantum statistical quantities like the average number of photons $\langle n\rangle$, the variances of $\hat{x}$ and $\hat{p}$, and the second-order correlations $g^{(2)}$ for the coherent states $|z\rangle$ at $z = 0, 1, i, 1+i$.

The probability for finding n photons in the photon state $|z\rangle$ is given by

$$P(n) = |\langle n|z\rangle|^2 = exp(-|z|^2)\frac{|z|^{2n}}{n!} = exp(-\langle n\rangle)\frac{\langle n\rangle^n}{n!}. \tag{2.61}$$

Figure (2.3) illustrates the distribution of the photon number for a coherent state $|z\rangle$ where $z = 2$. However, Figure (2.4) shows the probability of two different coherent states: $|z_1\rangle$ and $|z_2\rangle$ where $z_1 = i$ and $z_2 = 2 + 3i$.

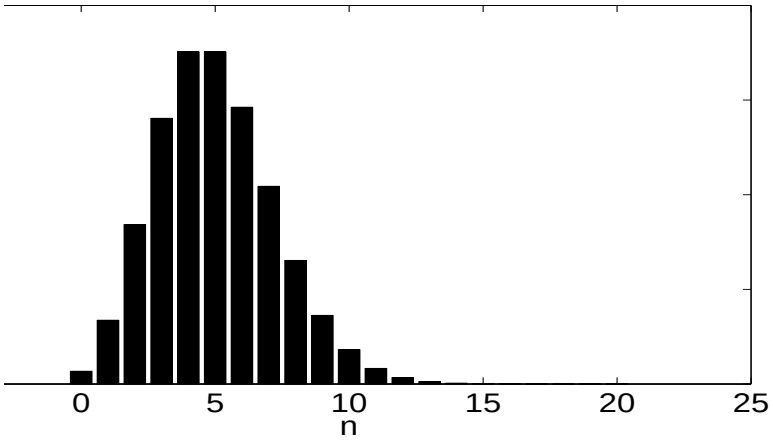

Figure 2.3: The Photon number probability distribution for coherent state $|2+i\rangle$

2.2.3 The time evolution of coherent state $|z\rangle$

The time evolution of a minimum uncertainty coherent state $|z\rangle$ where $z = s\exp(i\theta)$ under the harmonic oscillator is given by

$$|z\rangle_t = \exp(-iHt)|z\rangle = \exp(-it(\hat{a}^\dagger a))|z\rangle. \tag{2.62}$$

The expectation value of $\hat{x}$ in $|z\rangle$ at time $t \geq 0$ is:

$$\langle x\rangle_t = \sqrt{2}s\cos(\theta - t). \tag{2.63}$$

The expectation value of $\hat{p}$ in $|z\rangle$ at time $t \geq 0$ is:

$$\langle p\rangle_t = \sqrt{2}s\sin(\theta - t). \tag{2.64}$$

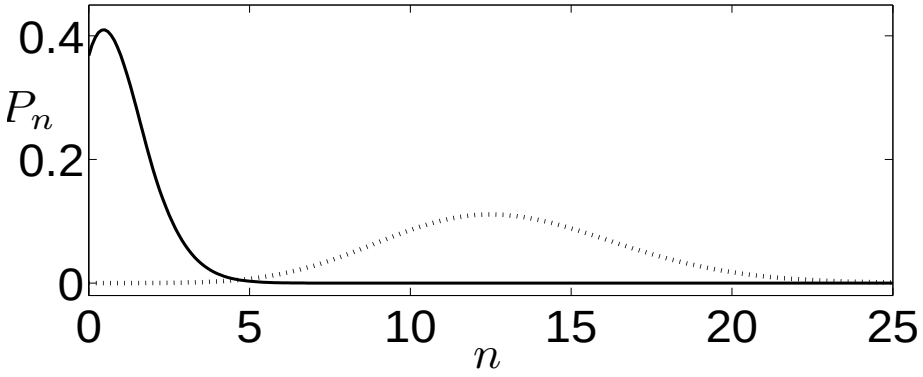

Figure 2.4: The Photon number probability distribution for $|z\rangle$, $z = i$ (solid line) and $|\beta\rangle$, $\beta = 2 + 3i$ (dot line).

The variance of $\hat{x}$ and $\hat{p}$ in $|z\rangle$ at time $t \geq 0$ is:

$$(\Delta x)_t^2 = (\Delta p)_t^2 = \frac{1}{2}. \tag{2.65}$$

Moreover, one can calculate the overlap between two different coherent states $|z_1\rangle$ and $|z_2\rangle$ [12]:

$$\langle z_1|z_2\rangle = \exp(-\frac{|z_1|^2}{2} - \frac{|z_2|^2}{2} + z_1^* z_2) \tag{2.66}$$

whereas the modulus (called sometimes **the state overlap**) is:

$$|\langle z_1|z_2\rangle|^2 = \exp(-|z_1 - z_2|^2). \tag{2.67}$$

The coherent states are not pairwise orthogonal. Since they can nevertheless

be used to represent any state by writing it as a superposition of them, they are called an over complete basis[13].

Furthermore, these states are evidently continuous in $z \in \mathbb{C}$ and admit a resolution of unity given by

$$1 = \frac{1}{\pi} \int_{\mathbb{C}} \int dz |z\rangle\langle z| \qquad dz = dRe(z) dIm(z), \tag{2.68}$$

where $z = Re(z) + iIm(z)$ and the integration is over the whole complex plane $\mathbb{C}$.

As the coherent states are labeled by a continuous complex plane in the Hilbert space that has a countable basis, they are over-complete. The above relation also shows that the coherent states can be normalized.

To prove this relation one should calculate the integral over the whole complex plane in the right hand side of equation Eq(2.68)

$$\int_{\mathbb{C}} \int dz |z\rangle\langle z| = \int_{\mathbb{C}} \int dz \exp(-|z|^2) \sum_{m,n} \frac{(z^*)^n z^m}{\sqrt{n!m!}}. \tag{2.69}$$

Now, writing z in polar form:

$z = s \exp(i\theta) \quad \Rightarrow \quad dz = s ds d\theta.$

We finally get:

$$\frac{1}{\pi} \int_{\mathbb{C}} \int dz |z\rangle\langle z| = \sum_{n=0}^{\infty} |n\rangle\langle n| = 1. \tag{2.70}$$

The photon number states $|n\rangle$ can be written as a superposition of co-

herent states $|z\rangle$:

$$|n\rangle = 1|n\rangle = \frac{1}{\pi}\int_{\mathbb{C}}\int dz|z\rangle\langle z|n\rangle = \frac{1}{\pi}\int_{\mathbb{C}}\int dz \exp\left(-\frac{|z|^2}{2}\right)\sum_{n=0}^{\infty}\frac{z^n}{\sqrt{n!}}|z\rangle. \tag{2.71}$$

The position-representation of coherent state $|z\rangle$ can be written as:

$$\langle x|z\rangle = \pi^{-1/4}\exp(-x^2/2 + \sqrt{2}zx - (Re(z))^2). \tag{2.72}$$

Figure (2.5) shows the wave function of two coherent states labeled as $|z_1\rangle$ and $|z_2\rangle$ where $z_1 = -1$ and $z_2 = 1$.

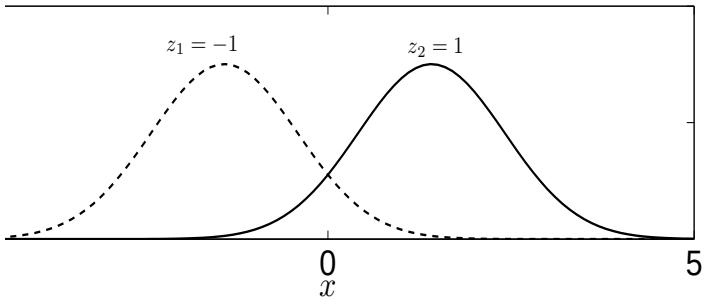

Figure 2.5: The wave function of two coherent states $|z_1\rangle$ and $|z_2\rangle$ where $z_1 = -1$ and $z_2 = 1$

The coherent state wave function $\langle x|z\rangle$ looks exactly like ground state, but shifted in momentum and position. It then moves as a classical particle, while keeping its shape fixed.

The coherent state is also called a '**Displaced Ground State**'

In summary, we have seen that the coherent states are minimal uncertainty wavepackets which remains minimal under time evolution. Furthermore, the time dependant expectation values of x and p satisfies the classical

equations of motion.

Table 2.3: The values of $\langle n\rangle$, $\langle n^2\rangle$ and $(\Delta n)^2$ for coherent states $|z\rangle$ at $z = 0, 1, i, 1+i$

$\|z\rangle$	$\langle n\rangle$	$\langle n^2\rangle$	$(\Delta n)^2$
0	0	0	0
1	1	2	1
i	1	2	1
$1+i$	2	6	2

Table 2.4: The values of $\langle x\rangle$, $\langle x^2\rangle$, $(\Delta x)^2$, $\langle p\rangle$, $\langle p^2\rangle$ and $(\Delta p)^2$ for coherent states $|z\rangle$ at $z = 0, 1, i, 1+i$

$\|z\rangle$	$\langle x\rangle$	$\langle x^2\rangle$	$(\Delta x)^2$	$\langle p\rangle$	$\langle p^2\rangle$	$(\Delta p)^2$
0	0	1/2	1/2	0	1/2	1/2
1	$\sqrt{2}$	5/2	1/2	0	1/2	1/2
i	0	1/2	1/2	$\sqrt{2}$	5/2	1/2
$1+i$	$\sqrt{2}$	5/2	1/2	$\sqrt{2}$	5/2	1/2

2.2.4 Even and odd coherent States $|z\rangle_e$ and $|z\rangle_o$

Superposition is a principle of quantum theory that describes a challenging concept about the nature and behavior of matter and forces at the sub-atomic level. The principle of superposition claims that while we do not know what the state of any object is, it is actually in all possible states simultaneously, as long as we don't look to check. It is the measurement itself that causes the object to be limited to a single possibility.

In 1935, Erwin Schrodinger proposed an analogy to show how superposition would operate in the every day world: the somewhat cruel analogy of Schrodinger's cat. Here's Schrdinger's (theoretical) experiment: We place a living cat into a steel chamber, along with a device containing hydrocyanic

acid. There is, in the chamber, a very small amount of a radioactive substance. If even a single atom of the substance decays during the test period, a relay mechanism will trip a hammer, which will, in turn, break the vial and kill the cat.

The observer cannot know whether or not an atom of the substance has decayed, and consequently, cannot know whether the vial has been broken, the hydrocyanic acid released, and the cat killed. Since we cannot know, the cat is both dead and alive according to quantum law, in a superposition of states. It is only when we break open the box and learn the condition of the cat that the superposition is lost, and the cat becomes one or the other (dead or alive)

The even coherent state $|z\rangle_e$ is a superposition of two macroscopically distinguishable coherent state and can be written as:

$$|z\rangle_e = N_e[|z\rangle + |-z\rangle], \tag{2.73}$$

where $N_e = [2(1 + \exp(-2|z|^2)]^{-1/2}$

The odd coherent state $|z\rangle_o$ is a superposition of two coherent state and can be written as:

$$|z\rangle_o = N_o[|z\rangle - |-z\rangle], \tag{2.74}$$

where $N_o = [2(1 - \exp(-2|z|^2)]^{-1/2}$ and for large number $z \quad N_e = N_o = \frac{1}{\sqrt{2}}$

They can also be created by a special displacement operator [14].

$$|z\rangle_{e,o} = D_{e,o}(z)|0\rangle = N_{e,o}[D(z) \pm D(-z)]|0\rangle. \tag{2.75}$$

Figure (2.6) displays the wave function of an even coherent state $|z\rangle_e$ where $z = i\pi$.

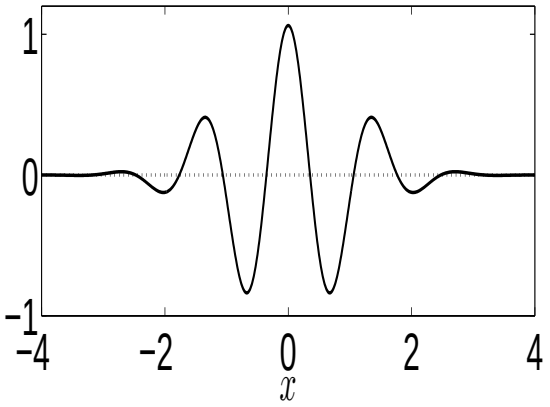

Figure 2.6: The wavefunction of the state $|i\pi\rangle_e$, the dot lines denotes to the imaginary part of its wavefunction

One can easily write the corresponding expansions for the even and odd coherent states [15].

$$|z\rangle_e = \exp\left(-\frac{|z|^2}{2}\right)\sum_{n=0}^{\infty}\frac{z^{2n}}{\sqrt{2n!}}\,|2n\rangle. \tag{2.76}$$

$$|z\rangle_o = \exp\left(-\frac{|z|^2}{2}\right)\sum_{n=0}^{\infty}\frac{z^{2n+1}}{\sqrt{(2n+1)!}}\,|2n+1\rangle. \tag{2.77}$$

The annihilation operator turns an even coherent state to an odd one (and vice versa).

$$a|z\rangle_e = z|z\rangle_o \qquad a|z\rangle_o = z|z\rangle_e. \tag{2.78}$$

The even and odd coherent states $|z\rangle_e$, $|z\rangle_o$ are orthonormalized eigen-

states of a^2 [16].

$$a^2|z\rangle_{e,o} = z^2|z\rangle_{e,o}. \tag{2.79}$$

The states $|z\rangle_e$ and $|z\rangle_o$ separately form complete sets in the Hilbert spaces of even and odd functions [15].

The even and odd coherent states and their relation to $SU(1,1)$ and $SU(2)$ Lie groups is clarified in Chapter(3).

2.2.5 Displaced number states $|z,n\rangle$

In this section we summarize various properties of the displaced number states. The displaced number states are defined as: [17]

$$|z,n\rangle = D(z)|n\rangle, \tag{2.80}$$

where $D(z)$ is the displacement operator.

For $n = 0$, the displaced number states, reduces to the well-known coherent states.

The mean number of photons for a system prepared in $|z,n\rangle$ as in [18, 19].

$$\langle n\rangle = \langle z,n|\hat{a}^\dagger\hat{a}|z,n\rangle = n + |z|^2. \tag{2.81}$$

Eq(2.81) agrees with the result of Eq(2.36) for $z = 0$ and agrees with the result of Eq(2.56) for $n = 0$.

The photon variance of $|z,n\rangle$

$$(\Delta n)^2 = \langle n^2\rangle - \langle n\rangle^2 = (2n+1)|z|^2. \tag{2.82}$$

The expectation value of the position operator $\hat{x}$ in the displaced number states $|z,n\rangle$ is

$$\langle x\rangle = \langle z,n|\hat{x}|z,n\rangle = \sqrt{2}Re(z). \tag{2.83}$$

The expectation value of the momentum operator $\hat{p}$ in the displaced number states $|z,n\rangle$ is

$$\langle p\rangle = \langle z,n|\hat{p}|z,n\rangle = \sqrt{2}Im(z) \tag{2.84}$$

The variance of $\hat{x}$ and $\hat{p}$ in the displaced number states $|z,n\rangle$

$$(\Delta x)^2 = (\Delta p)^2 = \frac{1}{2}(2n+1). \tag{2.85}$$

The second order coherence $g^{(2)}$ of $|z,n\rangle$

$$g^{(2)} = \frac{\langle n^2\rangle - \langle n\rangle}{\langle n\rangle^2} = \frac{|z|^4 + 4n|z|^2 + n^2 - n}{|z|^4 + 2n|z|^2 + n^2}. \tag{2.86}$$

Eq(2.86) agrees with the result of Eq(2.41) for $z = 0$ and agrees with the result of Eq(2.60) for $n = 0$.

The probability for finding l photons in the displaced number states $|z,n\rangle$ are given by

$$P_{|z,n\rangle}(l) = |\langle l|z,n\rangle|^2 = (\frac{n!}{l!})|z|^{2(l-n)}\exp(-|z|^2)[L_n^{l-n}(|z|^2)]^2 \quad l \geq n. \tag{2.87}$$

The photon distribution has formed two guassians in the displaced number states $|7,1\rangle$ as shown in Figure (2.7). However, when z remains as 7 and $n = 1$ three guissian are formed as shown in Figure (2.8). Similarly, when $n = 3$ which is shown in Figure (2.9) the number of guassian is 4 which

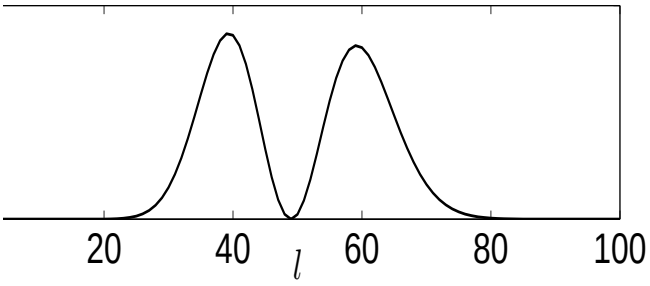

Figure 2.7: Photon distribution for the displaced number state $|7, 1\rangle$

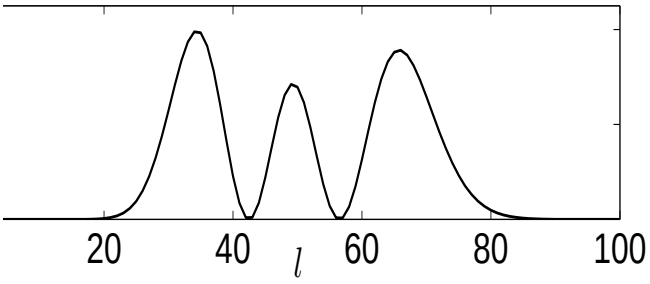

Figure 2.8: Photon distribution for the displaced number state $|7, 2\rangle$

indicates that the number of guassians depends on the value of n.

2.2.6 Squeezed states $|\xi, z\rangle$

We first define Squeezed states and then give some important properties. The squeezed state $|\xi, z\rangle$ is defined by [20].

$$|\xi, z\rangle = S(\xi)D(z)|0\rangle, \tag{2.88}$$

where $S(\xi) = \exp(\frac{1}{2}\xi a^{\dagger 2} - \frac{1}{2}\xi^* \hat{a}^2)$ is squeezing operator, and

$D(z) = \exp(z\hat{a}^\dagger - z^*\hat{a})$ is a displacement operator.

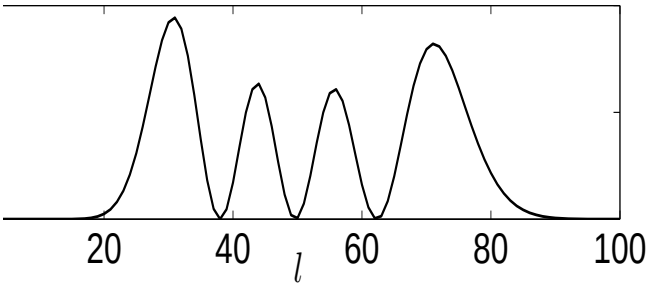

Figure 2.9: Photon distribution for the displaced number state $|7, 3\rangle$

We easily see that

$$S(\xi) = \exp(\frac{1}{2}\xi\hat{a}^{\dagger^2} - \frac{1}{2}\xi^*\hat{a}^2) = S(-\xi) = S^{-1}(\xi), \tag{2.89}$$

which indicates that operator $S(\xi)$ is a unitary operator one.

Let us assume that $\xi = r\exp(i\phi)$ and $z = s\exp(i\theta)$

the squeezing operator $S(\xi)$ satisfies:

$$S^\dagger(\xi)\hat{a}S(\xi) = \hat{a}\cosh r + \hat{a}^\dagger \exp(i\phi)\sinh r, \tag{2.90}$$

and

$$S^\dagger(\xi)\hat{a}^\dagger S(\xi) = \hat{a}^\dagger \cosh r + \hat{a}\exp(-i\phi)\sinh r. \tag{2.91}$$

It is easy to prove Eq (2.90) by using the expression:

$$\exp(hX)Y\exp(-hX) = Y + \frac{h}{1!}[X, Y] + \frac{h^2}{2!}[X, [X, Y]] + ... \tag{2.92}$$

We use this expression in Eq (2.92) with:

$$h \to r \qquad X \to (\frac{1}{2}\hat{a}^2 \exp(-i\phi) - \frac{1}{2}\hat{a}^{\dagger^2} \exp(i\phi)) \qquad Y \to \hat{a}, \tag{2.93}$$

and we get:

$$[X, Y] = [\frac{1}{2}\hat{a}^2 \exp(-i\phi) - \frac{1}{2}\hat{a}^{\dagger^2} \exp(i\phi), \hat{a}] = \exp(i\phi)\hat{a}^\dagger \tag{2.94}$$

$$[X, [X, Y]] = [\frac{1}{2}\hat{a}^2 \exp(-i\phi) - \frac{1}{2}\hat{a}^{\dagger^2} \exp(i\phi), \exp(i\phi)\hat{a}^\dagger] = \hat{a}. \tag{2.95}$$

When operator X occurs odd number of times, the result of a corresponding multiple operator will always be equal to the $\exp(i\phi)\hat{a}^\dagger$. Therefore, the general similarity expansion $S^\dagger(\xi)\hat{a}S(\xi)$ splits into two series; odd and even terms, and we get:

$$\begin{aligned} S^\dagger(\xi)\hat{a}S(\xi) &= \hat{a}(1 + \frac{r^2}{2!} + \frac{r^4}{4!} + ...) + \exp(i\phi)\hat{a}^\dagger(r + \frac{r^3}{3!} + \frac{r^5}{5!} + ...) \\ &= \hat{a}\cosh r + \hat{a}^\dagger \exp(i\phi)\sinh r \end{aligned} \tag{2.96}$$

It is clear that the coherent state is a special case of the squeezed state because:

$|0, z\rangle = S(0)D(z)|0\rangle = D(z)|0\rangle = |z\rangle$.

The squeezed state is normalized

$$\langle \xi, z | \xi, z \rangle = 1. \tag{2.97}$$

The average photon number $\langle \hat{n} \rangle$ in the squeezed state $|\xi, z\rangle$ is given by [21, 22].

$$\langle n \rangle = |z|^2 + \sinh^2 r. \tag{2.98}$$

The variance of photon number $(\Delta \hat{n})^2$ in the squeezed state $|\xi, z\rangle$ is

$$(\Delta n)^2 = |z|^2 \{\exp(-2r)\cos^2(\theta - \frac{1}{2}\phi) + \exp(2r)\sin^2(\theta - \frac{1}{2}\phi) + 2\sinh^2 r \cosh^2 r\}. \tag{2.99}$$

The expectation value of the position operator $\hat{x}$ in the squeezed state $|\xi, z\rangle$ is given by [22]:

$$\langle x \rangle = \sqrt{2} s \{\cos(\theta)\cosh r + \cos(\theta - \phi)\sinh r\}. \tag{2.100}$$

The expectation value of the momentum operator $\hat{p}$ in the squeezed state $|\xi, z\rangle$ is given by [22]:

$$\langle p \rangle = \sqrt{2} s \{\sin(\theta)\cosh r - \sin(\theta - \phi)\sinh r\}. \tag{2.101}$$

The variance of the position operator $\hat{x}$ in the squeezed state $|\xi, z\rangle$ is given by [22]:

$$(\Delta x)^2 = \frac{1}{2}\{\cosh 2r + \cos(\phi)\sinh 2r\}. \tag{2.102}$$

The variance of the momentum operator $\hat{p}$ in the squeezed state $|\xi, z\rangle$ is

given by [22]:

$$(\Delta p)^2 = \frac{1}{2}\{\cosh 2r - \cos(\phi)\sinh 2r\}. \tag{2.103}$$

The position representation of $|\xi, z\rangle$ is [22]:

$$\langle x|\xi, z\rangle = (\pi \exp(2r))^{-1/4} \exp\{\frac{\exp(-2r)}{2}[x - \langle x\rangle]^2 + i\langle p\rangle x\}. \tag{2.104}$$

2.2.7 The time evolution of squeezed state $|\xi, z\rangle$

The time evolution of a minimum uncertainty state under the harmonic oscillator is given by:

$$|\xi, z\rangle_t = \exp(-iHt)|\xi, z\rangle = \exp(-it(\hat{a}^\dagger a + 1/2))|\xi, z\rangle. \tag{2.105}$$

For simplicity we take ξ to be a real number.

The expectation value of $\hat{x}$ in $|\xi, z\rangle$ at time $t \geq 0$ is:

$$\langle x\rangle_t = \sqrt{2}s\{cos(\theta - t)\cosh\xi + cos(\theta + t)\sinh\xi\}. \tag{2.106}$$

The expectation value of $\hat{p}$ in $|\xi, z\rangle$ at time $t \geq 0$ is:

$$\langle p\rangle_t = \sqrt{2}s\{\sin(\theta - t)\cosh\xi - \sin(\theta + t)\sinh\xi\}. \tag{2.107}$$

The variance of $\hat{x}$ in $|r, z\rangle$ at time $t \geq 0$ is:

$$(\Delta x)_t^2 = \frac{1}{2}\{\cosh 2r + \cos(2t)\sinh 2\xi\}. \tag{2.108}$$

Figure (2.10) shows the expectation value of $\langle x\rangle_t$ and $\langle p\rangle_t$ for th squeezed state $|1, \exp(\frac{i\pi}{4})\rangle$. However, Figure (2.11) shows the product of the variance of $\hat{x}$ and $\hat{p}$ at time t.

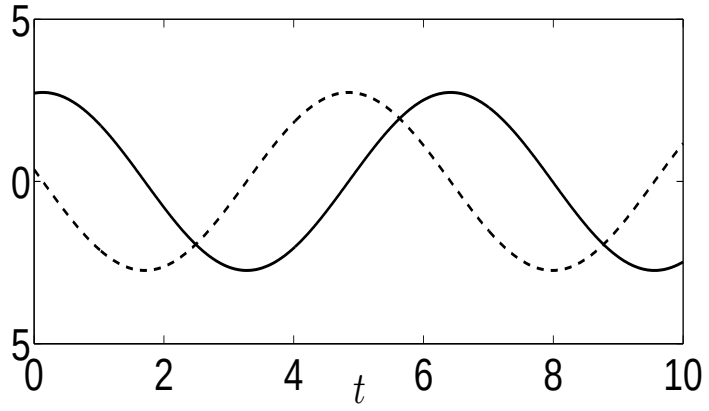

Figure 2.10: The expectation value of position and momentum $\langle x\rangle_t$ and $\langle p\rangle_t$ for the squeezed state $|\xi, z\rangle$ as a function of time t where $\xi = 1$ and $z = \exp(i\pi/4)$. The continuous line denotes to $\langle x\rangle_t$ and the cut lines denote to $\langle p\rangle_t$

The variance of $\hat{p}$ in $|\xi, z\rangle$ at time $t \geq 0$ is

$$(\Delta p)_t^2 = \frac{1}{2}\{\cosh 2\xi - \cos(2t)\sinh 2\xi\}. \tag{2.109}$$

2.3 Q-function of the quantum state $|\psi\rangle$

The expectation value of the density with respect to the coherent state $|z\rangle$, $z = x + iy$ is called the Q-function, or Husimi function [23, 24, 25, 26],

i.e $\quad Q(z) = Q(x, y) = \frac{1}{\pi}\langle z|\rho|z\rangle$

where $\quad \rho = |\psi\rangle\langle\psi|$

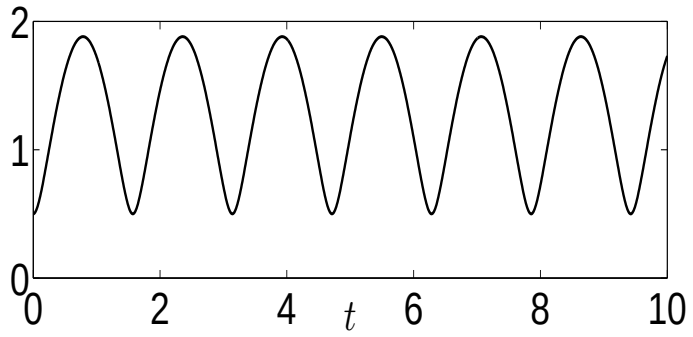

Figure 2.11: The plot of $(\Delta x)_t(\Delta p)_t$ for the squeezed state $|\xi, z\rangle$ at time $t \geq 0$ where $\xi = 1$ and $z = \exp(i\pi/4)$

2.3.1 The Q-function of the number state $|n\rangle$ and its zeros

The Q-function of the number states $|n\rangle$ is defined as:

$$Q_{|n\rangle}(z) = \frac{1}{\pi}\langle z|\rho|z\rangle = \frac{|z|^{2n}}{\pi(n!)}\exp(-|z|^2), \tag{2.110}$$

where $\rho = |n\rangle\langle n|$.

The Q-function $Q_{|n\rangle}(z) = 0$ if and only if $z^n = 0$.

It is very clear that Q-function of the ground state does not have zeros since $z^0 = 1 \neq 0$

Both figures (2.12) and (2.13) show the Q-function of two different states, the number state $|3\rangle$ and the coherent state $|2 - i\rangle$ respectively.

The Q-function of the superposition of two number states

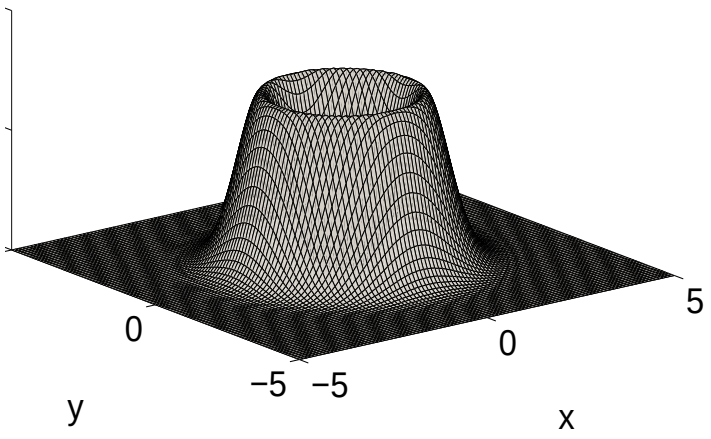

Figure 2.12: The Q-function of the number state $|3\rangle$

$|s\rangle = \frac{1}{\sqrt{2}}[|n_1\rangle + |n_2\rangle]$

$$Q_{|s\rangle}(z) = \frac{1}{2\pi}(\langle z|n_1\rangle\langle n_1|z\rangle + \langle z|n_2\rangle\langle n_2|z\rangle + \langle z|n_1\rangle\langle n_2|z\rangle + \langle z|n_2\rangle\langle n_1|z\rangle), \tag{2.111}$$

where

$$\langle z|n_i\rangle\langle n_j|z\rangle = \frac{1}{\pi}\frac{z^{n_i}z^{n_j}}{\sqrt{n_i!n_j!}}\exp(-|z|^2) \tag{2.112}$$

$$Q_{|s\rangle}(z) = \frac{1}{2\pi}\exp(-|z|^2)[\frac{|z|^{2n_1}}{n_1!} + \frac{|z|^{2n_2}}{n_2!} + \frac{(z^*)^{n_1}z^{n_2}}{\sqrt{n_1!n_2!}} + \frac{(z^*)^{n_2}z^{n_1}}{\sqrt{n_1!n_2!}}] \tag{2.113}$$

Notice that the Q-function $Q_{|n\rangle}(z) = 0$ iff

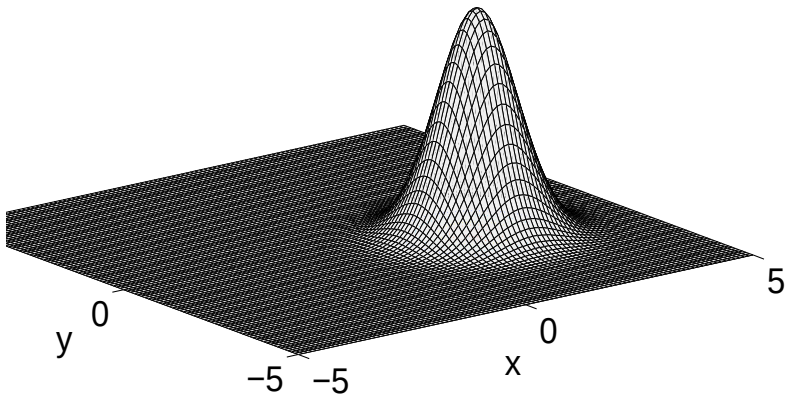

Figure 2.13: The Q-function of coherent state $|2-i\rangle$

$$\sum_{i=1}^{2}\sum_{j=1}^{2}\frac{(z^*)^{n_i}z^{n_j}}{\sqrt{n_i!n_j!}}=0, \tag{2.114}$$

and

$$\frac{r^{2n_1}}{n_1!}+\frac{r^{2n_2}}{n_2!}+2\frac{r^{n_1+n_2}}{\sqrt{n_i!n_j!}}\cos(n_i-n_j)\theta=0 \tag{2.115}$$

The Q-function of the coherent state $|\beta\rangle$ is:

$$Q_{|\beta\rangle}(z)=\frac{1}{\pi}\langle z|\rho|z\rangle=\frac{1}{\pi}exp(-|z-\beta|^2), \tag{2.116}$$

where $\rho=|\psi\rangle\langle\psi|$ and $Q_{|\psi\rangle}(z)>0$ for any complex number z .

The Q-function of coherent state always has a gaussian shape. As shown in figure 2.13 with coherent state $|2-i\rangle$.

Q-function of superposition of two coherent states

Let $|\beta\rangle$ be a superposition of two coherent states $|\beta_1\rangle$ and $|\beta_2\rangle$ i.e

$|\beta\rangle = N[|\beta_1\rangle + |\beta_2\rangle]$,

where N=$[2 + \langle\beta_1|\beta_2\rangle + \langle\beta_2|\beta_1\rangle]^{-1/2}$ and

$\langle\beta_i|\beta_j\rangle = \exp(-\frac{1}{2}[|\beta_i|^2 + |\beta_j|^2] + \beta_i^*\beta_j)$

The Q-function of $|\beta\rangle$ can be written as follows:

$$Q_{|\beta\rangle}(z) = \frac{N^2}{\pi}\sum_{i=1}^{2}\sum_{j=1}^{2}\exp(-|z|^2 - \frac{|\beta_i|^2}{2} - \frac{|\beta_j|^2}{2} + z^*\beta_i + \beta_j^* z). \qquad (2.117)$$

2.3.2 Examples of Q-function of the quantum states and their zeros

Example(1)

The Q-function of the superposition two number states $|s\rangle = \frac{1}{\sqrt{2}}[|0\rangle + |1\rangle]$ is:

$Q_{|s\rangle}(z) = \frac{1}{2\pi}\exp(-|z|^2)[1 + 2Re(z) + |z|^2]$

and it has only one zero $z = -1$ with multiplicity 2

Figure 2.14 and 2.15 show the Q-functions for the superposition of two number states namely $|0\rangle$, $|1\rangle$ and $|1\rangle$, $|2\rangle$ respectively. Their shapes are not gaussian due to the presence of the roots; in chapter 5 we will study the link between the roots of any Q-function and the negative region of its Wigner function.

Example(2)

The Q-function of the superposition of two number states $|s\rangle = \frac{1}{\sqrt{2}}[|1\rangle + |2\rangle]$ is:

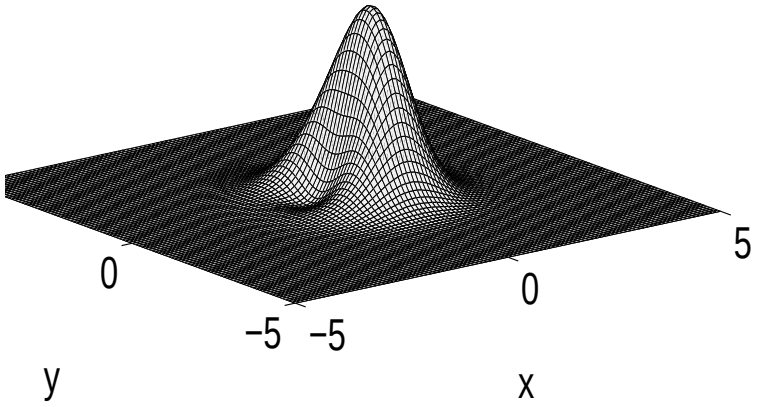

Figure 2.14: The Q-function of superposition of the number state$|0\rangle$ and the number state $|1\rangle$

$Q_{|s\rangle}(z) = \frac{1}{2\pi}\exp(-|z|^2)(\frac{|z|^2}{1!} + \frac{|z|^4}{2} + \frac{(z^*)^1 z^2}{\sqrt{2}} + \frac{(z^*)^2 z^1}{\sqrt{2}})$

and it has only two zeros $z = 0$ and $z = -\sqrt{2}$ with multiplicity 2

Both figures (2.16) and (2.17) show the Q-function of two different even coherent states $|3i\rangle_e$ and $|3 + 3i\rangle_e$ respectively.

2.4 Wigner and Weyl functions

The Wigner-Weyl function provides a deeper insight into the properties of a quantum state that cannot be easily seen from the wavefunction (either

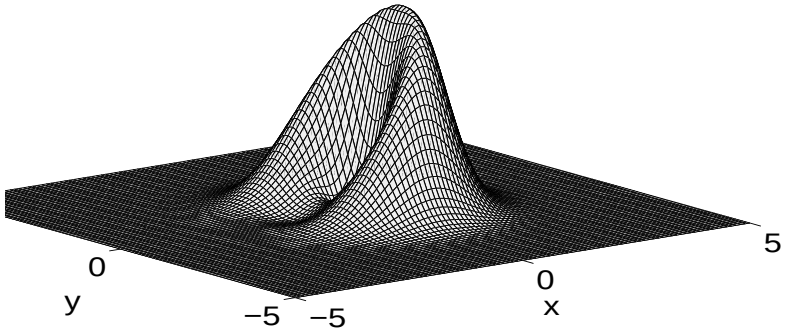

Figure 2.15: The Q-function of superposition of the number state$|1\rangle$ and the number state $|2\rangle$

in x or in p-representation). The Wigner function shows that the position and momentum of the particle in a way are consistent with the uncertainty principle, while the Weyl function shows quantum correlation.

The Wigner function $W(x,p)$ of a quantum state is described by a density matrix ρ and is defined by [27, 28]

$$W(x,p) = \frac{1}{2\pi}\int_{-\infty}^{\infty}\exp(ipX)\langle x - X/2|\rho|x + X/2\rangle dX \qquad (2.118)$$

$$W(x,p) = \frac{1}{2\pi}\int_{-\infty}^{\infty}\exp(-iPx)\langle p - P/2|\rho|p + P/2\rangle dP \qquad (2.119)$$

The probability $P(x)$ for finding the particle at x in phase space is

$$P(x) = \int_{-\infty}^{\infty} W(x,p)dp = \langle x|\rho|x\rangle \qquad (2.120)$$

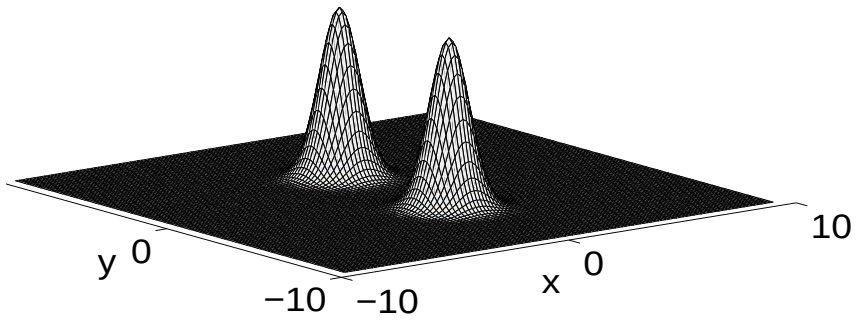

Figure 2.16: The Q-function of the even coherent state $|3i\rangle_e$

The probability $P(p)$ for finding the particle at p in phase space is

$$P(p) = \int_{-\infty}^{\infty} W(x,p)dx = \langle p|\rho|p\rangle \tag{2.121}$$

The Wigner function $W(x,p)$ is real, but it can be negative. Hence , it can not be regarded as a probability distribution. Eqs (2.120), (2.121) are the marginal properties of the Wigner function and they are important in the interpretation of the Wigner function as a pseudo-probability function. The negative regions of a Wigner function indicate the non-classical nature of a quantum state. Later we link the negative region of the Wigner function with the zeros of Bargmann function.

The Wigner function satisfies the following:

$$\int_{-\infty}^{\infty}\int_{-\infty}^{\infty} W(x,p)dxdp = 1 \tag{2.122}$$

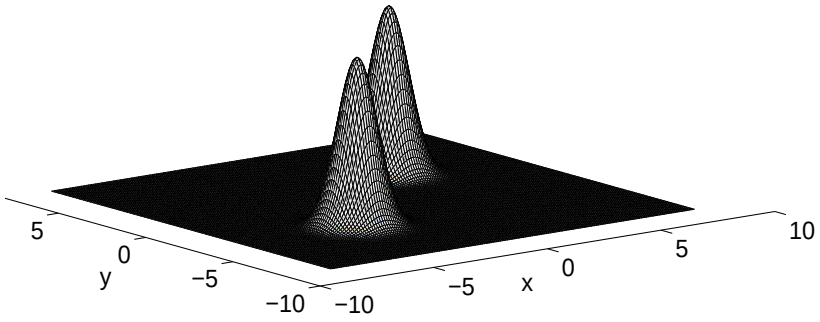

Figure 2.17: The Q-function of the even coherent state $|3+3i\rangle_e$

The Wigner function of any state $|\psi\rangle$ can be obtained by substitute the wave function of the state $|\psi\rangle$ into Eq (2.118)

The Wigner function of the number state $|n\rangle$ has the form [29, 30].

$$W_{|n\rangle}(x,p) = \frac{(-1)^n}{\pi}\exp(-x^2-p^2)L_n(2x^2+2p^2)) \tag{2.123}$$

where

$$L_n(x) = \frac{\exp(x)}{n!}\frac{d^n}{dx^n}(x^n\exp(-x)) \tag{2.124}$$

is the Laguerre polynomial of the order n.

The Wigner function of a number states has negative parts.

The Wigner function of the state $|s\rangle = \frac{1}{\sqrt{2}}[|m\rangle + |n\rangle]$.

$$W_{|s\rangle}(x,p) = \frac{1}{2}[W_{|n\rangle}(x,p) + W_{|m\rangle}(x,p) + W_{mn}(x,p) + W_{mn}(x,p)] \tag{2.125}$$

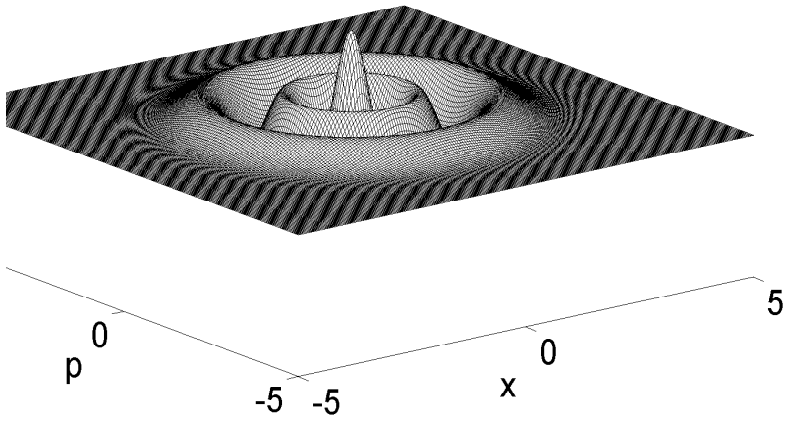

Figure 2.18: The Wigner function of number state $|4\rangle$

where $|m\rangle$ and $|n\rangle$ are number states and $W_{mn}(x,p)$ is defined as [31]:

$$W_{mn}(x,p) = \frac{(-1)^n}{\pi}\sqrt{\frac{n!}{m!}}(\sqrt{2}[x+ip])^{m-n}\exp(-x^2-p^2)L_n^{m-n}(2x^2+2p^2) \tag{2.126}$$

where $L_n^a(x)$ is a generalized Laguerre polynomial and can be defined as: [32]:

$$L_n^a(x) = \frac{x^{-a}\exp(x)}{n!}\frac{d^n}{dx^n}(x^{n+a}\exp(-x)) \tag{2.127}$$

The Wigner function of a coherent state $|z\rangle$ has the form [30]:

$$W_{|z\rangle}(x,p) = \frac{1}{\pi}\exp\{-[x-\sqrt{2}Re(z)]^2 - [p-\sqrt{2}Im(z)]^2\} \tag{2.128}$$

The Wigner function of an even coherent $|z\rangle_e$ and an odd state $|z\rangle_o$ have the form:

$$W_{|z\rangle_{e,o}}(x,p) = W_{|0\rangle}(\dot{x},\dot{p}) + W_{|0\rangle}(\ddot{x},\ddot{p}) \pm 2W_{|0\rangle}(x,p)\cos(4zIm(z)) \tag{2.129}$$

Where

$W_{|0\rangle}(x,p)$ is the Wigner function of ground state $|0\rangle$

$\dot{x} = x - Re(z), \quad \dot{p} = p - Im(z), \quad \ddot{x} = x + Re(z), \quad \ddot{p} = p + Im(z)$

Both figures (2.18) and (2.19) show the Wigner function of two different states, the number state $|4\rangle$ and the even coherent state $|3\rangle_e$ respectively.

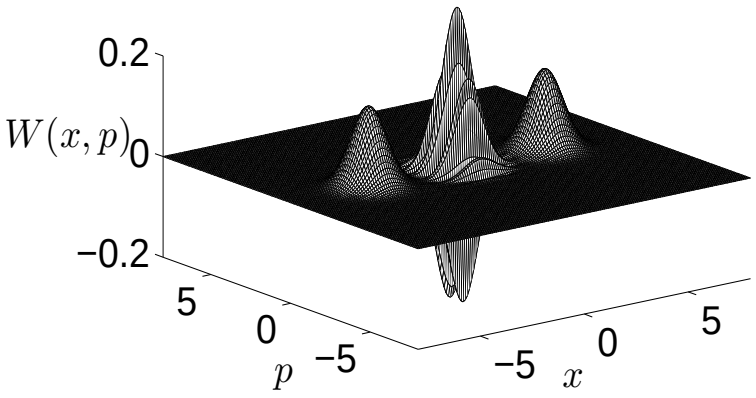

Figure 2.19: the plot of Wigner function for the even coherent state $|3\rangle_e$

The Wigner function of a squeezed state $|\xi, z\rangle$ has the form [27, 30]:

$$W_{|\xi,z\rangle}(x,p) = \frac{1}{\pi}\exp\{U+V\} \tag{2.130}$$

where

$$U = -\exp(2r)[(x-\sqrt{2}s\sin(\theta))\cos(\frac{\phi}{2}) + (p-\sqrt{2}s\cos(\theta))\sin(\frac{\phi}{2})]^2 \tag{2.131}$$

$$V = -\exp(-2r)[(x-\sqrt{2}s\sin(\theta))\sin(\frac{\phi}{2}) + (p-\sqrt{2}s\cos(\theta))\cos(\frac{\phi}{2})]^2 \tag{2.132}$$

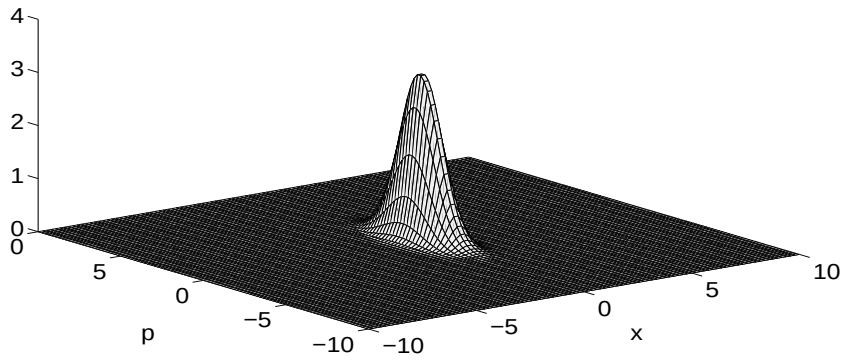

Figure 2.20: Wigner function of $|\xi, z\rangle$; $\xi = \frac{1}{2}$ and $z = \frac{1}{2}\exp(i\frac{\pi}{4})$

The Weyl function $\tilde{W}(X,P)$ that corresponds to a quantum state described by a density operator ρ is defined by:

$$\tilde{W}(X,P) = \frac{1}{2\pi}\int_{-\infty}^{\infty} \exp(iPx)\langle x - X/2|\rho|x + X/2\rangle dX \quad (2.133)$$

$$\tilde{W}(X,P) = \frac{1}{2\pi}\int_{-\infty}^{\infty} \exp(-ipX)\langle p - P/2|\rho|p + P/2\rangle dP \quad (2.134)$$

The Weyl function $\tilde{W}(X,P)$ is the two dimensional Fourier transform of the Wigner function $W(x,p)$, where X and P denotes to increments in position and momentum respectively [31] .

The Weyl function $\tilde{W}(X,P)$ is a complex function, in general, whose absolute value obeys $0 \leq |\tilde{W}(X,P)| \leq 1$.

A more detailed discussion and review of Wigner and Weyl functions, and their relationships can be found in the literature [33, 34].

In figures (2.21) and (2.22) the Wingner function of superposition of the number states $|0\rangle$ and $|1\rangle$ and its contour are shown. Similarly, the Wigner finction of superposition of the number states of $|1\rangle$ and $|2\rangle$ and its contour are shown in figures (2.23) and (2.24).

The Weyl function of the number states $|n\rangle$ has the form:

$$\tilde{W}(X,P) = \exp(\frac{-X^2 - P^2}{4})L_n\frac{(X^2 + P^2)}{2}) \quad (2.135)$$

The Weyl function of the coherent state $|z\rangle$ has the form:

$$\tilde{W}(X,P) = \exp(-(\frac{X}{2} + \sqrt{2}iIm(z))^2 - (\frac{P}{2} + \sqrt{2}iRe(z))^2 - 2|z|^2) \quad (2.136)$$

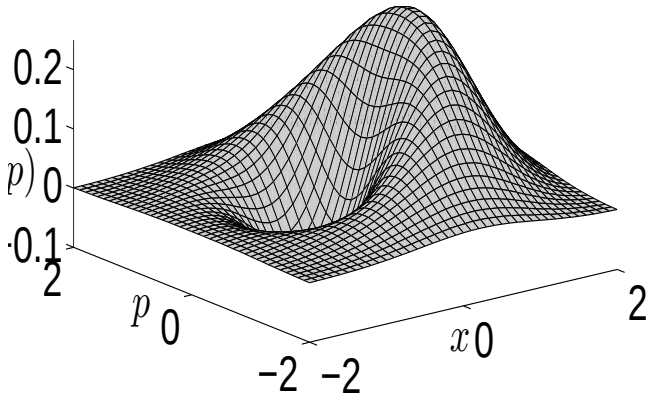

Figure 2.21: The Wigner function of the state $|s\rangle = \frac{1}{\sqrt{2}}(|0\rangle + |1\rangle)$

The Weyl function of the squeezed state $|\xi, z\rangle$ has the form:

$$\tilde{W}_{|\xi,z\rangle}(X,P) = \exp[-i(A) - \frac{1}{4}(B) - \frac{1}{4}(C)] \tag{2.137}$$

where

$$A = \sqrt{2}Xs\cos(\theta) - \sqrt{2}Ps\sin(\theta), \tag{2.138}$$

$$B = (X\cos(\frac{\phi}{2}) + P\sin(\frac{\phi}{2}))^2\exp(2r), \tag{2.139}$$

$$C = (X\sin(\frac{\phi}{2}) + P\cos(\frac{\phi}{2}))^2\exp(-2r), \tag{2.140}$$

and $z = s\exp(i\theta) \quad \xi = r\exp(i\phi)$

2.5 Bargmann Analytic Representation

The theory of analytic functions has played an important role in quantum mechanics. There are several representations which are using analytic func-

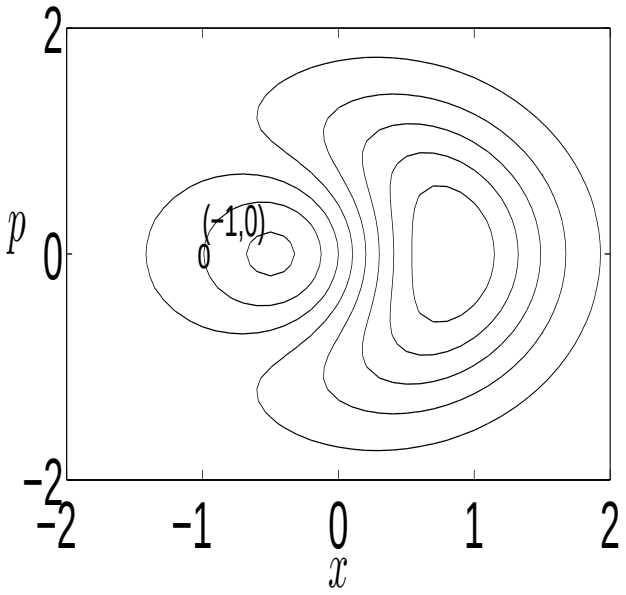

Figure 2.22: The contour of the Wigner function for $|s\rangle = \frac{1}{\sqrt{2}}(|0\rangle + |1\rangle)$.The Q-Function of the state $|s\rangle = \frac{1}{\sqrt{2}}(|0\rangle + |1\rangle)$ has only one zero $(-1, 0)$, and its Wigner function at $(0, 0)$ is zero as shown

tions. The Bargmann representation is the most well-known one, and uses analytic functions in the complex plane (Euclideangeometry). The Bargmann representation will be used in chapter 5 and chapter 6 to describe our new generalized coherent states.

Let $|f\rangle$ be any arbitrary state:

$$|f\rangle = \sum_{n=0}^{\infty} f_n |n\rangle; \qquad \sum_{n=0}^{\infty} |f_n|^2 = 1 \tag{2.141}$$

The conjugate of $|f\rangle$ is $\langle f|$ and can be written as:

$$\langle f| = \sum_{n=0}^{\infty} f_n^* \langle n| \tag{2.142}$$

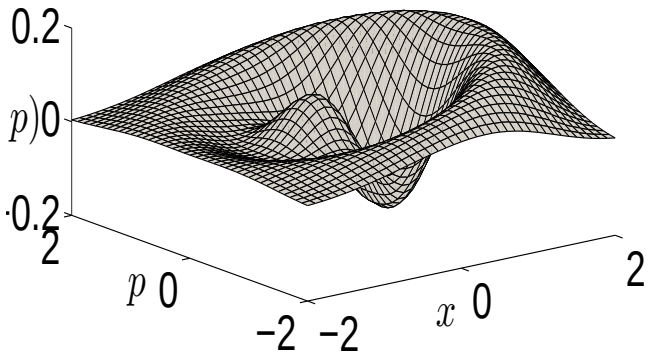

Figure 2.23: The Wigner function for $|s\rangle = \frac{1}{\sqrt{2}}(|1\rangle + |2\rangle)$

The Bargmann representation for the state $|f\rangle$ is:

$$f(z) = \exp(\frac{1}{2}|z|^2)\langle z^*|f\rangle \tag{2.143}$$

$$= \exp(\frac{1}{2}|z|^2)\langle f^*|z\rangle \tag{2.144}$$

$$= \sum_{n=0}^{\infty} \frac{f_n z^n}{\sqrt{n!}} \tag{2.145}$$

The Bargmann function $f(z)$ is analytic in the complex plane $\mathbb{C}$

The Bargmann representation for the creation operator $\hat{a}^\dagger$ and annihilation operator $\hat{a}$ are given by:

$$\hat{a}^\dagger \to z \tag{2.146}$$

$$\hat{a} \to \frac{d}{dz} \tag{2.147}$$

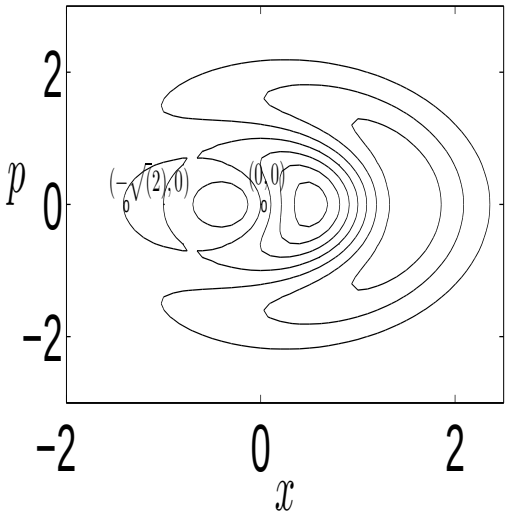

Figure 2.24: The contour of the Wigner function for $|s\rangle = \frac{1}{\sqrt{2}}(|1\rangle + |2\rangle)$,The Q-Function of the state $|s\rangle = \frac{1}{\sqrt{2}}(|1\rangle + |2\rangle)$ has two zeros $(0,0)$ and $(-\sqrt{2},0)$, and its Wigner function at these zeros is zero as shown

The Bargmann representation for the number states $|n\rangle$ is:

$$f(z) = \frac{z^n}{\sqrt{n!}} \tag{2.148}$$

The Bargmann representation for the coherent state $|\alpha\rangle$ is:

$$f(z) = \exp(\alpha z - \frac{1}{2}|\alpha|^2) \tag{2.149}$$

The Bargmann representation for the squeezed state $|\xi, \alpha\rangle$ is:

$$f(z) = (\cosh r)^{-1/2} \exp(-\frac{\mu}{2}z^2 + (\alpha^*\mu + \alpha)z - \frac{1}{2}|\alpha|^2) \tag{2.150}$$

where $\mu = \exp(i\phi)\tanh r$.

The inner product of two Bargmann analytic functions $f(z)$ and $g(z)$ are defined as:

$$\langle f|g\rangle = \frac{1}{\pi}\int\int_{\mathbb{C}} f^*(z)g(z)\exp(-|z|^2)dz \tag{2.151}$$

2.5.1 The growth of Bargmann analytic functions

The growth of analytic function $f(z)$ is defined by its order $\rho \geq 0$ and its type $\sigma \geq 0$ which are defined as: [35, 36]

$$\rho = \limsup_{R\to\infty} \frac{\ln\ln M(R)}{\ln R}, \tag{2.152}$$

$$\sigma = \limsup_{R\to\infty} \frac{\ln M(R)}{R^\rho}, \tag{2.153}$$

where $M(R)$ is the maximum value of $|f(z)|$ on the circle $|z| = R$

The function $f(z)$ has minimal type means $\sigma = 0$.

The function $f(z)$ has normal type means $0 < \sigma < \infty$.

The function $f(z)$ has maximal type means $\sigma = \infty$.

A function with growth (ρ, σ) has smaller growth than (ρ_1, σ_1) if $\rho < \rho_1$ or if both $\rho = \rho_1$ and $\sigma < \sigma_1$.

The growth is used below to study the convergence of the scalar product of Eq (2.151)

2.5.2 The relation between the wave function $f(x) = \langle x|f\rangle$ and its Bargmann fuction $f(z)$

The Bargmann function $f(z)$ is related to its wave function $f(x)$ as [37]

$$f(\frac{x}{\sqrt{2}}) = \frac{1}{\sqrt{2}\sqrt[4]{\pi^3}} \exp(-\frac{x^2}{4}) \int dy f(z) \exp(-\frac{y^2}{2}) \tag{2.154}$$

$$f(z) = \frac{1}{\sqrt[4]{\pi}} \int dx f(x) \exp(-\frac{x^2}{2} + \sqrt{2}zx - \frac{z^2}{2}) \tag{2.155}$$

The Bargmann function of the number states $|n\rangle$ is:

$$|n\rangle \rightarrow \langle z|n\rangle \rightarrow f(z) = \frac{z^n}{\sqrt{n!}} \tag{2.156}$$

and has order $\rho = 0$.

The Bargmann function of the coherent state $|\alpha\rangle$ is:

$$|\alpha\rangle \ \rightarrow \langle z|\alpha\rangle \rightarrow f(z) = \exp(\alpha z - \frac{|\alpha|^2}{2}) \tag{2.157}$$

which is of order order $\rho = 1$ and type $\sigma = |\alpha|$.

2.6 Convergence of scalar product of Bargmann functions

We consider the Bargmann function $g(z)$ whose growth can be given as (ρ, σ) where $\rho \geq 0$ and $\sigma \geq 0$.

The Bargmann function $g(z)$ is convergent in the following cases:

Case 1 The order $\rho < 2$ and the type $\sigma > 0$

Case 2 The order $\rho = 2$ and the type $\sigma < 1/2$

Any entire Bargmann function can be expanded as:

$$g(z) = \sum_{n=0}^{\infty} g_n z^n \tag{2.158}$$

The corresponding normalized Bargmann function of $g(z)$ is:

$H(z) = [M]^{-1/2} g(z)$ where

$$M = \int_{\mathbb{C}} \int |g(z)|^2 \exp(-|z|^2) d\mu(z), \qquad d\mu(z) = \frac{1}{\pi} dz \tag{2.159}$$

assuming that $g(z)$ exists

The Bargmann function $g(Az)$ exists (where A is a complex number)in the following cases:

Case 1:

The Bargmann function $g(Az)$ is convergent $\forall A \in \mathbb{C}$, when the order $\rho < 2$.

Case 2:

The Bargmann function $g(Az)$ is convergent for $\ni |A| \leq 1$; when the order $\rho \leq 2$ and the type $\sigma = 1/2$

The entire Bargmann function $g(Az)$ can be expanded as

$$g(Az) = \sum_{n=0}^{\infty} g_n (Az)^n = \sum_{n=0}^{\infty} g_n A^n z^n \tag{2.160}$$

The corresponding normalized Bargmann function of $g(Az)$ is

$H(Az) = [M(A)]^{-1/2} g(Az)$ where

$$M(A) = \int_{\mathbb{C}} \int |g(Az)|^2 \exp(-|z|^2) d\mu(z) \tag{2.161}$$

2.6.1 Examples for Convergence of Bargmann function

Example 1

The Bargmann function $f(z)$ of the number states $|n\rangle$ is convergent since the order $\rho = 0$.

Example 2

The Bargmann function $f(z)$ of the coherent state $|A\rangle$ is convergent since the order $\rho = 1$.

2.6.2 $\mathfrak{B}$ and $\mathfrak{B}_s$ Bargmann functions spaces

Let $\mathfrak{B}$ be the set of all Bargmann functions with order $\rho < 2$ or $\rho = 2$ and type $\sigma < \frac{1}{2}$, and $\mathfrak{B}_s$ be a sub set of $\mathfrak{B}$ with order $\rho < 2$.

If a Bargmann fuction $g(z)$ belongs to $\mathfrak{B}_s$ then for any complex number A, $g(Az)$ is also in $\mathfrak{B}_s$

The Bargmann function of the coherent state $|A\rangle$ is

$$f(z) = \exp(Az - \frac{|A|^2}{2}) \tag{2.162}$$

It has growth with $\rho = 1$,$\sigma = |A|$ and therefore it belongs to $\mathfrak{B}_s$

The Bargmann function of the squeezed state $|A, r, \phi\rangle$ is

$$f(z) = (1 - |A|^2)^{1/4} \exp(\frac{1}{2}Az^2 + \beta z + \gamma) \tag{2.163}$$

$\alpha = -\tanh(\frac{r}{2}) \exp(-i\phi)$, $\beta = A(1 - |\alpha|^2)^{1/2}$, and $\gamma = -\frac{1}{2}\alpha^* A^2 - \frac{1}{2}|A|^2$

It has growth with $\rho = 2$ and therefore it does not belong to $\mathfrak{B}_s$

An example of a state whose Bargmann function has growth with a given order ρ and given type σ (which may or may not be integers) is

$$|\rho, \sigma\rangle = \Sigma_{n=0}^{\infty} f_n |n\rangle; f_n = N \frac{\exp(in\theta)\sigma^{n/\rho}(n!)^{1/2}}{\Gamma(\frac{n}{\rho} + 1)} \tag{2.164}$$

where N is the normalization constant

$$N = \sqrt{\sum_{n=0}^{\infty} \frac{\sigma^{2n/\rho}(n!)}{\Gamma(\frac{n}{\rho} + 1)}} \tag{2.165}$$

N is finite when $0 \leq \rho < 1/2$; and also when $\rho = 2$ and $\sigma < 1/2$. The Bargmann function of this state is $NE_{1/\rho}(\exp(i\theta)\sigma^{1/\rho} z)$ where $E(\zeta)$ is the **Mittage-Leffler** function [38].

2.6.3 Zeros of the Bargmann function and the negative regions of the Wigner function

Let $F_A(x) = \langle x|A\rangle_{gcoh}$ be the wavefunction of the generalized of the coherent states $|A\rangle_{gcoh}$. The corresponding Wigner function is defined as:

$$W_A(z, z^*) = \int dq F_A(2^{1/2} Re(z) + q)[F_A(2^{1/2} Re(z) - q)]^* \exp(-i2^{1/2} Im(z) q) \tag{2.166}$$

and it is normalized as:

$$2\int d\mu(z)W_A(z,z^*)=1 \tag{2.167}$$

The Q-function (or Husmi function is given in terms of the Bargmann function as:

$$Q_A(z,z^*)=|g(Az)|^2\exp(-|z|^2) \tag{2.168}$$

Therefore the zeros of the Q-function are the zeros of the Bargmann function, with double multiplicity.

The Wigner function is related to Q-function as follows:

$$Q_A(z,z^*)=2\int_{\mathbb{C}}\int d\mu(\xi)\exp(-2|z-\xi|^2)W_A(\xi,\xi^*) \tag{2.169}$$

If z_0 is a zero of the Bargmann function, then $Q_A(z_0,z_0^*)=0$ and therefore:

$$\int_{\mathbb{C}} d\mu(\xi)\exp(-2|z_0-\xi|^2)W_A(\xi,\xi^*)=0 \tag{2.170}$$

The fact that the integral is equal to zero, implies that the $W_A(\xi,\xi^*)$ takes both positive and negative values near the point z_0. Therefore the Wigner function takes negative values close to the zeros of the Bargmann function. If the Bargmann has many zeros, the corresponding Wigner function has many islands with negative values near these zeros. We note that negative values of the Wigner function indicate nonclassical states.

2.6.4 Zeros of Bargmann function of the state $|s\rangle$ and its motion

In this section we consider a system with a Hamiltonian H, which at $t = 0$ is in some initial state. We study the time evolution of this state, and the motion of the zeros of its Bargmann function. We assume that at time $t = 0$ the system is on the state $|s\rangle$. and its Bargmann function $g(z)$ with zeros $\omega_n\}$. At time t the system is in the state $|s,t\rangle = \exp(iHt)|s,\rangle$ and has Bargmann function $g(z,t)$ with zeros $\{\omega_n(t)\}$. The number of zeros corresponding to $|s,t\rangle$ may change as a function of time. This is obvious from the fact that any two states can be related with a unitary transformation [39].

Example(1):

Let $|s\rangle$ be a superposition of two number states $|1\rangle$ and $|2\rangle$. The Bargmann function of this state has zeros at $\{\omega_0 = 0, \omega_1 = -\sqrt{2}\}$ and its motion can be shown in fig 2.25 and fig 2.26 according to $H = \hat{a}^\dagger\hat{a} + \hat{a}^\dagger + \hat{a}$ and $H = (\hat{a}^\dagger\hat{a})^2$ respectively. The zero $\omega_0 = 0$ corresponding to $|s,t\rangle$ changes as a function of time according to $H = \hat{a}^\dagger\hat{a} + \hat{a}^\dagger + \hat{a}$ and does not change according to $H = (\hat{a}^\dagger\hat{a})^2$.

Example(2):

Let $|s\rangle$ be a superposition of two number states $|1\rangle$ and $|3\rangle$. The Bargmann function of this state has zeros at $\{\omega_0 = 0, \quad \omega_1 = -\sqrt[4]{6}i, \quad \omega_2 = \sqrt[4]{6}i\}$ and its motion can be shown in fig 2.27 and fig 2.28 according to $H = (\hat{a}^\dagger\hat{a})$ $H = (\hat{a}^\dagger\hat{a})^2 + \hat{a}^\dagger + \hat{a}$ respectively.

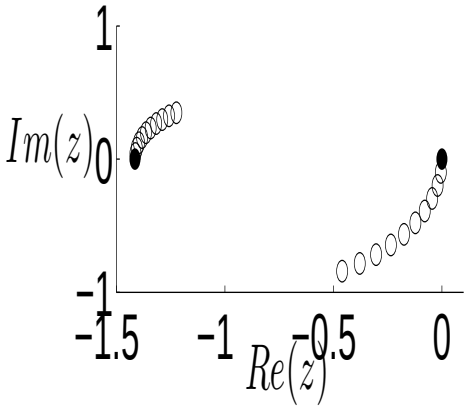

Figure 2.25: The time evolution of the zeros of the Bargmann function of the state $|s\rangle$, at time $t = [0 : .1 : 1]$.

2.7 Summary

In this chapter, we undertook a review of the phase space methods for the quantum particles on a real line $\Re$, and the basic formalisms of this phase space were introduced. Some special states such as number states, coherent states and squeezed states were studied, and the most popular functions used in phase space. The Wigner and Weyl function were described. The Bargmann analytic representation in the complex plane, which was defined by the Glauber coherent states, was also considered. In the next chapter we will study in more detail known classes of coherent states and in chapter four we will introduce our own generalization of coherent states.

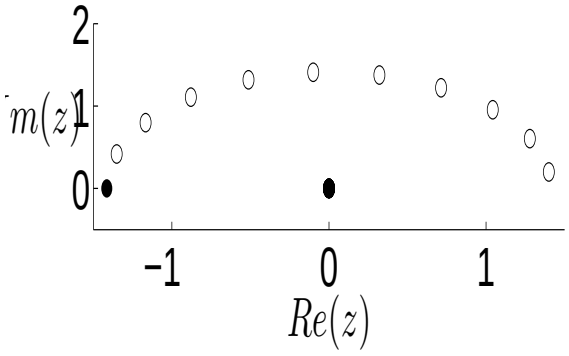

Figure 2.26: The time evolution of the zeros of the Bargmann function of the state $|s\rangle$, at time $t = [0 : .1 : 1]$.

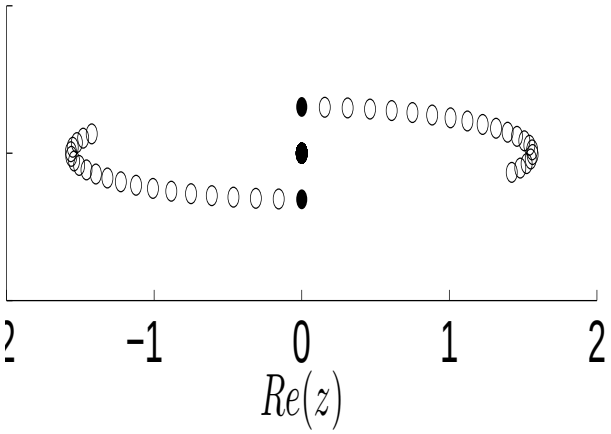

Figure 2.27: The time evolution of the zeros of the Bargmann function of the state $|s\rangle$, at time $t = [0 : .1 : 2]$.

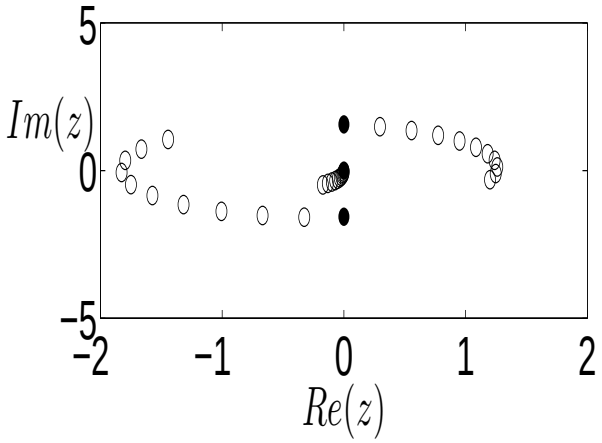

Figure 2.28: The time evolution of the zeros of the Bargmann function of the state $|s\rangle$, at time $t = [0 : .05 : .5]$.

Chapter 3

Generalized coherent states

3.1 Introduction

The subject of generalized coherent states has been addressed by many researchers in different contexts. In this chapter we introduce the concept of generalized coherent states by a new perception.

3.1.1 Group definition and $SU(1,1)$ Lie group

Group definition. A group $(G, *)$ is a set G together with a binary operation $*$ on G such that:

1- $g_1 * g_2 \in G$ for any $g_1, g_2 \in G$.

2- $(g_1 * g_2) * g_3 = g_1 * (g_2 * g_3)$ for any $g_1, g_2, g_3 \in G$.

3- There is an element $e \in G$ such that $e*g = g = g*e$ called an **identity** for any $g \in G$.

4- For any $g \in G$ there exists $g^{-1} \in G$ called **inverse** of g such that $g * g^{-1} = g^{-1} * g = e$.

The group G is said to be abelian if $g_1 * g_2 = g_2 * g_1$ for all $g_1, g_2 \in G$

The definition of an abelian group is also useful in discussing vector spaces and modules. The theory of abelian groups is generally simpler than that of their non-abelian counterparts, and finite abelian groups are very well understood. On the other hand, the theory of infinite abelian groups is an area of current research.

Lie groups lie at the intersection of two fundamental fields of mathematics: algebra and geometry. A Lie group is first of all a group. Secondly it is a smooth manifold which is a specific kind of geometric object. The circle and the sphere are examples of smooth manifolds. Finally the algebraic structure and the geometric structure must be compatible in a precise way. Informally, a Lie group is a group of symmetries where the symmetries are continuous. A circle has a continuous group of symmetries for example you can rotate the circle an arbitrarily small amount and it looks the same. This is in contrast to the hexagon, for example. If you rotate the hexagon by a small amount then it will look different. Only rotations that are multiples of one-sixth of a full turn are symmetries of a hexagon.

A Lie algebra consists of a (finite dimensional) vector space, over a field F, and a multiplication on the vector space (denoted by [ ], pronounced bracket, the image of a pair (X, Y) of vectors denoted by [X Y] or [X,Y], with the properties:

(a) Anti-commutativity $[X, Y] = -[Y, X]$.

(b) Jacobi identity $[X, [Y, Z]] + [Y, [Z, X]] + [Z, [X, Y]] = 0$.

3.2 Generalized coherent states based on $SU(1,1)$

3.2.1 $SU(1,1)$ Lie group

The group $SU(1,1)$ is a non abelian group (i.e. its elements do not commute) with its element $g = \begin{pmatrix} a & b \\ b^* & a^* \end{pmatrix}$, with determinant $|g| = 1$

The Lie algebra corresponding to the group $SU(1,1)$ is spanned by the three group generators K_0, K_1, K_2 [16, 40].

$$[K_0, K_1] = -iK_2, \quad [K_1, K_2] = iK_0, \quad [K_2, K_0] = iK_1 \tag{3.1}$$

The raising and lowering generators are defined as:

$$K_+ = K_1 + iK_2, \quad K_- = K_1 - iK_2 \tag{3.2}$$

The $SU(1,1)$ generators K_0, K_+, K_- obey the following relations:

$$[K_0, K_\pm] = \pm K_\pm, \quad [K_-, K_+] = 2K_0 \tag{3.3}$$

The Casimir operator K^2 of $SU(1,1)$ is given by:

$$K^2 = K_0^2 - \frac{1}{2}(K_+K_- + K_-K_+) = k(k-1)\mathbf{1} \tag{3.4}$$

The generators of $SU(1,1)$ algebra in terms of creation and annihilation operators are given by [41]:

$$K_1 = \frac{1}{4}(\hat{a}^\dagger\hat{a}^\dagger + \hat{a}\hat{a}) \qquad K_2 = \frac{1}{4i}(\hat{a}^\dagger\hat{a}^\dagger - aa) \tag{3.5}$$

$$K_+ = \frac{1}{2}\hat{a}^\dagger\hat{a}^\dagger, \qquad K_- = \frac{1}{2}\hat{a}\hat{a}, \qquad K_0 = \frac{1}{4}(\hat{a}\hat{a}^\dagger + \hat{a}^\dagger\hat{a}), \tag{3.6}$$

In this case the Casimir operator reduced identically to:

$$K^2 = -\frac{3}{16}. \tag{3.7}$$

Therefore there are two irreducible representation: $k = 1/4$ and $k = 3/4$. The state space $H_{1/4}$ is the even Fock subspace with the orthogonal basis consisting of even number eigenstates $|n, 1/4\rangle = |2n\rangle$ $(n = 0, 1, 2, ...)$; the state space $H_{3/4}$ is the odd Fock subspace with the orthogonal basis consisting of odd number eigenstates $|n, 3/4\rangle = |2n + 1\rangle$ $(n = 0, 1, 2, ...)$.

The $SU(1, 1)$ number state $|n, k\rangle$ can be defined as [42, 29, 43].

$$K^2|n, k\rangle = k(k-1)|n, k\rangle \tag{3.8}$$

$$K_0|n, k\rangle = (n + k)|n, k\rangle \tag{3.9}$$

$$K_-|n, k\rangle = \sqrt{n(n + 2k - 1)}|n - 1, k\rangle \tag{3.10}$$

$$K_+|n, k\rangle = \sqrt{(n + 1)(n + 2k)}|n + 1, k\rangle \tag{3.11}$$

$SU(1, 1)$ coherent states in the unit disc $D = \{z \in C : |z| < 1\}$ are defined as follows:

$$|z,k\rangle = (1-|z|^2)^k \sum_{n=0}^{\infty} d(n,k) z^n |n,k\rangle \tag{3.12}$$

$$d(n,k) = \sqrt{\frac{\Gamma(n+2k)}{\Gamma(n+1)\Gamma(2k)}} \tag{3.13}$$

The $SU(1,1)$ coherent state for $k = 1/4$ is given by:

$$|z,1/4\rangle = (1-|z|^2)^{1/4} \sum_{n=0}^{\infty} \frac{(\sqrt{2n})!}{2^n n!} z^n |2n\rangle \tag{3.14}$$

The $SU(1,1)$ coherent state for $k = 3/4$ is given by [42, 44]:

$$|z,3/4\rangle = (1-|z|^2)^{3/4} \sum_{n=0}^{\infty} \frac{(\sqrt{2n+1})!}{2^n n!} z^n |2n+1\rangle \tag{3.15}$$

It is not difficult to see that the states $|z,1/4\rangle$ and $|z,3/4\rangle$ coincide with the even and odd coherent states correspondingly [41].

$$|z,1/4\rangle = |z\rangle_e = \frac{1}{\sqrt{2(1+\exp(-2|z|^2))}}[|z\rangle + |-z\rangle] \tag{3.16}$$

$$|z,3/4\rangle = |z\rangle_o = \frac{1}{\sqrt{2(1-\exp(-2|z|^2))}}[|z\rangle - |-z\rangle] \tag{3.17}$$

The inner product of two $SU(1,1)$ coherent states $|z_1,k\rangle$ and $|z_2,k\rangle$ are defined as:

$$\langle z_1,k|z_2,k\rangle = \frac{(1-|z_1|^2)^k(1-|z_2|^2)^k}{(1-z_1^* z_2)^{2k}} \tag{3.18}$$

The resolution of the identity of the states $|z,k\rangle$ is given by:

$$\int d\mu_k(z)|z,k\rangle\langle z,k| = \hat{1} \tag{3.19}$$

where $d\mu_k(z)$ is given by:

$$d\mu_k(z) = \pi^{-1}(2k-1)(1-|z|^2)^{-2}, \quad k > 1/2 \tag{3.20}$$

The integral diverges for $k \leq 1/2$.

3.3 Generalized coherent states based on $SU(2)$

3.3.1 $SU(2)$ Lie group

The group $SU(2)$ is an abelian group which its element $g = \begin{pmatrix} a & b \\ -b^* & a^* \end{pmatrix}$, with determinant $|g| = 1$

The lie algebra corresponding to the group $SU(2)$ is spanned by the three group generators J_1, J_2, J_3, which are related by the following identities:

$$[J_1, J_2] = iJ_3, \quad [J_2, J_3] = iJ_1, \quad [J_3, J_1] = iJ_2. \tag{3.21}$$

The raising and lowering generators are defined as:

$$J_+ = J_1 + iJ_2, \quad J_- = J_1 - iJ_2. \tag{3.22}$$

The $SU(2)$ generators J_3, J_+, J_- obey the following relations:

$$[J_3, J_\pm] = \pm J_\pm, \quad [J_-, J_+] = -2J_3. \tag{3.23}$$

The Casimir operator J^2 of $SU(2)$ is given by:

$$J^2 = J_1^2 + J_2^2 + J_3^2 = j(j+1)\hat{1}. \tag{3.24}$$

The representation of the $SU(2)$ is determined by a single number j that can be a positive integer or half integer: $j = \frac{1}{2}, 1, \frac{3}{2}, 2...$

The representation Hilbert space is spanned by the orthogonal basis $|j, m\rangle$ $(m = -j, -j+1...., j-1, j)$.

The orthogonal basis $|j, m\rangle$ can be defined as:

$$J_+|j, m\rangle = [j(j+1) - m(m+1)]^{1/2}|j, m+1\rangle \tag{3.25}$$

$$J_-|j, m\rangle = [j(j+1) - m(m-1)]^{1/2}|j, m-1\rangle \tag{3.26}$$

$$J^2|j, m\rangle = j(j+1)|j, m+1\rangle. \tag{3.27}$$

The $SU(2)$ coherent states are defined as follows:

$$|j, \zeta\rangle = (1 + |z|^2)^{-j} \sum_{m=-j}^{j} d(j, m)\zeta^{j+m}|j, m\rangle \tag{3.28}$$

$$d(j, m) = \sqrt{\frac{(2j)!}{(j+m)!(j-m)!}}. \tag{3.29}$$

The inner product of two $SU(2)$ coherent states $|j, \zeta_1\rangle$ and $|j, \zeta_2\rangle$ are defined as:

$$\langle j,\zeta_1|j,\zeta_2\rangle = (1+|\zeta_1|^2)^{-j}(1+|\zeta_2|^2)^{-j}(1+\zeta_1^*\zeta_2)^{2j} \tag{3.30}$$

The resolution of the identity of the states $|j,\zeta\rangle$ is given by:

$$\int d\mu_j(\zeta)|j,\zeta\rangle\langle j,\zeta| = \hat{1} \tag{3.31}$$

where $d\mu_j(\zeta)$ is given by:

$$d\mu_j(\zeta) = \pi^{-1}(2j-1)(1+|\zeta|^2)^{-2}d^2\zeta, \tag{3.32}$$

The generators of $SU(2)$ algebra in terms of creation and annihilation operators are given by:

$$J_+ = [(2j+1)-\hat{a}^\dagger\hat{a}]^{1/2}\hat{a}^\dagger, \qquad J_- = \hat{a}[(2j+1)-\hat{a}^\dagger\hat{a}]^{1/2} \tag{3.33}$$

$$J_3 = \hat{a}^\dagger\hat{a} - j, \qquad J^2 = j(j+1)\hat{1}, \tag{3.34}$$

3.4 Summary

In this chapter we have studied the $SU(1,1)$ and $SU(2)$ coherent states. In the next chapter we will introduce novel coherent states based on the Bargmann formalism.

Chapter 4

A new class of Generalized coherent states

4.1 Generalized coherent state $|A\rangle_{gcoh}$ and its Bargmann function

Let $g(z) \in B_s$ then $g(Az) \in B_s$ and can be written as infinite series

$$g(Az) = \sum_{n=0}^{\infty} g_n (Az)^n \tag{4.1}$$

Let Z_g be the set of all integers n such that $g_n \neq 0$. We consider functions $g(Az)$ for which Z_g is an infinite subset of the non negative integers i.e, the expansion of $g(z)$ is not a polynomial but an infinite series. We denote it as $|A\rangle_{gcoh}$, the corresponding normalized quantum state. Then the state $|A\rangle_{gcoh}$

can be written as:

$$|A\rangle_{gcoh} = [M(A)]^{-1/2} \sum_{n \in Z_g} (n!)^{1/2} g_n A^n |n\rangle, \tag{4.2}$$

where $M(A)$ has been given in Eq(2.161) as a corresponding normalized Bargmann function of $g(Az)$.

We have two cases for the complex number A:

Case 1

If $0 \in Z_g$ that means $g_0 \neq 0$ then $A \in \mathbb{C}$.

Case 2

If $0 \notin Z_g$ that means $g_0 = 0$ then $A \in \mathbb{C}^*$ (because if $A = 0$ then $g = 0$).

4.1.1 The linear map τ from $\mathfrak{B}$ into $\mathfrak{B}$

We consider the following linear map from $\mathfrak{B}$ into $\mathfrak{B}$:

$$\tau(A) : g(z) \to g(Az), \qquad A \in \mathbb{C}^* = \mathbb{C} - \{0\} \tag{4.3}$$

The linear map τ from $\mathfrak{B}$ into $\mathfrak{B}$ can be written in a Dirac notation as:

$$\tau(A) : |1\rangle_{gcoh} \to |A\rangle_{gcoh}, \qquad A \in \mathbb{C}^* = \mathbb{C} - \{0\} \tag{4.4}$$

$\tau(A)$ is a map from $\mathfrak{B}$ to $\mathfrak{B}$ which is not bijective and has no inverse. Indeed, if the growth of the Bargmann function of $|1\rangle_{gcoh}$ is $(2, \sigma)$, then the growth of Bargmann function of $|A\rangle_{gcoh}$ is $(2, |A|^2\sigma)$. For $|A| > 1$, there are states for which $|A|^2\sigma > 1/2$ and therefore they are not normalizable. For $|A| < 1$ the map from $\mathfrak{B}$ to $\mathfrak{B}$ is not surjective.

To avoid these problem we restrict below this map into $\mathfrak{B}_s$.

4.1.2 The linear map τ from $\mathfrak{B}_s$ into $\mathfrak{B}_s$

We consider the following linear bijective map from $\mathfrak{B}_s$ into $\mathfrak{B}_s$:

$$\tau(A) : g(z) \to g(Az), \qquad A \in \mathbb{C}^* = \mathbb{C} - \{0\} \tag{4.5}$$

The linear map τ from $\mathfrak{B}_s$ into $\mathfrak{B}_s$ can be written in a Dirac notation as:

$$\tau(A) : |1\rangle_{gcoh} \to |A\rangle_{gcoh}, \qquad A \in \mathbb{C}^* = \mathbb{C} - \{0\} \tag{4.6}$$

This map is not preserving the inner product and it is bijective only in the subspace $B_s \subset B$. This map can be written in terms of the operator $\tau(A)$ [45]:

$$\tau(A) = \exp[(\ln|A| + i\theta_A)\hat{a}^\dagger\hat{a}] \tag{4.7}$$

where $A = |A|\exp(i\theta_A) \in \mathbb{C}^* = \mathbb{C} - \{0\}$.

These operators are unitary when $|A| = 1$.

The set $G_\tau = \{\tau(A) : A = |A|\exp(i\theta_A) \in \mathbb{C}^*\}$ forms an abelian group:

1- Closure

For any $\tau(A)$, and $\tau(B) \in G_\tau$

$$\begin{aligned}
\tau(A)\tau(B) &= \exp[(\ln|A| + i\theta_A)\hat{a}^\dagger\hat{a}]\exp[(\ln|B| + i\theta_B)\hat{a}^\dagger\hat{a}] \\
&= \exp[(\ln|A| + \ln|B| + i\theta_A + i\theta_B)\hat{a}^\dagger\hat{a}] \\
&= \exp[(\ln[AB| + i(\theta_A + \theta_B))\hat{a}^\dagger\hat{a}] \\
&= \exp[(\ln[AB| + i(\theta_{AB}))\hat{a}^\dagger\hat{a}] \\
&= \tau(AB) \in G_\tau \qquad (4.8)
\end{aligned}$$

2- Identity element $\tau(1)$

The Identity element $\tau(1)$ can be written as

$$\tau(1) = \exp[(\ln(1) + 0i)\hat{a}^\dagger\hat{a}] = \exp[\hat{0}] = \hat{1} \qquad (4.9)$$

3- Associativity

For any $\tau(A)$, $\tau(B)$ and $\tau(B) \in G_\tau$

$$\begin{aligned}
(\tau(A)\tau(B))\tau(C) = &= (\tau(AB))\tau(C) \\
&= \tau(ABC) \\
&= \tau(A)(\tau(BC)) \\
&= \tau(A)(\tau(B)\tau(C)) \qquad (4.10)
\end{aligned}$$

4- The inverse element $(\tau(A))^{-1}$

There is a unique element $(\tau(A))^{-1} = \tau(A^{-1}) \in G_\tau$ holds

$$\tau(A)\tau(A^{-1}) = \hat{1} = \tau(A^{-1})\tau(A) \quad \forall \tau(A) \in G_\tau \tag{4.11}$$

The set G_τ is an Abelian group that means, for any $\tau(A)$ and $\tau(B) \in G_\tau$

$$\tau(A)\tau(B) = \tau(AB) = \tau(BA) = \tau(B)\tau(A) \tag{4.12}$$

Therefore the set G_τ is an Abelian group. This group is isomorphic to the multiplicative group of complex numbers in $\mathbb{C}^*$.

We next prove that

$$\tau(A)|1\rangle_{gcoh} = [M(A)]^{-1/2}|A\rangle_{gcoh} \tag{4.13}$$

where $[M(A)]$ is a normalization factor of $g(Az)$.

There are special cases for the operator $\tau(A)$:

Case 1: (Fractional Fourier operator)

For $|A| = 1$ the operator $\tau(A)$ by definition becomes:

$$\tau(A) = \exp[(i\theta_A)\hat{a}^\dagger\hat{a}]. \tag{4.14}$$

and is called fractional Fourier operator.

Case 2: (Fourier operator).

For $A = \exp(i\pi/2)$ the operator $\tau(A)$ by definition becomes:

$$\tau(A) = \exp[(i\pi/2)\hat{a}^\dagger\hat{a}] = \hat{U}(\pi/2) \tag{4.15}$$

and is called the Fourier operator.

Case 3: (Parity operator)

For $A = \exp(i\pi)$ the operator $\tau(A)$ by definition becomes

$$\tau(A) = \exp[(i\pi)\hat{a}^\dagger\hat{a}] = \hat{U}(\pi) \tag{4.16}$$

and called parity operator.

4.1.3 Example (The Schrödinger cat states)

The even and odd coherent states, introduced in 1970 by Dodono V, Malkin and Man'ko, later called 'Schrödinger cat' states, are superposition of coherent states; they are close to coherent and squeezed states. Since Schrödinger cat states have a wide class of application in quantum optics, they have been much studied in recent years. The wigner function has been studied under several physical conditions. The Wigner function of Schrodinger cat states typical Gaussian like probabilities located at two different regions of phase space, with an additional interference term that takes negative regions.

As an example we consider the case where the Bargmann function is a sinusoidal function. In this case

$$g(Az) = i[sinh(\pi^2|A|^2)]^{-1/2}\sin(\pi Az) \tag{4.17}$$

The corresponding generalized coherent states are the Schrödinger cat states:

$$|A\rangle_{sin} = [2 - 2\exp(-2\pi|A|^2)]^{-1/2}[|i\pi A\rangle - |-i\pi A\rangle]] \tag{4.18}$$

The index 'sin' in the notation of this state, indicates that its Bargmann function is sinusoidal. It is easily seen that these states belong in the space H_{odd} spanned by the odd number states $|2n+1\rangle$. According to our general theory the set $\{|A\rangle_{sin}\}$ is total in H_{odd}. Their zeros are $\zeta_n = N/A$ where N is an integer, and they can be factorized as:

$$\sin(\pi A z) = \pi A z \prod_{N=1}^{\infty} (1 - \frac{z^2}{N^2 A^{-2}}). \tag{4.19}$$

A similar argument can be given for the states with Bargmann function $\cos(\pi A z)$. The set of these states is total in H_{even} spanned by even number states $|2n\rangle$.

For example the state $|1\rangle_{sin}$

$$|1\rangle_{sin} = [2 - 2\exp(-2\pi)]^{-1/2}[|i\pi\rangle - |-i\pi\rangle]] \tag{4.20}$$

Figure 4.1 shows the first 11^{th} zeros of Bargmann function of the state $|1\rangle_{sin}$ and its motion according to the $H = \hat{a}^\dagger\hat{a} - i\hat{a}^\dagger + i\hat{a}$ at $t = [0 : .05 : 0.3]$. According to this Hamiltonian the path of positive zeros is moving upwards while the path for negative zeros is moving downwards.

4.2 Summary

Starting from a Bargmann function $g(z)$ in B_s we have considered the states with Bargmann function $g(Az)$ (with a normalization factor). We have explained that the dilation from z to Az on Bargmann functions considered here are different from the dilation on wavefunctions in the context of the az+b

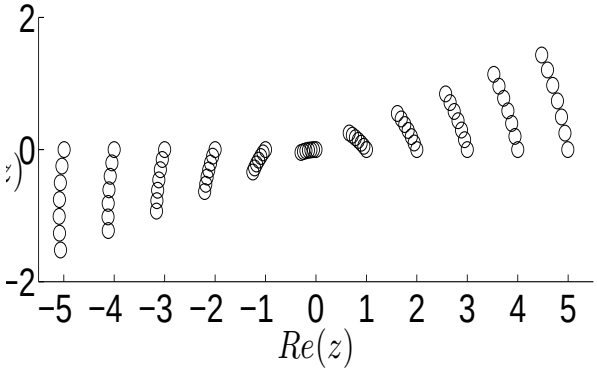

Figure 4.1: The time evolution of the zeros of the Bargmann function of the state $|1\rangle_{sin}$, for Hamiltonian $H = \hat{a}^\dagger\hat{a} - i\hat{a}^\dagger + i\hat{a}$ and for the time interval $t = [0 : .05 : 0.3]$.

group. These states are generalized coherent sates in the sense that they have the following three properties: (i) they are a total set in some Hilbert space but we have not found a resolution of the identity. (ii) they can be written as $[N(A)]^{\frac{-1}{2}}\tau(A)|1\rangle_{gcoh}$ where $\tau(A)$ form a representation of the multiplicative group of non-zero complex number C^* and (iii) they have the property of temporal stability that remains invariant under the corresponding time evolution. The Glauber coherent states are an example of these states. But there are many other examples, which comprise highly non-classical states, with many zeros and Wigner functions with many islands of negative values. We have studied the Schrödinger cat states as an example, and their Bargmann functions. The Bargmann zeros of these states are on a straight line. We have also considered a system which at $t = 0$ is in Schrödinger cat state, and studied the paths of the Bargmann zeros as the system evolves

in time with Hamiltonian $H = \hat{a}^\dagger \hat{a} - i\hat{a}^\dagger + i\hat{a}$ as an example. In the next two chapters two more examples based on the Gamma and the Riemann ξ functions are considered.

Chapter 5

The Gamma states $|A; B; k\rangle_\Gamma$

5.1 The Gamma function $\Gamma(z)$

The Gamma function was first introduced by the Swiss mathematician Leonhard (1707-1783) in his goal to generalize the factorial to non integer values.

The Gamma function $\Gamma(z)$ is a complex function defined as [46, 47]:

$$\Gamma(z) = \int_0^\infty t^{z-1} \exp(-t) dt \tag{5.1}$$

It is an analytic function of the complex variable z which in any finite domain has no singularities other than simple poles, situated at the points $z = 0, -1, -2, -3, -4, ...$[48].

The n-th derivative of the Gamma function is:

$$\frac{d^n}{dz^n} = \int_0^\infty t^{z-1} exp(-t)(\ln t)^n dt. \tag{5.2}$$

This can be derived by differentiating the integral form of the Gamma

function with respect to z, and using the technique of differentiation under the integral sign.

This equation above will be used for the derivative of ξ in table 6.1 .

If the real part of the complex number z is positive, then the integral above converges absolutely. By using integral by parts, we can show that

$$\Gamma(z+1) = z\Gamma(z) \tag{5.3}$$

If z is a real variable, then only when z is a natural number, we have

$$\Gamma(z+1) = z! \tag{5.4}$$

Figures 5.1 and 5.2 show the plots of $\Gamma(x)$ and $\frac{1}{\Gamma(x)}$ respectively.

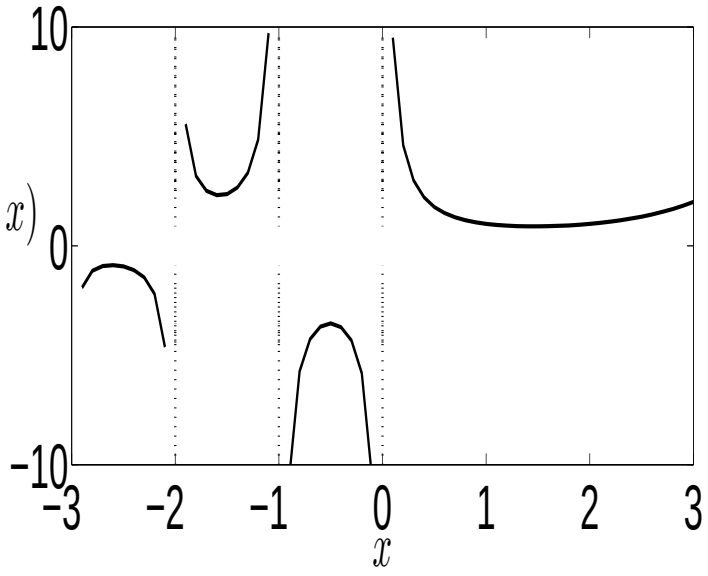

Figure 5.1: The plot of $y = \Gamma(x)$ for all $-3 \leq x \leq 3$

For non-natural values of z, the above equation does not apply, since the factorial function is not defined. The Euler's reflection formula for Gamma function is [49]:

$$\Gamma(1-z)\Gamma(z) = \frac{\pi}{\sin(\pi z)} \tag{5.5}$$

Perhaps the most well-known value of the Gamma function at a non-integer argument is:

$$\Gamma(\frac{1}{2}) = \sqrt{\pi} \tag{5.6}$$

For any non null integer n, we have

$$\Gamma(z) = \frac{\Gamma(z+n)}{z(z+1)...(z+n-1)} \qquad z+n>0 \tag{5.7}$$

The inverse Gamma function $\frac{1}{\Gamma(z)}$ is an entire function in all of the complex plane. $\frac{1}{\Gamma(z)}$ can be written as an infinite series as follows [50]:

$$\frac{1}{\Gamma(z)} = \sum_{k=1}^{\infty} c_n z^n \tag{5.8}$$

where c_n satisfies:

$$(nc_1 - 1)c_n = c_2 c_{n-1} - \sum_{k=2}^{n} (-1)^k \zeta(k) c_{n-k} \tag{5.9}$$

where $c_0 = 0$, $c_1 = 1$, $c_2 = \gamma \approx .5771$, γ is the Euler constant and $\zeta(k)$ is Riemann's zeta function discussed in more detail later. The zeros of $\frac{1}{\Gamma(z)}$ are $z = 0, -1, -2, -3, ...$

For any real number z, except on negative integers $z = 0, -1, -2, -3, ...$, we have infinite product.

The Gamma function $\Gamma(z)$ is a function from the complex plane $\mathbb{C}$ to itself i.e, $\Gamma : \mathbb{C} \to \mathbb{C}$, its graph can't be represented as a 3D image. Instead, the real part and the imaginary part are plotted and can be shown in figure 5.3 and figure 5.4. In addition the absolute value of $\Gamma(z)$ and $\frac{1}{\Gamma(z)}$ can be shown in figures 5.5 and 5.6 respectively.

The Hadamard product representation of the ξ function $\frac{1}{\Gamma(z)}$ is:

$$\frac{1}{\Gamma(z)} = z\exp(\gamma z)\prod_{p=1}^{\infty}(1+\frac{z}{p})\exp(-z/p) \tag{5.10}$$

From this product we see that Euler's constant is deeply related to the Gamma function and the poles are clearly the negative or null integers.

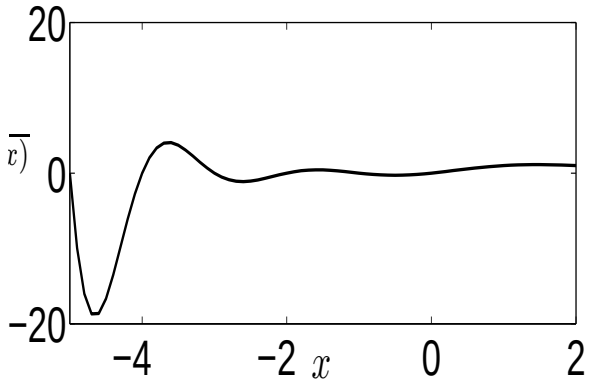

Figure 5.2: The plot of $y = \frac{1}{\Gamma(x)}$ for all $-5 \leq x \leq 2$

We consider the entire function $\Omega_{|A,B,k\rangle_\Gamma}(z)$ as follows:

$$\begin{aligned} \Omega_{|A,B,k\rangle_\Gamma}(z) &= \frac{\exp(Bz)}{[\Gamma(Az)]^k} \qquad k = 1,2,3... \\ &= \exp(Bz) \qquad k = 0 \end{aligned} \tag{5.11}$$

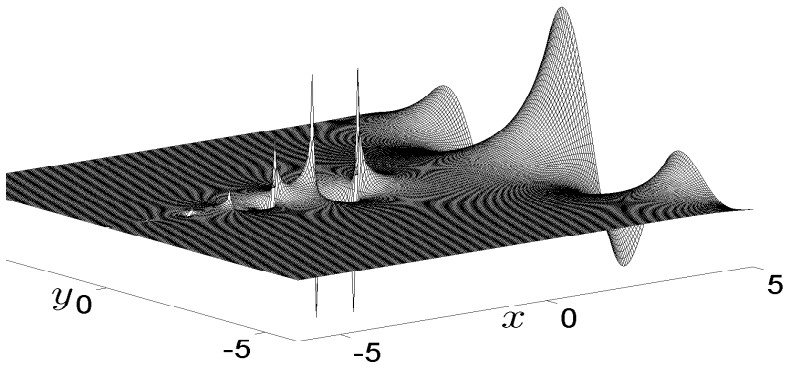

Figure 5.3: The plot of real part of $\Gamma(z)$ where $z = x + iy$ for all $-5 \leq x \leq 5$ and $-5 \leq y \leq 5$

The growth of both $\exp(Bz)$ and the $\frac{1}{\Gamma(Az)}$ has order $\rho = 1$ and therefore the $\Omega_{|A,B,k\rangle_\Gamma}(z)$ has growth with order $\rho = 1$ and qualifies as a Bargmann function. The corresponding normalized Bargmann function is $N(A)^{-1/2}\Omega_{|A,B,k\rangle_\Gamma}(z)$ where

$$N(A) = \int_{\mathbb{C}} \int \frac{\exp(-|z|^2 + Bz + B^* z^*)}{[\Gamma(Az)]^{2k}} d\mu(z) \tag{5.12}$$

We denote the corresponding normalized state as $|A;B;k\rangle_\Gamma$ (where $A \neq 0$).

The most common application is to a complex analytic function determined near a point z_0 by a power series.

We next consider the power expansion series of our Bargmann function $\Omega_{|A,B,k\rangle_\Gamma}(z)$ at $z_0 = 0$ as:

$$\Omega_{|A,B,k\rangle_\Gamma}(z) = \sum_{N=k}^{\infty} c_N(A,B,k) z^N \tag{5.13}$$

where c_N represents the coefficient of the n-th term, and will be used in

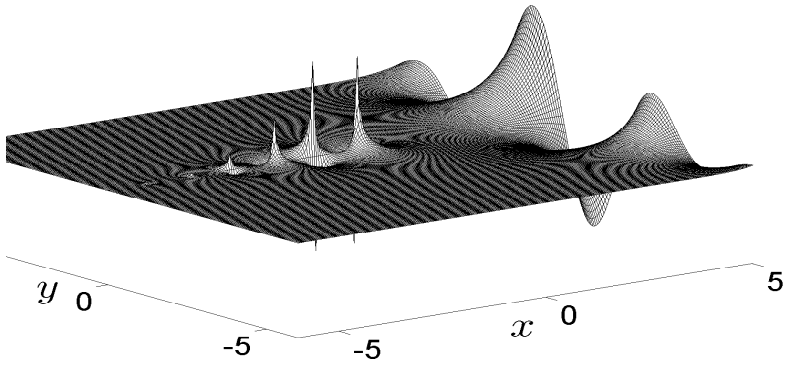

Figure 5.4: The plot of imaginary part of $\Gamma(z)$ where $z = x + iy$ for all $-5 \leq x \leq 5$ and $-5 \leq y \leq 5$

subsection 5.1.3 to compute the overlap f_n of Gamma states.

The summation starts from $N = k$ because $z = 0$ is a zero of this function with multiplicity k. The states $|A;B;k\rangle_\Gamma$ with fixed B, k and $A \in C - \{0\}$ are generalized coherent states in the sense described in section 4.1. The set of all these states is total in the space H_s spanned by the number states $|k\rangle$,$|k+1\rangle$ and it does not include any $|N\rangle$ for which $c_N = 0$. The states $|A;B;k\rangle_\Gamma$ with fixed A,$k$and $B \in C$ are also generalized coherent states in the sense described in section (4.1) The zeros of $\Omega_{|A,B,k\rangle_\Gamma}(z)$ are $\zeta_N = -NA^{-1}$ (where N is a non-negative integer), with multiplicity k. The zeros of an analytic function do not define the function uniquely, and in our case all state with fixed values of A,k have the same zeros. The fact that $\zeta_N = -NA^{-1}$ are zeros with multiplicity k of the Bargmann function $\Omega_{|A,B,k\rangle_\Gamma}(z)$ of $|A;B;k\rangle_\Gamma$, implies that The state $|A;B;k\rangle_\Gamma$ is the eigenstate of $\Theta_{m,A,k}$ where $\Theta_{m,A,k}$ can

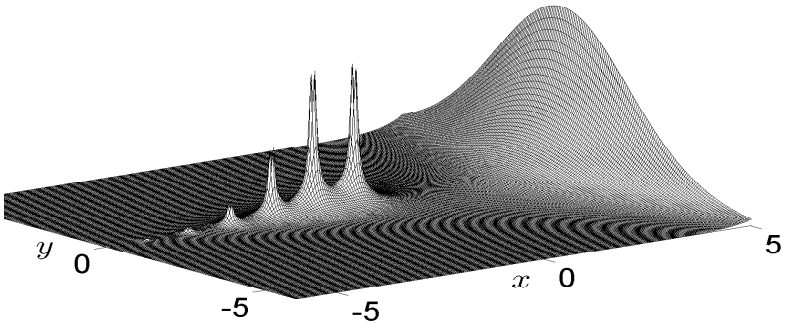

Figure 5.5: The plot of absolute value of $\Gamma(z)$ where $z = x + iy$ for all $-5 \leq x \leq 5$ and $-5 \leq y \leq 5$

be defined as

$$\Theta_{m,A,k} = [A\hat{a}^\dagger(A\hat{a}^\dagger + 1)...(A\hat{a}^\dagger + m - 1)]^k \exp(\frac{m}{A}\hat{a}) \tag{5.14}$$

The operator $\Theta_{m,A,k}$ can be written in a Bargmann representation as

$$\Theta_{m,A,k} = [Az(Az + 1)...(Az + m - 1)]^k \exp(\frac{m}{A}\partial_z) \tag{5.15}$$

To prove that

$$\Theta_{m,A,k}|A;B;k\rangle_\Gamma = \exp(\frac{mB}{A})|A;B;k\rangle_\Gamma \tag{5.16}$$

By using the definition of $\Theta_{m,A,k}$ in Eq(5.14)

$$\Theta_{m,A,k}|A;B;k\rangle_\Gamma = [Az(Az+1)...(Az+m-1)]^k \exp(\frac{m}{A}\partial_z)\Omega_{|A,B,k\rangle_\Gamma}(z) \tag{5.17}$$

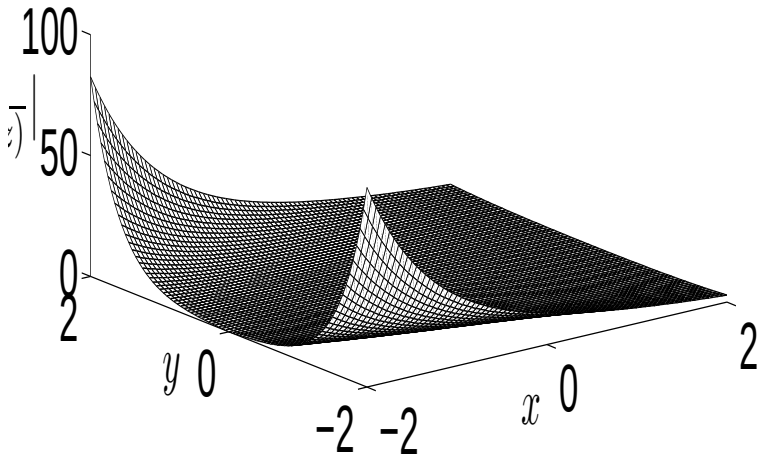

Figure 5.6: The plot of $w = |\frac{1}{\Gamma(z)}|$ where $z = x + iy$ for all $-2 \leq x \leq 2$ and $-2 \leq y \leq 2$

$$\Theta_{m,A,k}|A;B;k\rangle_\Gamma = [Az(Az+1)...(Az+m-1)]^k \exp(\frac{m}{A}\partial_z)\frac{\exp(Bz)}{[\Gamma(Az)]^k} \quad (5.18)$$

The shifting operator $\exp(\frac{m}{A}\partial_z)$ acts on $\frac{\exp(Bz)}{[\Gamma(Az)]^k}$ we get

$$\begin{aligned} \exp(\frac{m}{A}\partial_z)\frac{\exp(Bz)}{[\Gamma(Az)]^k} &= \frac{\exp(B(z+\frac{m}{A}))}{[\Gamma(A(z+\frac{m}{A}))]^k} \\ &= \frac{\exp(Bz+\frac{Bm}{A})}{[\Gamma(Az+m)]^k} \\ &= \exp(\frac{Bm}{A})\frac{\exp(Bz)}{[\Gamma(Az+m)]^k} \end{aligned} \quad (5.19)$$

By using the relation $z(z+1)...(z+m-1)\Gamma(z)=\Gamma(z+m)$

$$\exp(\frac{m}{A}\partial_z)\frac{\exp(Bz)}{[\Gamma(Az)]^k}=\exp(\frac{mB}{A})\frac{\exp(Bz)}{[[Az(Az+1)...(Az+m-1)]^k\Gamma(Az)]^k} \tag{5.20}$$

Then the Eq(5.20), shows that the state $|A;B;k\rangle_\Gamma$ is the eigenstate of the operator $\Theta_{m,A,k}$(for all positive integer m):

$$\Theta_{m,A,k}|A;B;k\rangle_\Gamma=\exp(\frac{mB}{A})|A;B;k\rangle_\Gamma \tag{5.21}$$

The zeros of an analytic function do not define the function uniquely, and in our case states with fixed values of A,k have the same zeros.

The Bargmann function of our state $|A;B;k\rangle_\Gamma$ has zeros at $-NA^{-1}$ with multiplicity k

If the derivative of order l with respect to z for $\Omega_{|A,B,k\rangle_\Gamma}(z)$ has zeros at $-NA^{-1}$ then the state $|A;B;k\rangle_\Gamma$ is orthogonal to all coherent states $a^l|-NA^{-1}\rangle$ with $l=0,1,...k-1$ and $N=0,1,2...$

We next act with the fractional fourier operator on both sides of $\Theta_{m,A,k}$ and we get

$$\exp(i\theta\hat{a}^\dagger\hat{a})\Theta_{m,A,k}\exp(-i\theta\hat{a}^\dagger\hat{a})=\Theta_{m,A',k};\quad A'=A\exp(i\theta) \tag{5.22}$$

It is easy to show Eq(5.22) by using the formula

$$\exp(i\theta\hat{a}^\dagger\hat{a})f(\hat{a},\hat{a}^\dagger)\exp(-i\theta\hat{a}^\dagger\hat{a})=f(\hat{a}\exp(-i\theta),\hat{a}^\dagger\exp(i\theta)) \tag{5.23}$$

That means replace $\hat{a}$ by $\hat{a}\exp(-i\theta)$ and $\hat{a}^\dagger$ by $\hat{a}^\dagger\exp(i\theta)$

$$\exp(i\theta\hat{a}^\dagger\hat{a})\Theta_{m,A,k}\exp(-i\theta\hat{a}^\dagger a) = \Theta_{m,A\exp(i\theta),k} \tag{5.24}$$

$$\exp(i\theta\hat{a}^\dagger\hat{a})|A;B;k\rangle_\Gamma = |A\exp(i\theta);B\exp(i\theta);k\rangle_\Gamma \tag{5.25}$$

We can prove that by taking the overlap of both sides with a coherent state, it is clear that these states have the property of temporal stability.

5.1.1 Factorization of the entire $\Omega_{|A,B,k\rangle_\Gamma}(z)$

The $\Omega_{|A,B,k\rangle_\Gamma}(z)$ can be factorized as:

$$\Omega_{|A,B,k\rangle_\Gamma}(z) = Az[\prod_{N=1}^{\infty}(1+\frac{Az}{N})^k\exp(-\frac{Az}{N})]\exp(\gamma Az)\exp(Bz) \tag{5.26}$$

The $\Omega_{|A,B,k\rangle_\Gamma}(z)$ is related to $\sin(\pi Az)$ as follows:

$$\sin(\pi Az) = \pi\Omega_{|A,B,1\rangle_\Gamma}(z)\Omega_{|A,B,1\rangle_\Gamma}(\frac{1}{A}-z)\exp(-\frac{B}{A}) \tag{5.27}$$

Therefore the Bargmann function of the Schrodiger cat state is the product of Bargmann function of our Gamma states. For $A=1$ and $B=0$, the zeros of the Bargmann of $|1\rangle_{sin}$ on the negative axis coincide with the zeros of the Bargmann function of $|1,0,1\rangle_\Gamma$. The zeros of the Bargmann function of $|1\rangle_{sin}$ on the positive axis coincide with the zeros of $\Omega_{|1,0,1\rangle_\Gamma}(1-z)$, which is the Bargmann function for the state $N\tau_\pi\exp(-a)|1,0,1\rangle_\Gamma$ (where a is the annihilation operator and N is a normalization factor).

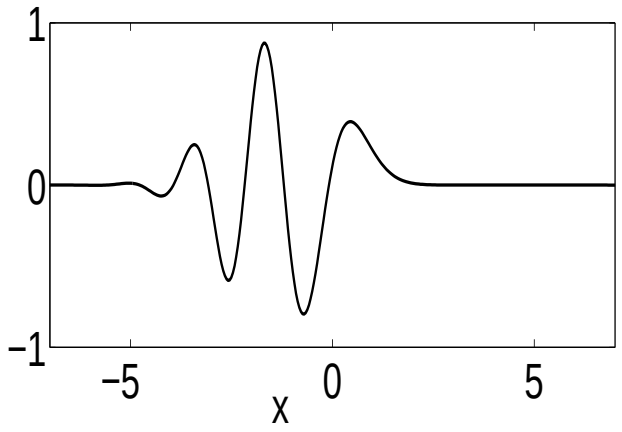

Figure 5.7: The plot of $F(x,1,0,1)$

5.1.2 The wavefunction of $|A,B,k\rangle_\Gamma$

We denote $F(x;A;B;k) = \langle x|A;B;k\rangle_\Gamma$ as the wavefunction of the state $|A,B,k\rangle_\Gamma$ and can be written as:

$$F(\frac{x}{\sqrt{2}};A;B;k) = \frac{1}{\sqrt{2}\sqrt[4]{\pi^3}}\exp(-\frac{x^2}{4})\int dy\Omega_{|A,B,k\rangle_\Gamma}(z)\exp(-\frac{y^2}{2}) \qquad (5.28)$$

$$F(\frac{x}{\sqrt{2}};A;B;k) = \frac{1}{\sqrt{2}\sqrt[4]{\pi^3}}\exp(-\frac{x^2}{4})\int dy\frac{\exp(Bz)}{[\Gamma(Az)]^k}\exp(-\frac{y^2}{2}) \qquad (5.29)$$

It is easy to show that $F(x;A;B;k)$ is a real function by using the fact that $|\Gamma(z)|^* = |\Gamma(z^*)|$.

Using equation(5.29), we calculated the wavefunction $F(x,1,0,1)$ and the result is shown in figure 5.7.

5.1.3 The overlap of Gamma states with number states

The overlap $f_n = \langle N|1,0,1\rangle_\Gamma$ can be calculated by different methods. In this section we present two methods. The first method is a well known method that uses the Bargmann function of Gamma state to compute f_n Whereas, the second one is a new method that has been proposed to compute the f_n using the wave function of Gamma state.

Method 1

We use the expansion of the bargmann function of the Gamma state $|A,0,1\rangle_\Gamma$

$$\Omega_|A,0,1\rangle_\Gamma(z) = \frac{1}{\Gamma(Az)} = \sum_{n=1}^{\infty} c_n (Az)^n \tag{5.30}$$

The Bargmann function $\frac{1}{\Gamma(Az)}$ can also be expressed in $n-$representation as follows:

$$\frac{1}{\Gamma(Az)} = \sum_{n=1}^{\infty} \frac{f_n}{\sqrt{n!}} (Az)^n \tag{5.31}$$

So the relation between the normalized coefficients of the overlaps f_n and c_n can be written as:

$$f_n = c_n \sqrt{n!} M^{-1/2}, \qquad M = \sum_{n=1}^{k} |c_n|^2 (n!) \tag{5.32}$$

Method 2

The overlap f_n can be expressed buy using the wave function $F(x,A,B,k)$ as follows:

$$f_n = \int_{-\infty}^{\infty} F(x,A,B,k) U_n(x) dx \tag{5.33}$$

where $U_n(x)$ is a wave function of the number state $|n\rangle$ and F(x,A,B,k) is a wave function of the state $|A,B,k\rangle_\Gamma$.

The coefficients f_n for the state $|1;0;1\rangle_\Gamma$ can be shown in table 5.1 by using Method 1 and Method 2.

Table 5.1: The coefficients f_n for the state $|1;0;1\rangle_\Gamma$ by using Method1 and Method2

n	Method1	Method2
1	0.275497454109021	0.275497685283495
2	0.224890285856650	0.224890474006347
3	-0.442605010554867	-0.442605370760393
4	-0.056689124182813	-0.056689164984884
5	0.502600772796255	0.502601168615769
6	-0.311941369122938	-0.311941622720611
7	-0.188190166086860	-0.188190310615659
8	0.399347968135548	0.399348332230931
9	-0.193369290122090	-0.193369564564189
10	-0.112960203880015	-0.112960064616746
11	0.222882509742501	0.222882204347078
12	-0.121404440991182	-0.121403515627903
13	-0.027185616146742	-0.027187644503849
14	0.092164169511051	0.092167887609552
15	-0.064783138573200	-0.064789377799676
16	0.007707288506432	0.007717143563691
17	0.025989396728844	0.025974778226824
18	-0.026039878468228	-0.026019699432077
19	0.010025978847910	0.010000313713691
20	0.003344150549284	0.003373811717604
21	-0.007279744530954	-0.007310121755611
22	0.004710976014662	0.004737039198377
23	-0.000911638685507	-0.0009279287991457
24	-0.001161674783025	-0.001159368639999
25	0.001325927806304	0.001347030885182

The approximate mean number of photons for a system prepared in $|1,0,1\rangle_\Gamma$ equals:

$$\langle n\rangle = \sum_{n=0}^{200} n|f_n|^2 = 5.5556. \tag{5.34}$$

The approximate photon variance $\langle\triangle n\rangle^2$ in the Gamma state $|1,0,1\rangle_\Gamma$ is:

$$\langle\triangle n\rangle^2 = \langle n^2\rangle - \langle n\rangle^2 = 39.5329 - (5.5556)^2 = 8.6682. \tag{5.35}$$

The approximate expectation value of the position operator $\hat{x}$ in the Gamma state $|1,0,1\rangle_\Gamma$ equals:

$$\langle x\rangle = \int x|F(x,1,0,1)|^2 dx = -1.2802. \tag{5.36}$$

The approximate expectation value of the momentum operator $\hat{p}$ in the Gamma state $|1,0,1\rangle_\Gamma$ equals:

$$\langle p\rangle = \int p|F(p,1,0,1)|^2 dp = 2.5760. \tag{5.37}$$

The approximate variance of the position operator $\hat{x}$ in the Gamma state $|1,0,1\rangle_\Gamma$ equals:

$$\langle\triangle x\rangle^2 = \langle x^2\rangle - \langle x\rangle^2 = .9986. \tag{5.38}$$

The approximate variance of the momentum operator $\hat{p}$ in the Gamma state $|1,0,1\rangle_\Gamma$ equals:

$$\langle\triangle p\rangle^2 = \langle p^2\rangle - \langle p\rangle^2 = 3.0781. \tag{5.39}$$

The second order coherence $g^{(2)}$ of $|1,0,1\rangle_\Gamma$ equals:

$$g^{(2)} = \frac{\langle \hat{a}^\dagger \hat{a}^\dagger \hat{a} \hat{a} \rangle}{\langle \hat{a}^\dagger \hat{a} \rangle^2} = 1.1008. \tag{5.40}$$

Figures 5.8, 5.9 and 5.10 show $\langle n \rangle$, $\langle n^2 \rangle$ and $g^{(2)}$, as functions of A (for real A), for the state $|A, 0, 1\rangle_\Gamma$

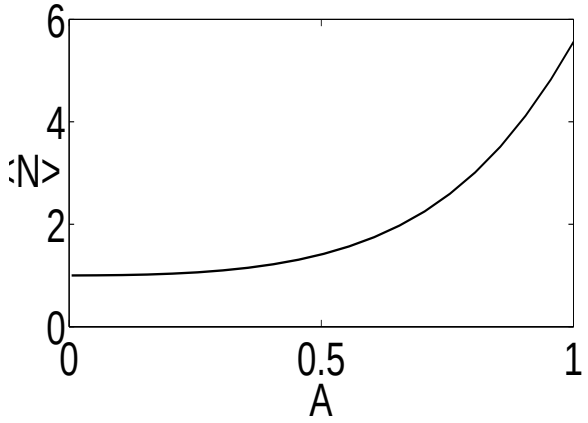

Figure 5.8: The plot of the expectation value of number state $\langle n \rangle$ as a function of A for the state $|A, 0, 1\rangle_\Gamma$

5.1.4 The Wigner function $W_{|A,B,k\rangle_\Gamma}(x,p)$ of the state $|A, B, k\rangle_\Gamma$

The Wigner function of the state $|A, B, k\rangle_\Gamma$ can be written as

$$W_{|A,B,k\rangle_\Gamma}(x,p) = \frac{1}{2\pi} \int_{-\infty}^{\infty} \exp(ipX) \langle x - X/2 | \rho | x + X/2 \rangle dX \tag{5.41}$$

$$W_{|A,B,k\rangle_\Gamma}(x,p) = \frac{1}{2\pi} \int_{-\infty}^{\infty} \exp(-iPx) \langle p - P/2 | \rho | p + P/2 \rangle dP \tag{5.42}$$

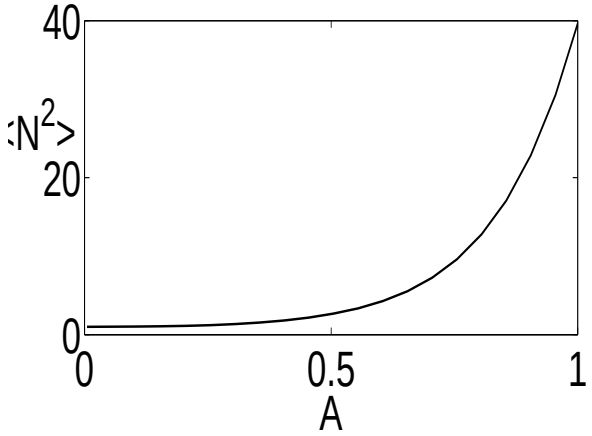

Figure 5.9: The plot of the expectation value $\langle n^2\rangle$ as a function of A for the state $|A,0,1\rangle_\Gamma$

where ρ is the density operator of the state $|A,B,k\rangle_\Gamma$ is given by:

$$\rho = |A,B,k\rangle_{\Gamma\Gamma}\langle A,B,k| \tag{5.43}$$

The Wigner function has been calculated using equation (5.41). Figures 5.12, 5.14, 5.16 and 5.18 show the Wigner functions for the states $|1;0;1\rangle_\Gamma$, $|0.1,0,1\rangle_\Gamma$, $|1,0.1,1\rangle_\Gamma$ and $|1,0.1\pi i,1\rangle_\Gamma$ correspondingly.

The contour of Wigner functions for the states $|1;0;1\rangle_\Gamma$, $|0.1,0,1\rangle_\Gamma$, $|1,0.1,1\rangle_\Gamma$ and $|1,0.1\pi i,1\rangle_\Gamma$ can be shown in figures 5.13, 5.15, 5.17 and 5.19 correspondingly.

The relation between zeros of Bargmann function of the state $|1,0,1\rangle_\Gamma$ and negative region of its Wigner function can be shown in figure 5.13 and also the state $|0.1,0,1\rangle_\Gamma$ in figure 5.15. The signs + and − denote to the positive and negative regions of Wigner function respectively. We note that in $|1,0,1\rangle_\Gamma$ the values of Wigner function at the first four zeros $z = 0,-1,-2,-3$ of its

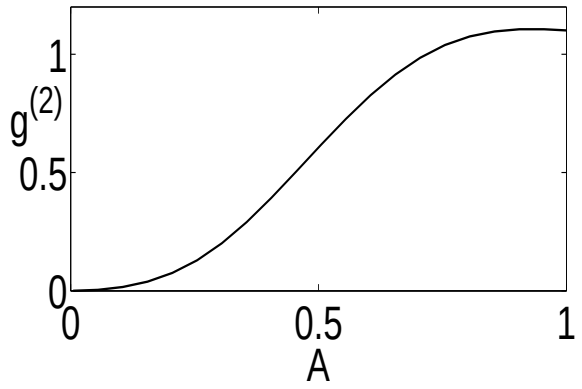

Figure 5.10: The plot of second order correlation $g^{(2)}$ as a function of A for the state $|A,0,1\rangle_\Gamma$

Bargmann state are all negatives.

5.1.5 Time evolution: motion of the zeros

The state of a quantum system is not constant in time and the system evolves according to the Schrodinger equation:

$$-i\frac{d}{dt}|\psi(t)\rangle = H\psi(t)\rangle \tag{5.44}$$

where H is the corresponding Hamiltonian.

The solution of Eq(5.44) can be written as:

$$|\psi(t)\rangle = \exp(iHt)|\psi(t_0)\rangle \tag{5.45}$$

where $|\psi(t_0)$ is an initial state.

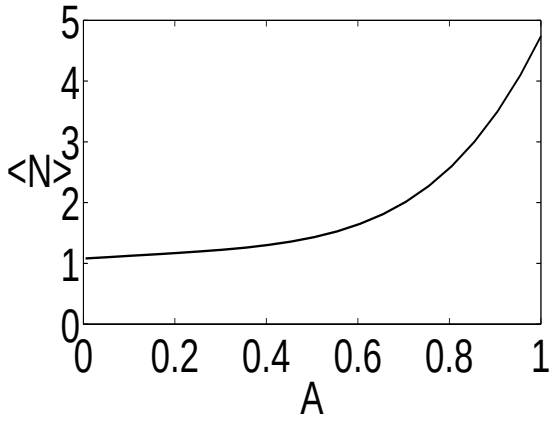

Figure 5.11: The plot of the expectation value of number state $\langle n\rangle$ as a function of A for the state $|A, 0.2, 1\rangle_\Gamma$

5.1.6 Bargmann function of Gamma states and its zeros

In this section we consider a system with a Hamiltonian H, which at $t = 0$ is in some initial state. We study the time evolution of this state, and the motion of the zeros of its Bargmann function. We assume that at time $t = 0$ the system is on the state $|A, B, k\rangle_\Gamma$. and its Bargmann function $\Omega_{|A,B,k\rangle_\Gamma}(z)$ with zeros $\{\varsigma_n\}$. At time t the system is in the state $|A, B, k, t\rangle_\Gamma = \exp(iHt)|A, B, k\rangle_\Gamma$ and has Bargmann function $\Omega_{|A,B,k\rangle_\Gamma}(z, t)$ with zeros $\{\varsigma_n(t)\}$. The number of zeros corresponding to $|A, B, k, t\rangle_\Gamma$ may change as a function of time. This is obvious from the fact that any two states can be related with a unitary transformation [39].

The zeros of a Bargmann function may all have paths or may not even have a path. If we consider figure 5.20 we notice that the first six zeros of the Bargmann function $\frac{1}{\Gamma(z)}$ all have paths under the Hamiltonian $H =$

$0.5[(\hat{a}^\dagger)^2+\hat{a}^2]$ on the other hand, in figure 5.21 under $H=[\hat{a}^\dagger\hat{a}]$; there is no path for $\varsigma_0=0$. If we compare two different Bargmann functions with the same roots under the same Hamiltonian we will have different paths. Comparing figure 5.20 for the Bargmann function $\frac{1}{\Gamma(z)}$ and figure 5.22 for the Barmann function $\frac{\exp(0.5z)}{\Gamma(z)}$, which are both under the $H=0.5[(\hat{a}^\dagger)^2+\hat{a}^2]$. It is clear that the correspondig zeros do not follow the same paths.

Figure 5.23 shows the first six zeros of Bargmann function of the state $|1,0,1\rangle_\Gamma$ and its motion according to the $H=0.1[(\hat{a}^\dagger)^2\hat{a}^2]$ at $t=[0:.05:0.3]$.

A zero can have two paths as shown in figure 5.24 under $H=0.5[(\hat{a}^\dagger)^2+\hat{a}^2]$ and figure 5.25 under $H=0.01[\hat{a}^\dagger\hat{a}]^2$. Each zero has two different paths as a result of multiplicity 2.

5.2 Summary

We have given an example of our generalized coherent states based on the Gamma function. In the next chapter we give another example based on the Riemann ξ function.

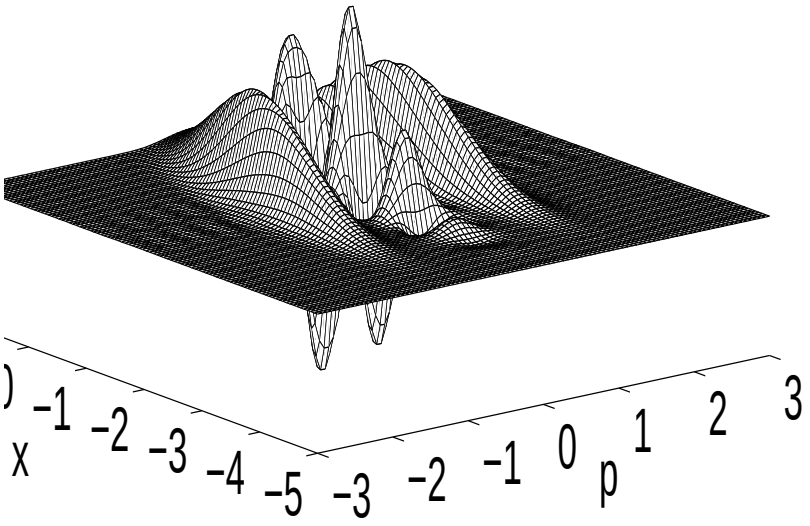

Figure 5.12: The Wigner function of the state $F(x, 1, 0, 1)$ for all $-5 \leq x \leq 1$ and $-3 \leq p \leq 3$

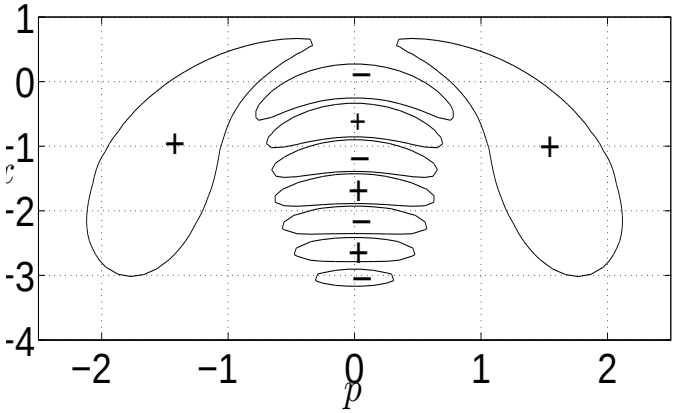

Figure 5.13: The contour of Wigner function of the state $F(x, 1, 0, 1)$for all $-4 \leq x \leq 1$ and $-2.5 \leq p \leq 2.5$

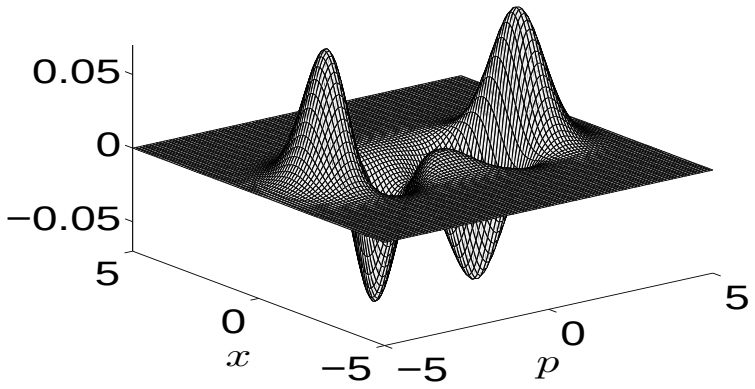

Figure 5.14: The Wigner function of the state $|0.1, 0, 1\rangle_\Gamma$

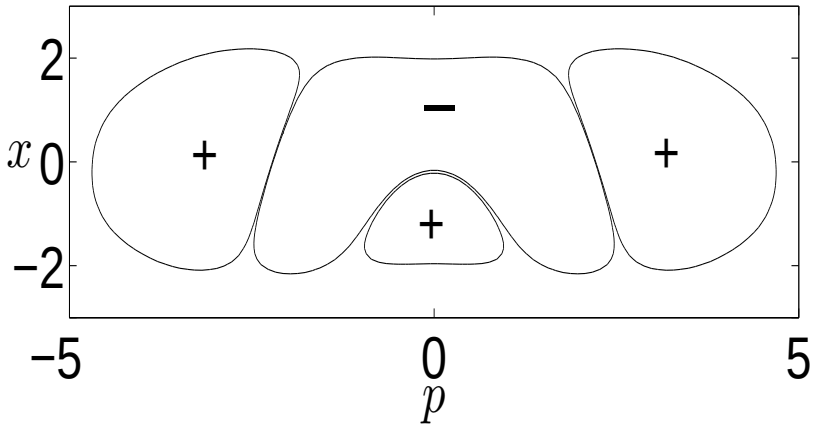

Figure 5.15: The contour of Wigner function for the state $|0.1, 0, 1\rangle_\Gamma$

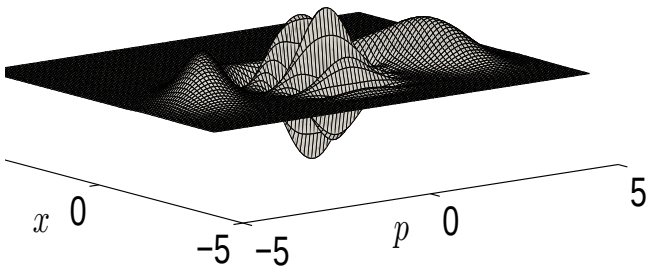

Figure 5.16: The Wigner function of the state $|1, 0.1, 1\rangle_\Gamma$

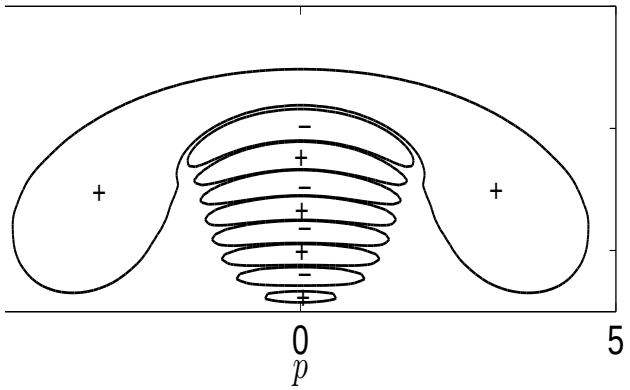

Figure 5.17: The contour of Wigner function of the state $|1, 0.1, 1\rangle_\Gamma$

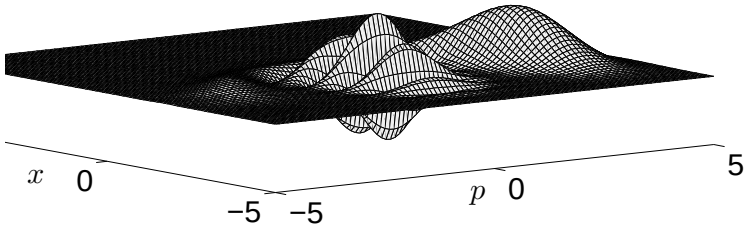

Figure 5.18: The Wigner function of the state $|1, 0.1\pi i, 1\rangle_\Gamma$

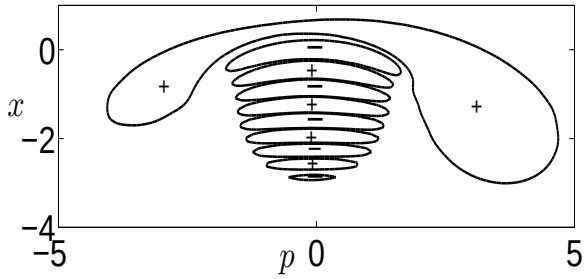

Figure 5.19: The contour of Wigner function for the state $|1, 0.1\pi i, 1\rangle_\Gamma$

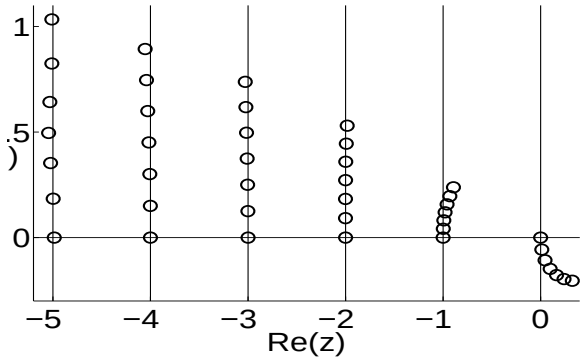

Figure 5.20: The time evolution of the zeros of the Bargmann function for the state $|1,0,1\rangle_\Gamma$, for Hamiltonian $H = 0.5[(\hat{a}^\dagger)^2 + \hat{a}^2]$ and for the time interval $t = [0 : .05 : 0.3]$. At $t = 0$ the Bargmann function is $\frac{1}{\Gamma(z).}$ Figure 5.20 shows the first six zeros of Bargmann function of the state $|1,0,1\rangle_\Gamma$ and its motion according to the Hamiltonian $H = 0.5[(\hat{a}^\dagger)^2+\hat{a}^2]$ at $t = [0 : .05 : 0.3]$. For $t = 0$ the system is on the state $|1,0,1\rangle_\Gamma$. and its Bargmann function $\Omega_{|1,0,1\rangle_\Gamma}(z)$ with first six zeros $\varsigma_0 = 0, \varsigma_1 = -1, \varsigma_2 = -2, \varsigma_3 = -3, \varsigma_4 = -4, \varsigma_5 = -5$. At any time t the system is in the state $|1,0,1,t\rangle_\Gamma = \exp(iHt)|1,0,1\rangle_\Gamma$ and has Bargmann function $\Omega_{|1,0,1\rangle_\Gamma}(z,t)$ with zeros $\{\varsigma_n(t)\}$.

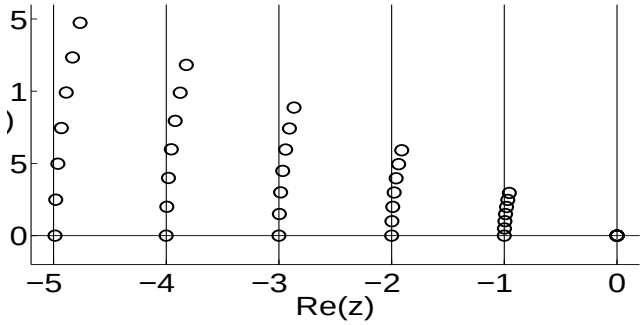

Figure 5.21: The time evolution of the zeros of the Bargmann function of the state $|1,0,1\rangle_\Gamma$, for Hamiltonian $H = [\hat{a}^\dagger \hat{a}]$ and for the time interval $t = [0 : .05 : 0.3]$. At $t = 0$ the Bargmann function is $\frac{1}{\Gamma(z).}$ Figure 5.21 shows the first six zeros of Bargmann function of the state $|1,0,1\rangle_\Gamma$ and its motion according to the Hamiltonian $H = \hat{a}^\dagger \hat{a}$ at $t = [0 : .05 : 0.3]$. For $t = 0$ the system is on the state $|1,0,1\rangle_\Gamma$. and its Bargmann function $\Omega_{|1,0,1\rangle_\Gamma}(z)$ with first six zeros $\varsigma_0 = 0, \varsigma_1 = -1, \varsigma_2 = -2, \varsigma_3 = -3, \varsigma_4 = -4, \varsigma_5 = -5$. At any time t the system is in the state $|1,0,1,t\rangle_\Gamma = \exp(iHt)|1,0,1\rangle_\Gamma$ and has Bargmann function $\Omega_{|1,0,1\rangle_\Gamma}(z,t)$ with zeros $\{\varsigma_n(t)\}$.

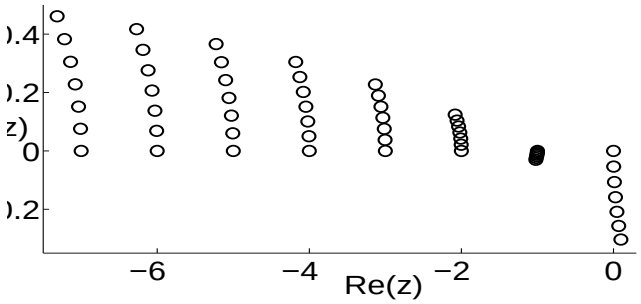

Figure 5.22: The time evolution of the zeros of the Bargmann function of the state $|1, 0.5, 1\rangle_\Gamma$, for Hamiltonian $H = 0.5[(\hat{a}^\dagger)^2 + a^2]$ and for the time interval $t = [0 : .05 : 0.3]$. At $t = 0$ the Bargmann function is $\frac{\exp(0.5z)}{\Gamma(z)}$. Figure 5.22 shows the first eight zeros of Bargmann function of the state $|1, 0.5, 1\rangle_\Gamma$ and its motion according to the $H = 0.5[(\hat{a}^\dagger)^2 + \hat{a}^2]$ at $t = [0 : .05 : 0.3]$. For $t = 0$ the system is on the state $|1, 0.5, 1\rangle_\Gamma$. and its Bargmann function $\Omega_{|1,0.5,1\rangle_\Gamma}(z)$ with first eight zeros $\varsigma_0 = 0, \varsigma_1 = -1, \varsigma_2 = -2, \varsigma_3 = -3, \varsigma_4 = -4, \varsigma_5 = -5, \varsigma_6 = -6, \varsigma_7 = -7$. At any time t the system is in the state $|1, 0.5, 1, t\rangle_\Gamma = \exp(iHt)|1, 0.5, 1\rangle_\Gamma$ and has Bargmann function $\Omega_{|1,0.5,1\rangle_\Gamma}(z, t)$ with zeros $\{\varsigma_n(t)\}$.

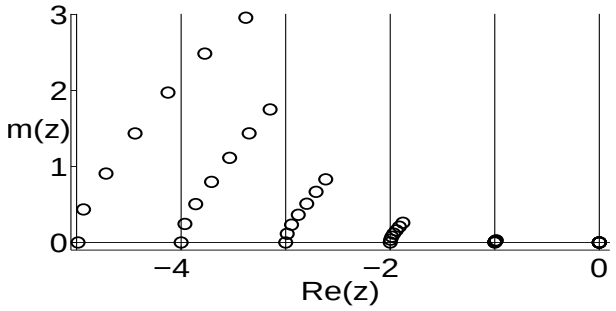

Figure 5.23: The time evolution of the zeros of the Bargmann function of the state $|1,0,1\rangle_\Gamma$, for Hamiltonian $H = 0.1[(\hat{a}^\dagger)^2\hat{a}^2]$ and for the time interval $t = [0 : .05 : 0.3]$. At $t = 0$ the Bargmann function is $\frac{1}{\Gamma(z).}$ Figure 5.23 shows the first six zeros of Bargmann function of the state $|1,0,1\rangle_\Gamma$ and its motion according to the $H = 0.1[(\hat{a}^\dagger)^2\hat{a}^2]$ at $t = [0 : .05 : 0.3]$. For $t = 0$ the system is on the state $|1,0,1\rangle_\Gamma$. and its Bargmann function $\Omega_{|1,0,1\rangle_\Gamma}(z)$ with first six zeros $\varsigma_0 = 0, \varsigma_1 = -1, \varsigma_2 = -2, \varsigma_3 = -3, \varsigma_4 = -4, \varsigma_5 = -5$. At any time t the system is in the state $|1,0,1,t\rangle_\Gamma = \exp(iHt)|1,0,1\rangle_\Gamma$ and has Bargmann function $\Omega_{|1,0,1\rangle_\Gamma}(z,t)$ with zeros $\{\varsigma_n(t)\}$.

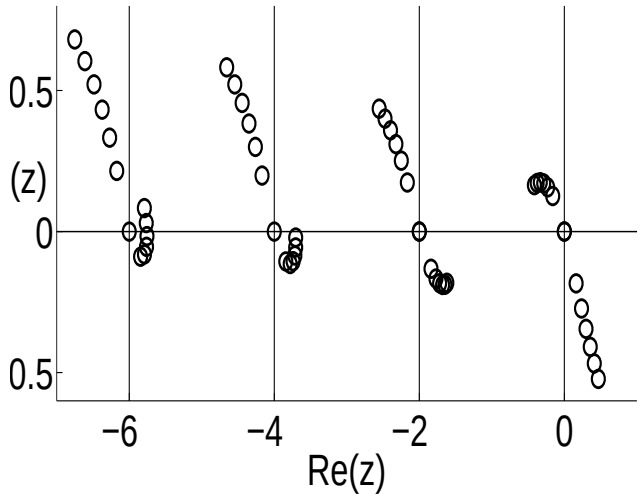

Figure 5.24: The time evolution of the zeros of the Bargmann function of the state $|0.5, 0, 2\rangle$, for Hamiltonian $H = 0.5[(\hat{a}^\dagger)^2 + \hat{a}^2]$ and for the time interval $t = [0 : .05 : 0.3]$. At $t = 0$ the Bargmann function is $\frac{1}{(\Gamma(0.5z))^2.}$ Figure 5.24 shows the first four zeros of Bargmann function of the state $|0.5, 0, 2\rangle_\Gamma$ and its motion according to the Hamiltonian $H = 0.5[(\hat{a}^\dagger)^2 + \hat{a}^2]$ at $t = [0 : .05 : 0.3]$. For $t = 0$ the system is on the state $|0.5, 0, 2\rangle_\Gamma$. and its Bargmann function $\Omega_{|0.5,0.5,2\rangle_\Gamma}(z)$ with first four zeros $\varsigma_0 = 0, \varsigma_2 = -2, \varsigma_4 = -4, \varsigma_6 = -6$ with multiplicity 2. At time t the system is in the state $|0.5, 0, 2, t\rangle_\Gamma = \exp(iHt)|0.5, 0, 2\rangle_\Gamma$ and has Bargmann function $\Omega_{|0.5,0,2\rangle_\Gamma}(z, t)$ with zeros $\{\varsigma_n(t)\}$. In this case we denote that each zero follows two different paths one is moving up while the other is moving down. This because the original zero has multiplicity two

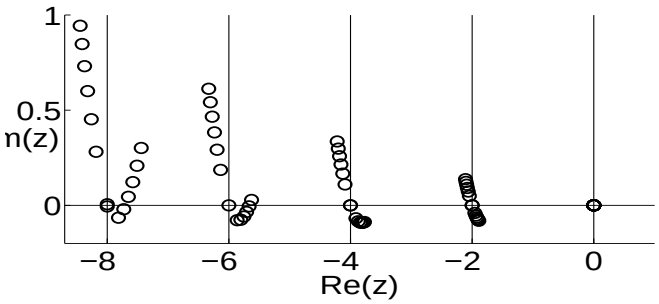

Figure 5.25: The time evolution of the zeros of the Bargmann function of the state $|0.5, 0, 2\rangle$, for Hamiltonian $H = 0.01[\hat{a}^\dagger \hat{a}]^2$ and for the time interval$t = [0 : .05 : 0.3]$. At $t = 0$ the Bargmann function is $\frac{1}{(\Gamma(0.5z))^2}$. Figure 5.25 shows the first five zeros of Bargmann function of the state $|0.5, 0, 2\rangle_\Gamma$ and its motion according to the Hamiltonian $H = 0.01[\hat{a}^\dagger a]^2$ at $t = [0 : .05 : 0.3]$. For $t = 0$ the system is on the state $|0.5, 0, 2\rangle_\Gamma$. and its Bargmann function $\Omega_{|0.5,0,2\rangle_\Gamma}(z)$ with first five zeros $\varsigma_0 = 0, \varsigma_1 = -2, \varsigma_2 = -4, \varsigma_3 = -6, \varsigma_4 = -8, \varsigma_5 = -5$ with multiplicity two. At any time t the system is in the state $|0.5, 0, 2, t\rangle_\Gamma = \exp(iHt)|0.5, 0, 2\rangle_\Gamma$ and has Bargmann function $\Omega_{|0.5,0,2\rangle_\Gamma}(z, t)$ with zeros $\{\varsigma_n(t)\}$. In this case we denote that each zero has two different paths one is moving up while the other is moving down.

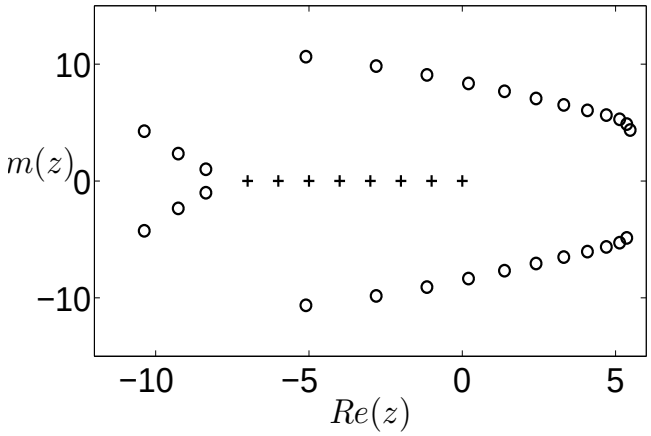

Figure 5.26: The zeros of the approximate polynomial for the state $|1,0,1\rangle_\Gamma$ where [+] denotes to real zeros and [o] denotes to the spurious zeros.

Chapter 6

Riemann ξ state $|A\rangle_\xi$

6.1 The Riemann Zeta function $\zeta(z)$

The Riemann zeta function is an extremely important function in mathematics and physics that arises in definite integration and is intimately related to very deep results surrounding the prime number theorem. While many of the properties of this function have been investigated, their remain important fundamental conjectures that remain unproved to this day. The Riemann zeta function can be defined by the following integral:

$$\zeta(x) \equiv \frac{1}{\Gamma(x)} \int_0^\infty \frac{u^{x-1}}{\exp(u)-1} du, \quad x > 1 \tag{6.1}$$

where $\Gamma(x)$ is the Gamma function.

If x is an integer k, then we have the simplified identity:

$$\begin{aligned}\frac{u^{k-1}}{\exp(u)-1} &= \frac{u^{k-1}\exp(-u)}{1-\exp(-u)} \\ &= u^{k-1}\exp(-u)\sum_{n=0}^{\infty}\exp(-nu) \\ &= \sum_{n=1}^{\infty}u^{k-1}\exp(-nu)\end{aligned}$$

By integrating both sides:

$$\int_0^\infty \frac{u^{k-1}}{\exp(u)-1} = \sum_{n=1}^{\infty}\int_0^\infty u^{k-1}\exp(-nu)$$

To evaluate $\zeta(k)$, we let $y \equiv nu$ so that $dy \equiv ndu$ and plug in the above identity to obtain:

$$\begin{aligned}\zeta(k) &= \frac{1}{\Gamma(k)}\sum_{n=1}^{\infty}\int_0^\infty u^{k-1}\exp(-nu)du \\ &= \frac{1}{\Gamma(k)}\sum_{n=1}^{\infty}\int_0^\infty (\frac{y}{n})^{k-1}\exp(-y)\frac{dy}{n} \\ &= \frac{1}{\Gamma(k)}\sum_{n=1}^{\infty}\frac{1}{n^k}\int_0^\infty y^{k-1}\exp(-y)dy\end{aligned}$$

Evaluating the integral above gives $\Gamma(k)$, which cancels the factor $\frac{1}{\Gamma(k)}$ and gives the most common form of the Riemann zeta function:

$$\zeta(k) = \sum_{n=1}^{\infty}\frac{1}{n^k} \tag{6.2}$$

The Riemann Zeta function $\zeta(z)$ is a complex function defined as [51, 52, 53, 54]:

$$\zeta(z) = \sum_{n=1}^{\infty} \frac{1}{n^z} \qquad \forall Re(z) > 1 \tag{6.3}$$

where the sum on the right-hand side is taken over all n, the natural numbers.

The relation between Riemann Zeta function $\zeta(z)$ and prime numbers, p is given by [55, 56]:

$$\begin{aligned}
\zeta(z) &= \frac{1}{1^z} + \frac{1}{2^z} + \frac{1}{3^z} + \frac{1}{4^z} + \frac{1}{5^z} + \frac{1}{6^z} + \frac{1}{7^z} + ... \\
&= (\frac{1}{1^z} + \frac{1}{2^z} + \frac{1}{4^z} + \frac{1}{8^z} + ...)(\frac{1}{1^z} + \frac{1}{3^z} + \frac{1}{9^z}...)(\frac{1}{1^z} + \frac{1}{5^z} + ...) \\
&= \prod_p \sum_{k=0}^{\infty} p^{-kz} \\
\zeta(z) &= \prod_p (1 - \frac{1}{p^z})^{-1}, \qquad Re(z) = x > 1
\end{aligned} \tag{6.4}$$

The Euler product formula given above expresses the zeta function as a product over the primes p, and consequently provides a link between the analytic properties of the zeta function and the distribution of primes in the integers.

It is clear that $\zeta(z)$ at $z = 1$ is the harmonic series [57, 58]:

$$\zeta(1) = \sum_{n=1}^{\infty} \frac{1}{n} = 1 + \frac{1}{2} + \frac{1}{3} + \frac{1}{4} + ... = \infty \tag{6.5}$$

and is divergent by the P-test, hence $P = 1$ [57, 58].

In complex analysis, **analytic continuation** is a technique that extends the domain of a given analytic function. Analytic continuation often succeeds in defining further values of a function, for example in a new region where an infinite series representation in terms of which it is initially defined becomes divergent.

The functional equation, which provide the analytic continuation of $\zeta(z)$ for $Re(z) < 1$ is

$$\zeta(z) = 2^z \pi^{z-1} sin(\frac{\pi z}{2}) \Gamma(1-z)\zeta(1-z) \tag{6.6}$$

The zeta function $\zeta(z)$ is analytic in the whole complex plane except for the simple pole at $z = 1$ with residue 1 [51, 59].

The limit of $(z-1)\zeta(z)$ is equal to 1 at $z \to 1$, i.e.

$$\lim_{z\to 1}(z-1)\zeta(z) = 1 \tag{6.7}$$

The function $(z-1)\zeta(z)$ is analytic in the whole complex plane and can be expressed as a Taylor expansion at any $z \in \mathbb{C}$ [55, 56].

The ζ function $\zeta(z)$ is a function from the complex plane $\mathbb{C} - \{0\}$ to $\mathbb{C}$ i.e, $\zeta : \mathbb{C} - \{0\} \to \mathbb{C}$, its graph can't be represented as a 3D image. Instead, the real valued ζ function $\zeta(x)$ and $(x-1)\zeta(x)$ are plotted and can be shown in figure 6.1 and figure 6.2. In addition the absolute value of $\zeta(z)$ can be shown in figure 6.3

Some other well known values of the Riemann Zeta are:

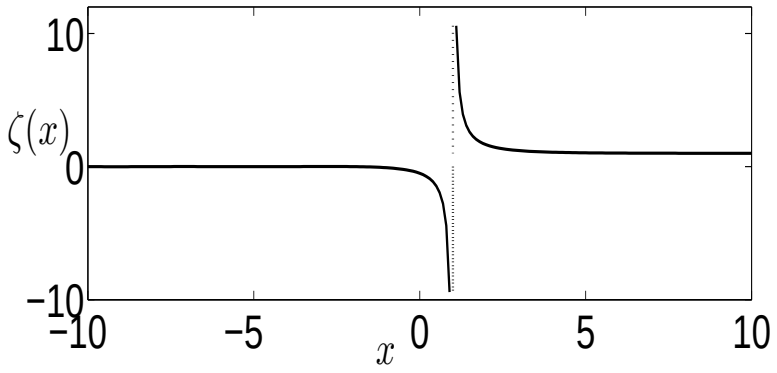

Figure 6.1: The plot of real valued Riemann Zeta function $\zeta(x)$ for all $-10 \leq x \leq 10$

$$\zeta(0) = \frac{-1}{2}, \quad \zeta(2) = \frac{\pi^2}{6}, \quad \zeta(4) = \frac{\pi^4}{90} \tag{6.8}$$

A **nontrival zero** of the Riemann Zeta function is defined to be a root $\zeta(z) = 0$ with the property that $0 \leq Re(z) \leq 1$.

Any other zero of the zeta function is called a **trival zero**.

The Riemann zeta function has zeros at the negative even integers. Since $\zeta(z)$ has no zeros for $Re(z) > 1$, and Γ has no zeros for at all, we see from the functional Eq(6.6) that the only zeros of the functions $z \to \sin(\frac{\pi z}{2})$ at points -2,-4,-6,... These are called the **trival zeros** of $\zeta(z)$ and some of them can be shown in figure 6.4.

The Riemann hypothesis is concerned with the non-trival zeros, and states that:

The real part of any non-trival zero of the Zeta function is $\frac{1}{2}$ [60], thus the non-trival zeros should lie on the critical line $\frac{1}{2} + it$ where t is a real number

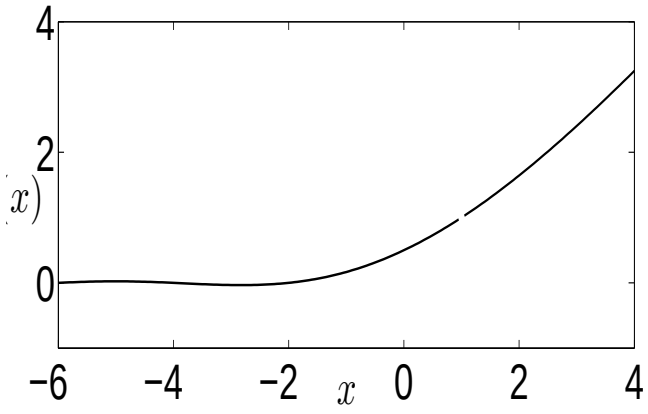

Figure 6.2: The plot of real valued Riemann Zeta function $(x-1)\zeta(x)$ for all $-6 \leq x \leq 4$

as shown in figure 6.4.

The Riemann Zeta function $\zeta(z)$ satisfies:

$$\zeta(z^*) = \zeta(z)^* \tag{6.9}$$

Therefore if ζ_n is a zero of $\zeta(z)$ then ζ_n^* is also a zero .

The Riemann Zeta function has **non-trival zeros** at $0.5 \pm 14.134725i$, $0.5 \pm 21.022040i$, $-0.5 \pm 25.010858i$, $0.5 \pm 30,424876i$,$0.5 \pm 32.935062i$...

The Riemman Zeta function $\zeta(z) \neq 0$ for all $Re(z) = x > 1$.

We can prove from Euler's product and $Re(z) > 1$ that $1 - p^{-z} \neq 0$, for all prime p.

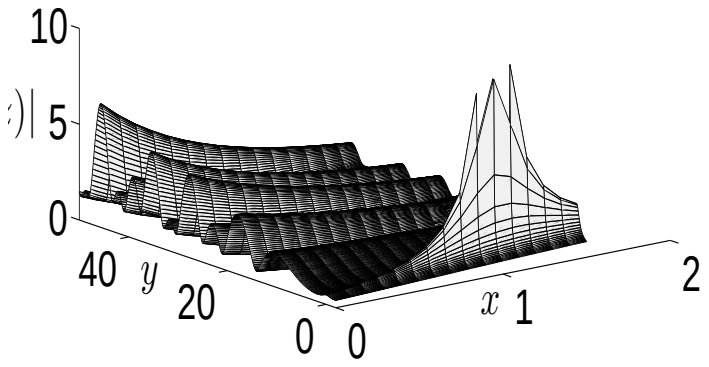

Figure 6.3: The plot of $|\zeta(z)|$,$0 \leq x \leq 1,5$ and $-2 \leq y \leq 50$

6.1.1 Zeros of the Zeta Function, and the Riemann Hypothesis

As we have said, $\zeta(z)$ has zeros at the negative even integers, and these are the only such zeros for $Re(z) < 0$. Also, for $Re(z) > 1$, $\zeta(z)$ has no zeros. This leaves the region $0 < Re(z) < 1$, which is called the critical strip. It turns out that $\zeta(z)$ has no zeros on the lines $Re(z) = 0$ or 1. And, we already know that if ζ_n is a root, then ζ_n^* is also a root. The famous Riemann Hypothesis asserts that in the critical strip, all the roots of $\zeta(z)$ lie on the line $Re(z) = \frac{1}{2}$. The truth (falsity) of this conjecture would have profound consequences concerning the distribution of prime numbers.

The n-th derivative of Riemann zeta function at $z = 0$ can be defined as [61]:

$$\zeta^n(0) = \frac{(-1)^n n!}{\pi}[\frac{Im(z_0^{n+1})}{(n+1)!} + \sum_{k=0}^{n-1} a_k \frac{Im(z_0^{n-k})}{(n-k)!}]. \tag{6.10}$$

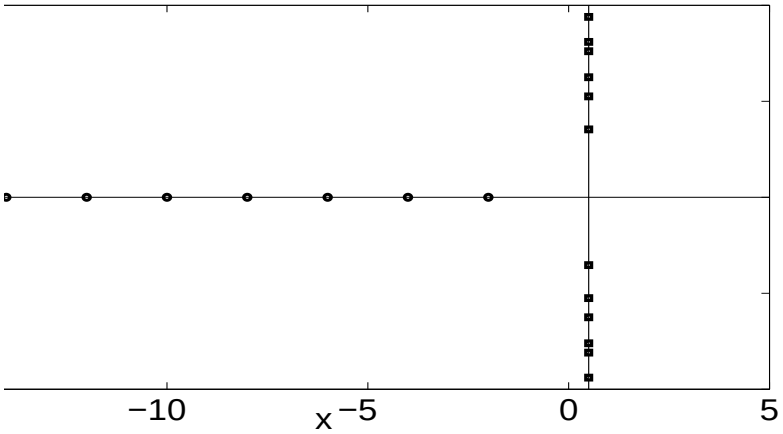

Figure 6.4: The trival and non trival zeros of zeta function for all $-15 \leq x \leq 5$ and $-40 \leq y \leq 40$

Here we have a_n and the Stieltjes constants γ_k, which are defined by:

$$a_n = \frac{\Gamma^{n+1}(1)}{(n+1)!} + \sum_{k=0}^{n} \frac{(-1)^k \gamma_k \Gamma^{n-k}(1)}{k!(n-k)!} \qquad n > 0 \tag{6.11}$$

$$\gamma_k = \lim_{N\to\infty} (\sum_{k=1}^{N} \frac{\ln^k(i)}{t}) - \frac{\ln^{k+1}(N)}{k+1} \tag{6.12}$$

where γ_0 is Euler constant and $z_0 = -\ln(2\pi) - \frac{\pi i}{2}$.

The first four derivatives of $\zeta(z)$ at $z = 0$ are given by:

$\zeta^{'}(0) = -0.9189, \quad \zeta^{''}(0) = 1.6449, \quad \zeta^{'''}(0) = 1.2021, \quad \zeta^{(4)}(0) = 1.0823$

6.2 The Riemann ξ function $\xi(z)$

The Riemann ξ function is defined as the product [62, 63, 56]:

$$\xi(z) = \frac{1}{2}z(z-1)\pi^{-\frac{1}{2}z}\Gamma(\frac{1}{2}z)\zeta(z) \tag{6.13}$$

where Γ denotes to the Gamma function and ζ denotes to the Zeta function. The zero of $z-1$ cancels the pole of $\zeta(z)$, and the real zeros of $\zeta(z)$ are canceled by the (simple) poles of $\Gamma(\frac{1}{2}z)$, which never vanish. Thus, $\xi(z)$ is an entire function.

The plot of $\xi(x)$, as a function of x where $-4 \leq x \leq 4$ also can be shown in figure 6.5.

The ξ function $\xi(z)$ is a function from the complex plane $\mathbb{C}$ to itself i.e. $\xi : \mathbb{C} \to \mathbb{C}$, its graph can not be represented as a 3D image. Instead, the real part and the imaginary part are plotted and can be shown in figure 6.6 and figure 6.7 In addition, the absolute value of $\xi(z)$ can be shown in figure 6.8.

The Riemann xi function $\xi(z)$ satisfies the functional equation [64]:

$$\xi(z) = \xi(1-z) \tag{6.14}$$

Therefore if ω_n is a zero of $\xi(z)$ then $1-\omega_n$ is also a zero.

The first 15^{th} zeros of Riemann xi function $\xi(z)$ can be shown in table 6.2.

From this functional equation (6.14), we notice from the n-th derivative that we can attain:

$$\frac{d^n\xi(z)}{dz^2} = (-1)^n\frac{d^n\xi(1-z)}{dz^2} \tag{6.15}$$

We can clearly explain from this relationship above why the same odd

derivative of $\xi(z)$ and $\xi(1-z)$ have different signs which can be noticed in table 6.1

The Riemann $\xi(z)$ is an analytic function and can be expressed as a Taylor expansion $\sum_{n=0}^{\infty} c_n(z-z_0)^n$.

The first 14^{th} coefficients c_n of $\xi(z)$ at $z=0$ and $z=1$ can be shown in table 6.1.

This can be derived by differentiating Eq (6.13) of the ξ function with respect to z, and using the technique of differentiation rules.

Table 6.1: The first 14^{th} coefficients of Riemann xi function $\xi(z)$ at z=0 and z=1

n	$c_n(z=0)$	$c_n(z=1)$
0	0.50000	0.50000
1	-0.01154	0.01154
2	-1.81397	-1.81397
3	2.19609	-2.19609
4	-1.43344	-1.43344
5	0.870594	-0.870594
6	-0.47145	-0.47145
7	0.24789	-0.24789
8	-0.12691	-0.12691
9	0.06429	-0.06429
10	0.03235	0.03235
11	0.01623	-0.01623
12	-0.00813	-0.00813
13	0.00363	-0.00363

Every entire function can be represented as a product involving its zeroes. Examples are the sine and cosine function.

The Hadamard product representation of the ξ function $\xi(z)$ [63].

$$\xi(z) = \frac{1}{2}\exp(Bz)\prod_{\omega_n}(1-\frac{z}{\omega_n})\exp(\frac{z}{\omega_n}) \tag{6.16}$$

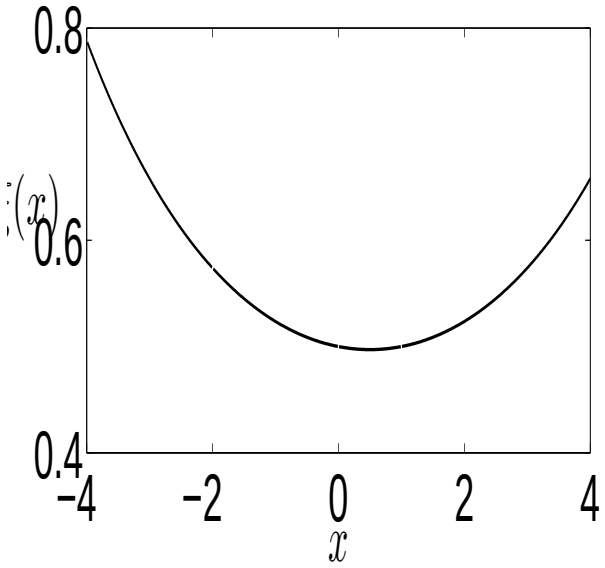

Figure 6.5: The plot of $\xi(x)$, as a function of x where $-4 \leq x \leq 4$

Here the product is over all nontrivial zeros ω_n of ζ. and B is the negative real number [65, 66]

$$B = \frac{1}{2}\log 4\pi - 1 - \frac{1}{2}\gamma \simeq -0.023095... \tag{6.17}$$

The real $\bullet$ and spurious zeros $\circ$ of Bargmann function for the $|1\rangle_\xi$ by using Eq(6.16) can be shown in figure 6.11 .

The function $\xi(z)$ also has a slow enough rate of growth that it can be written as a product over its zeroes:

$$\xi(z) = \xi(0)\prod_{\omega_n}(1 - \frac{z}{\omega_n}) \tag{6.18}$$

The order of its growth is $\rho = 1$ and therefore $\xi(Az)$ qualifies as a

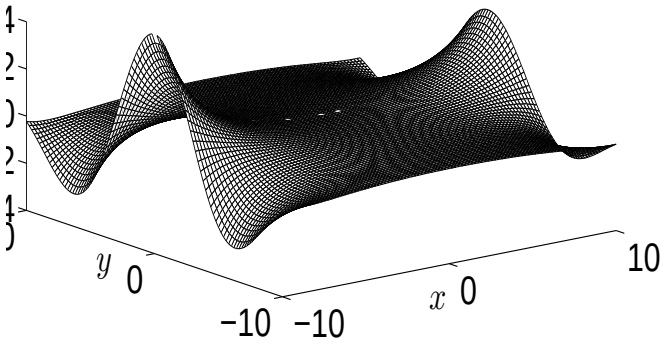

Figure 6.6: The real value of $\xi(z)$ where $z = x + iy$

Bargmann function [39]. The corresponding ket state is:

$$|A\rangle_\xi = N\xi(0)\prod_{\omega_n}(1 - \frac{\hat{a}^\dagger}{A^{-1}\omega_n})|0\rangle_\xi \tag{6.19}$$

The zeros of $\xi(z)$ are the nontrivial zeros of Zeta function $\zeta(z)$ and can be shown in figure 6.10.

6.2.1 The wavefunction of $|A\rangle_\xi$

We denote $F(x;A)_\xi$ as the wavefunction of the state $|A\rangle_\xi$ and can be written as:

$$F(\frac{x}{\sqrt{2}};A)_\xi = \frac{1}{\sqrt{2}\sqrt[4]{\pi^3}}\exp(-\frac{x^2}{4})\int dy\xi(Az)\exp(-\frac{y^2}{2}) \tag{6.20}$$

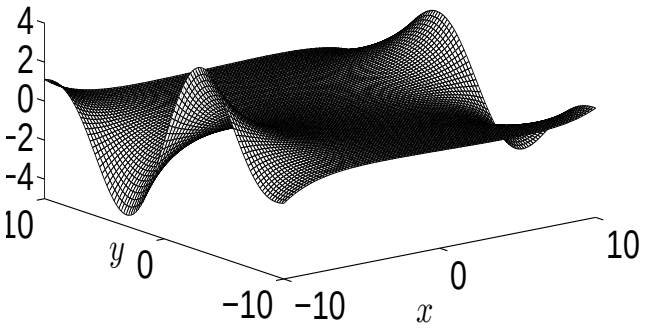

Figure 6.7: The image value of $\xi(z)$ where $z = x + iy$

6.2.2 The Wigner function $W_{|A\rangle_\xi}(x,p)$ of the state $|A\rangle_\xi$

The Wigner function of the state $|A\rangle_\xi$ can be written as:

$$W_{|A\rangle_\xi}(x,p) = \frac{1}{2\pi}\int_{-\infty}^{\infty} \exp(ipX)\langle x - X/2|\rho|x + X/2\rangle dX \quad (6.21)$$

$$W_{|A\rangle_\xi}(x,p) = \frac{1}{2\pi}\int_{-\infty}^{\infty} \exp(-iPx)\langle p - P/2|\rho|p + P/2\rangle dP \quad (6.22)$$

Where ρ is the density operator of the state $|A\rangle_\xi$.

$$\rho = |A\rangle_{\xi\xi}\langle A| \quad (6.23)$$

Figure 6.12 and 6.13 show wave and Wigner funtions for the state $|5\rangle_\xi$ and the cut lines denotes to the imaginary part of wave function.

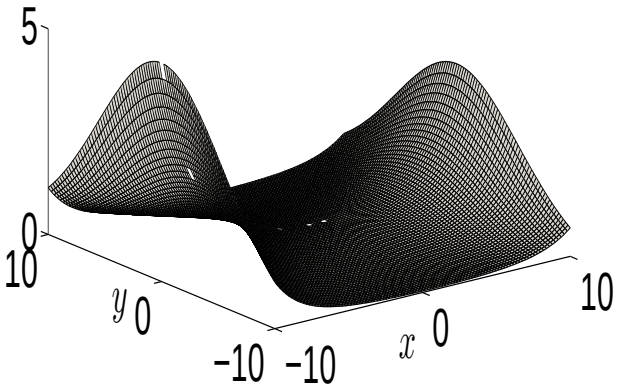

Figure 6.8: The absolute value of $\xi(z)$ where $z = x + iy$

The second coherence $g^{(2)}$ for the states $|A\rangle_\xi$ can be calculated by

$$g^{(2)} = \frac{\langle \hat{a}^\dagger \hat{a}^\dagger \hat{a} \hat{a} \rangle}{\langle \hat{a}^\dagger \hat{a} \rangle^2} = \frac{\langle n^2 \rangle - \langle n \rangle^2}{\langle n \rangle^2} \tag{6.24}$$

The values of $g^{(2)}$ for the states $|A\rangle_\xi$ at $A = [3 : 0.2 : 6]$ are shown in table 6.3

Figure 6.14 shows the the second coherence $g^{(2)}$ for the states $|A\rangle_\xi$ as a function of A.

6.2.3 Bargmann function of Riemann ξ states and its zeros

In this section we consider a system with a Hamiltonian H, which at $t = 0$ is in some initial state. We study the time evolution of this state, and the motion of the zeros of its Bargmann function. We assume that at time $t = 0$ the system is on the state $|A\rangle_\xi$, and its Bargmann function $\Omega_{|A\rangle_\xi}(z)$ with

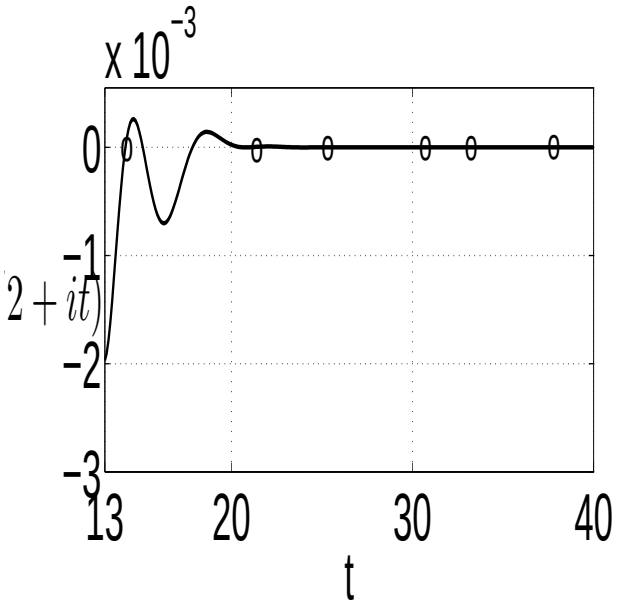

Figure 6.9: The plot of $\xi(1/2+it)$, as a function of t

zeros $\{\varsigma_n\}$. At time t the system is in the state $|A,t\rangle_\xi = \exp(iHt)|A\rangle_\xi$ and has Bargmann function $\Omega_{|A\rangle_\xi}(z,t)$ with zeros $\{\varsigma_n(t)\}$. The number of zeros corresponding to $|A,t\rangle_\xi$ may change as a function of time. This is obvious from the fact that any two states can be related with a unitary transformation [39].

The first six zeros of the approximate polynomial with degree $n = 6$ by using Eq(6.18) for Bargmann function of the state $|1\rangle_\xi$ according to the Hamiltonian $H = 0.1[(\hat{a}^\dagger)\hat{a}]^2$ is shown in figure (6.15). The paths of the first two zeros are in the same direction however, they differ from the remaining zeros. when we doubled the degree n and changed the H to $[(\hat{a}^\dagger)\hat{a}]$, the number of zeros became 12. Its motion has been illustrated in figure (6.16) and all the paths are in the same direction.

Table 6.2: The first 15^{th} zeros of Riemann xi function $\xi(z)$

n	ω_n
1	0.5+14.13472i
2	0.5+21.02203i
3	0.5+25.01085i
4	0.5+30.42487i
5	0.5+ 32.93506i
6	0.5+ 37.58617i
7	0.5+ 40.91871i
8	0.5+43.32707
9	0.5+48.00515i
10	0.5+49.77383i
11	0.5+ 52.97032i
12	0.5+52.97032i
13	0.5+ 59.34704i
14	0.5+ 60.83177i
15	0.5+ 65.11254i

The sign $\bullet$ denotes to the zeros at $t = 0$ while $\circ$ denotes to the zeros at $t > 0$

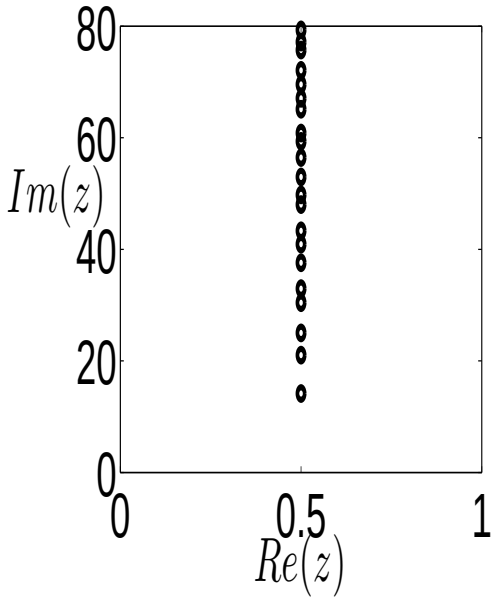

Figure 6.10: The zeros of ξ function

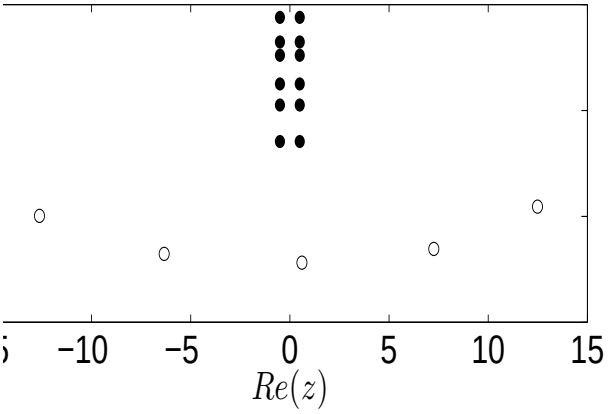

Figure 6.11: The real • and spurious zeros ∘ of Bargmann function for the $|1\rangle_\xi$ by using Eq(6.16).

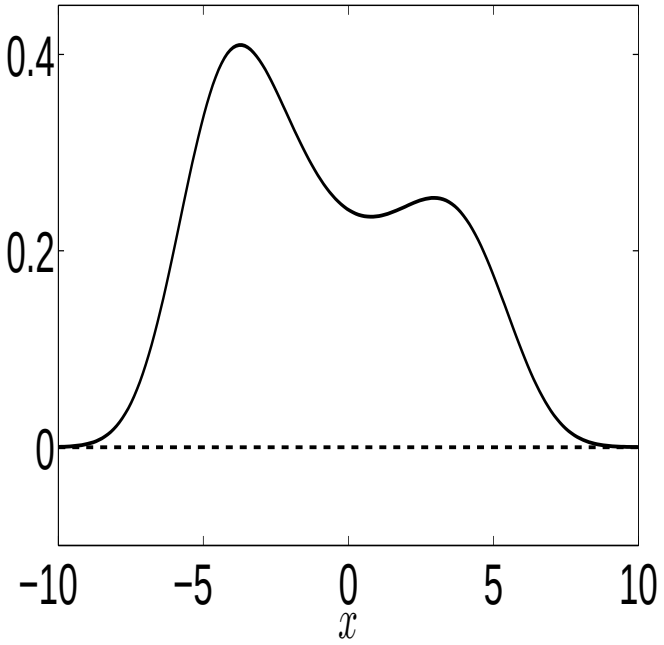

Figure 6.12: The wave function of the state $|5\rangle_\xi$

Table 6.3: This table shows the values of second coherence $g^{(2)}$ for the states $|A\rangle_\xi$ at $A = [3 : 0.2 : 6]$.

A	$g^{(2)}$	A	$g^{(2)}$
3.0	7.0842	4.6	2.2093
3.2	5.8705	4.8	1.9278
3.4	4.9565	5.0	1.6776
3.6	4.2559	5.2	1.4419
3.8	3.7002	5.4	1.2926
4.0	3.2460	5.6	1.1928
4.2	2.8588	5.8	1.1243
4.4	2.5196	6.0	1.079

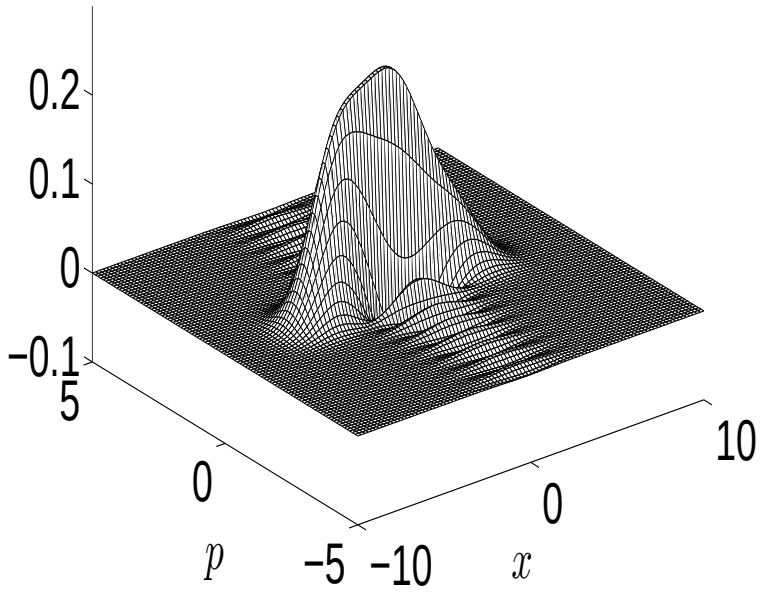

Figure 6.13: The Wigner function of the state $|5\rangle_\xi$

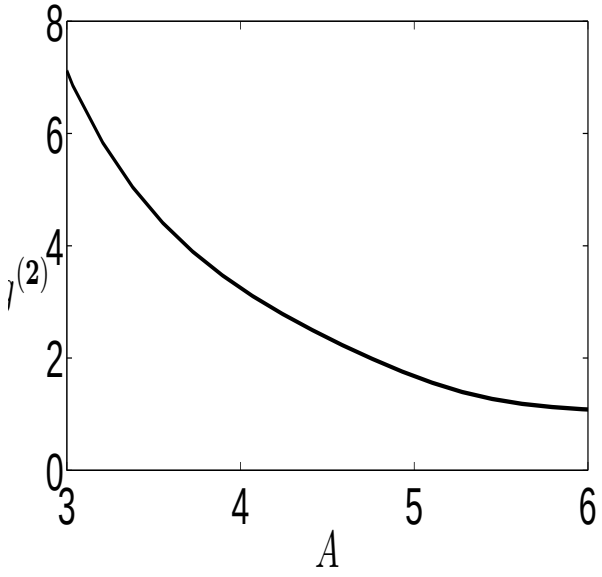

Figure 6.14: The second order coherence $g^{(2)}$ of $|A\rangle_\xi$ for $3 \leq A \leq 6$

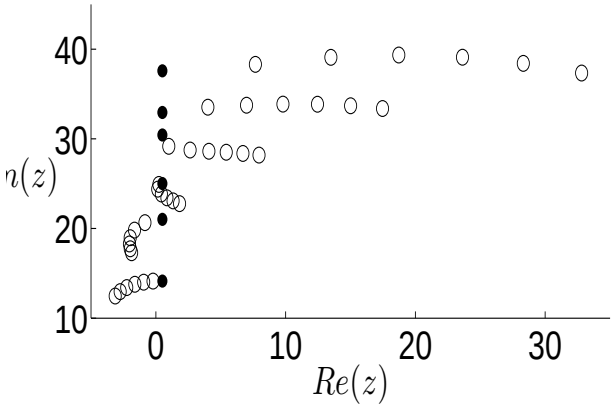

Figure 6.15: The time evolution of the zeros of the approximate polynomial with degree $n = 6$ for Bargmann function of the state $|1\rangle_\xi$, for Hamiltonian $H = 0.1[(\hat{a}^\dagger)\hat{a}]^2$ and for the time interval $t = [0 : .05 : 0.3]$.

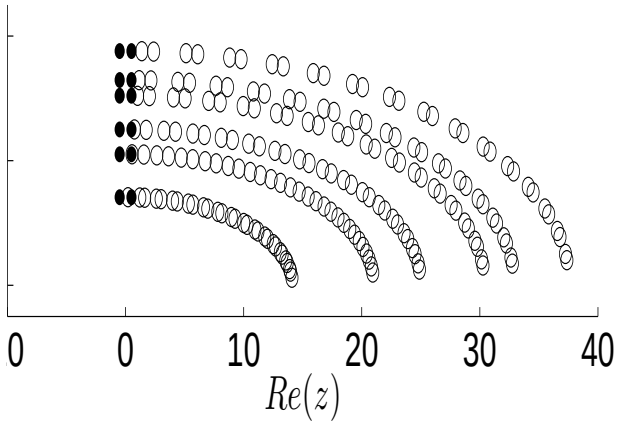

Figure 6.16: The time evolution of the zeros of the approximate polynomial with degree $n = 11$ for Bargmann function of the state $|1\rangle_\xi$ by using Eq(6.16), for Hamiltonian $H = (\hat{a}^\dagger)\hat{a}$ and for the time interval $t = [0 : 0.05 : 1.5]$. The sign $\bullet$ denotes to the zeros at $t = 0$ while $\circ$ denotes to the zeros at $t > 0$. The path according to $H = (\hat{a}^\dagger)\hat{a}$ is a circular curve.

Chapter 7

Discussion

Various analytic representations have been used in quantum mechanics. The Bargmann function in the complex plane has been used with the coherent states formalism. The analytic representation of infinite quantum systems has a great role in quantum optics. For each analytic function there is a corresponding quantum state.

In the present work we considered quantum systems with positions and momenta in real line. We introduced a new class of generalized coherent states which have three following properties:

- The set of coherent state is a **total set** in the Hilbert space. Our states may not have the stronger property of the resolution of the identity.
- We get all coherent states by acting on one of these states **fiducial vector** with operators which form a representation of the multiplicative group of non-zero complex numbers $\mathbb{C}^* = \mathbb{C} - \{0\}$.
- **Temporal stability** [2, 3] i.e. for some Hamiltonian H, the set of co-

herent states remains invariant under the corresponding time evolution (i.e, if $|s\rangle$ is a coherent state then $\exp(itH)|s\rangle$ is also a coherent state).

We have studied in detail two well known analytic functions on a complex plane based on Γ and ξ function (see table 7.1). The set of Gamma states $\{|A,B,k\rangle_\Gamma : \quad A,B \in \mathbb{C} \quad and \quad k = 1,2,3,...\}$ was based on the $g(z) = \frac{\exp(Bz)}{[\Gamma(Az)]^k}$. We have also studied quantum states corresponding to the analytic function $\xi(z)$.

In our work, we established a new methodology to generalize the concept of coherent states in a way which was not presented before. However, when this method was applied to certain coherent states, some essential properties could not be shown, such as the **resolution of the identity**.

The two previous examples illustrate the relation between the set of Quantum states and its analytic function.

The zeros of these function have been analyzed. The time evolution of the corresponding quantum states have been studied.

Table 7.1: The quantum state in ket and Bargmann representation

A	$Quantum-state$	$Ket-rep$	$Bargmann-rep$
1	Gamma state	$\|A,B,k\rangle_\Gamma$	$\frac{\exp(Bz)}{[\Gamma(Az)]^k}$
2	Riemann state	$\|A\rangle_\xi$	$\xi(Az)$

7.1 Further Work

The work is a contribution to the areas of coherent states, Bargmann functions and their zeros. Given a set of states which are a total set in some space,

it is an interesting problem to find the resolution of the identity. From a theoretical point of view, our methodology enlarges the concept of coherent states and leads to many novel sets of such states. We can use our methodology with many other examples in order to get other **novel sets of coherent states**. The work may be expanded to study more Bargmann functions and represent them as a set of new coherent states. A more general question is whether the total set property is a sufficient condition for the resolution of the identity property. I would like to work further on the goal of establishing a generalized methodology which maintains all the properties of coherent states.

References

[1] E. Colavita and S. Hacyan, "Wigner functions of free" schrodinger cat" states," *Revista mexicana de física*, vol. 49, no. 1, pp. 45–52, 2003.

[2] J. Klauder, "The current state of coherent states," *Arxiv preprint quant-ph/0110108*, 2001.

[3] J. Klauder and B. Skagerstam, *Coherent states: applications in physics and mathematical physics*. World Scientific Pub Co Inc, 1985.

[4] M. França Santos, E. Solano, and R. de Matos Filho, "Conditional large Fock state preparation and field state reconstruction in Cavity QED," *Physical Review Letters*, vol. 87, no. 9, p. 93601, 2001.

[5] A. Vourdas, "Quantum systems with finite Hilbert space," *Reports on Progress in Physics*, vol. 67, p. 267, 2004.

[6] D. Walls, "Squeezed states of light," *Nature*, vol. 306, no. 5939, pp. 141–146, 1983.

[7] D. Walls and G. Milburn, *Quantum optics*. Springer Verlag, 2008.

[8] B. Sutton, "18.338 J/16.394 J: The Mathematics of Infinite Random Matrices Tridiagonal Matrices, Orthogonal Polynomials and the Classical Random Matrix Ensembles,"

[9] A. W, "Hermite and Laguerre 2D polynomials," *Journal of computational and applied mathematics*, vol. 133, no. 1-2, pp. 665–678, 2001.

[10] S. Ali, J. Antoine, and J. Gazeau, *Coherent states, wavelets and their generalizations*. Springer Verlag, 2000.

[11] J. Klauder, "Coherent states for the hydrogen atom," *Journal of Physics A: Mathematical and General*, vol. 29, p. L293, 1996.

[12] J. Radcliffe, "Some properties of coherent spin states," *Journal of Physics A: General Physics*, vol. 4, p. 313, 1971.

[13] A. Perelomov, "On the completeness of a system of coherent states," *Theoretical and Mathematical Physics*, vol. 6, no. 2, pp. 156–164, 1971.

[14] M. Nieto, "Analytic description of the motion of a trapped ion in an even or odd squeezed state," *Physics Letters A*, vol. 219, no. 3-4, pp. 180–186, 1996.

[15] V. Dodonov, I. Malkin, and V. Man'Ko, "Even and odd coherent states and excitations of a singular oscillator," *Physica*, vol. 72, no. 3, pp. 597–615, 1974.

[16] C. Brif, A. Vourdas, and A. Mann, "Analytic representations based on SU (1, 1) coherent states and their applications," *Journal of Physics A: Mathematical and General*, vol. 29, p. 5873, 1996.

[17] M. Nieto, "Displaced and squeezed number states," *Physics Letters A*, vol. 229, no. 3, pp. 135–143, 1997.

[18] F. De Oliveira, M. Kim, P. Knight, and V. Buek, "Properties of displaced number states," *Physical Review A*, vol. 41, no. 5, pp. 2645–2652, 1990.

[19] S. Roy and V. Singh, "Generalized coherent states and the uncertainty principle," *Physical Review D*, vol. 25, no. 12, pp. 3413–3416, 1982.

[20] W. A. Man'ko, V.I, "Properties of squeezed-state excitations," *Quantum and Semiclassical Optics: Journal of the European Optical Society Part B*, vol. 9, p. 381, 1997.

[21] Y. Ben-Aryeh and B. Huttner, "Squeezed states and the quantum noise of measurement," *Physical Review A*, vol. 36, no. 3, pp. 1249–1257, 1987.

[22] K. Poels, I. Schoenmakers, and P. Tuyls, "Quantum Key Exchange,"

[23] A. Lukš and V. Peřinová, "Ordering of," *Physica Scripta*, vol. 1993, p. 94, 1993.

[24] G. Milburn, "Quantum and classical Liouville dynamics of the anharmonic oscillator," *Physical Review A*, vol. 33, no. 1, pp. 674–685, 1986.

[25] W. Schleich, A. Bandilla, and H. Paul, "Phase from Q function via linear amplification," *Physical Review A*, vol. 45, no. 9, pp. 6652–6654, 1992.

[26] K. Vogel, V. Akulin, and W. Schleich, "Quantum state engineering of the radiation field," *Physical review letters*, vol. 71, no. 12, pp. 1816–1819, 1993.

[27] D. Smithey, M. Beck, M. Raymer, and A. Faridani, "Measurement of the Wigner distribution and the density matrix of a light mode using optical homodyne tomography: Application to squeezed states and the vacuum," *Physical review letters*, vol. 70, no. 9, pp. 1244–1247, 1993.

[28] J. Vaccaro, "New Wigner function for number and phase," *Optics Communications*, vol. 113, no. 4-6, pp. 421–426, 1995.

[29] V. Bužek, A. Vidiella-Barranco, and P. Knight, "Superpositions of coherent states: Squeezing and dissipation," *Physical Review A*, vol. 45, no. 9, pp. 6570–6585, 1992.

[30] T. Williams, "Transformation of Squeezed Quadratures under Feed-Forward Amplification and Post-Selection," 2005.

[31] S. Chountasis and A. Vourdas, "The extended phase space: a formalism for the study of quantum noise and quantum correlations," *Journal of Physics A: Mathematical and General*, vol. 32, p. 6949, 1999.

[32] A. Jellal, "Coherent states for generalized Laguerre functions," *Arxiv preprint hep-th/0109028*, 2001.

[33] S. Chountasis and A. Vourdas, "Weyl functions and their use in the study of quantum interference," *Physical Review A*, vol. 58, no. 2, pp. 848–855, 1998.

[34] W. Schleich, *Quantum optics in phase space*. Vch Verlagsgesellschaft Mbh, 2001.

[35] C. Berg and H. Pedersen, "On the order and type of the entire functions associated with an indeterminate Hamburger moment problem," *Arkiv för Matematik*, vol. 32, no. 1, pp. 1–11, 1994.

[36] R. Boas, *Entire functions*, vol. 5. Academic Press, 1954.

[37] L. Stergioulas and A. Vourdas, "The Bargmann analytic representation in signal analysis," *Journal of Computational and Applied Mathematics*, vol. 167, no. 1, pp. 183–192, 2004.

[38] A. Vourdas, "The completeness of sequences of generalized coherent states," *Journal of Optics B: Quantum and Semiclassical Optics*, vol. 5, p. S413, 2003.

[39] A. Vourdas, "The growth and zeros of Bargmann functions," in *Journal of Physics: Conference Series*, vol. 213, p. 012001, IOP Publishing, 2010.

[40] C. Gerry, "Generalised coherent states and group representations on Hilbert spaces of analytic functions," *Journal of Physics A: Mathematical and General*, vol. 16, p. L1, 1983.

[41] C. Brif, "Photon states associated with the Holstein-Primakoff realization of the SU (1, 1) Lie algebra," *Quantum and Semiclassical Optics: Journal of the European Optical Society Part B*, vol. 7, p. 803, 1995.

[42] A. Vourdas, "SU (2) and SU (1, 1) phase states," *Physical Review A*, vol. 41, no. 3, pp. 1653–1661, 1990.

[43] K. Fujii, "Basic properties of coherent and generalized coherent operators revisited," *Arxiv preprint quant-ph/0009012*, 2000.

[44] C. Brif, "SU (2) and SU (1, 1) algebra eigenstates: A unified analytic approach to coherent and intelligent states," *International Journal of Theoretical Physics*, vol. 36, no. 7, pp. 1651–1682, 1997.

[45] A. Mohamed, C. Lei, and A. Vourdas, "Weak coherent states related to the multiplicative group," *Journal of Physics A: Mathematical and Theoretical*, vol. 44, pp. 215–304, 2011.

[46] A. Laurinčikas and R. Garunkštis, *The Lerch zeta-function*. Kluwer Academic Pub, 2002.

[47] P. Sebah and X. Gourdon, "Introduction to the gamma function," *numbers. computation. free. fr/Constants/constants. html*, 2002.

[48] H. Srivastava and C. Junesang, *Series associated with the zeta and related functions*. Springer Netherlands, 2001.

[49] M. Coffey, "Relations and positivity results for the derivatives of the Riemann [xi] function," *Journal of Computational and Applied Mathematics*, vol. 166, no. 2, pp. 525–534, 2004.

[50] W. Quay, N. Smiriga, and W. Haugeland, "Mathematical model and computer representation for nonlinear response systems," *Computers and Biomedical Research*, vol. 5, no. 3, pp. 239–246, 1972.

[51] C. Calderón, "The Riemann Hypothesis," *Monografías de la Real Academia de Ciencias Exactas, Físicas, Químicas y Naturales de Zaragoza*, no. 26, p. 1, 2004.

[52] J. Choi, H. Srivastava, and J. Quine, "Some series involving the zeta function," *Bulletin of the Australian Mathematical Society*, vol. 51, no. 03, pp. 383–393, 1995.

[53] T. Kim, "Euler numbers and polynomials associated with zeta functions," in *Abstract and Applied Analysis*, vol. 11, Hindawi Publishing Corporation, 2008.

[54] A. Odlyzko and A. Schönhage, "Fast algorithms for multiple evaluations of the Riemann zeta function," *Transactions of the American Mathematical Society*, vol. 309, no. 2, pp. 797–809, 1988.

[55] E. Titchmarsh and D. Heath-Brown, *The theory of the Riemann zeta-function*. Oxford University Press, USA, 1986.

[56] S. Patterson, *An introduction to the theory of the Riemann zeta-function*. Cambridge Univ Pr, 1995.

[57] T. Bromwich, *An introduction to the theory of infinite series*. Chelsea Publishing Company, Incorporated, 2005.

[58] W. Granville, *Elements of the differential and integral calculus*. Budge Pr, 2007.

[59] J. Choi, Y. Cho, and H. Srivastava, "Series involving the Zeta function and multiple Gamma functions," *Applied Mathematics and Computation*, vol. 159, no. 2, pp. 509–537, 2004.

[60] G. Hardy and J. Littlewood, "The zeros of Riemann's zeta-function on the critical line," *Mathematische Zeitschrift*, vol. 10, no. 3, pp. 283–317, 1921.

[61] N. Salazar, "Derivatives of the dedekind zeta function attached to a complex quadratic field extention," 2010.

[62] B. Conrey, "Zeros of derivatives of Riemann's xi-function of the critical line. II," *Journal of Number Theory*, vol. 17, no. 1, pp. 71–75, 1983.

[63] H. Edwards, *Riemann's zeta function*. Academic Pr, 1974.

[64] J. Choi, H. Srivastava, and V. Adamchik, "Multiple Gamma and related functions," *Applied Mathematics and Computation*, vol. 134, no. 2-3, pp. 515–534, 2003.

[65] E. Elizalde, *Ten physical applications of spectral zeta functions*. Springer Verlag, 1995.

[66] S. Gelbart and S. Miller, "Riemann's zeta function and beyond," *Bulletin of the American Mathematical Society*, vol. 41, no. 1, p. 59, 2004.